Research paper

Design, synthesis and biological evaluation of novel 2,4-thiazolidinedione derivatives able to target the human BAG3 protein

Federica Budassi [a,2], Chiara Marchioro [b,2], Martina Canton [b], Annagiulia Favaro [c], Mattia Sturlese [c], Chiara Urbinati [d], Marco Rusnati [d], Romeo Romagnoli [e], Giampietro Viola [b,f,**,1], Elena Mariotto [b,f,*,1]

[a] *Synthetic Chemistry, DDD, Aptuit an Evotec Company, Via Alessandro Fleming 4, 37135, Verona, Italy*
[b] *Laboratory of Pediatric Hematology-Oncology Department of Women's and Children's Health, University of Padova, Via Giustiniani 3, 35128, Padova, Italy*
[c] *Molecular Modeling Section (MMS), Department of Pharmaceutical and Pharmacological Sciences, University of Padova, via Marzolo 5, 35131, Padova, Italy*
[d] *Experimental Oncology and Immunology, Department of Molecular and Translational Medicine, University of Brescia, Viale Europa11, 25121, Brescia, Italy*
[e] *Dipartimento di Scienze Chimiche, Farmaceutiche e Agrarie, Università degli Studi di Ferrara, Via Luigi Borsari 46, 44121, Ferrara, Italy*
[f] *Istituto di Ricerca Pediatrica (IRP), Corso Stati Uniti 4F, 35127, Padova, Italy*

ARTICLE INFO

ABSTRACT

The Bcl-2-associated athanogene 3 (BAG3) protein plays multiple roles in controlling cellular homeostasis, and it has been reported to be deregulated in many cancers, leading tumor cell apoptosis escape. BAG3 protein is then an emerging target for its oncogenic activities in both leukemia and solid cancers, such as medulloblastoma. In this work a series of forty-four compounds were designed and successfully synthesized by the modification and optimization of a previously reported 2,4-thiazolidinedione derivative **28**. Using an efficient cloning and transfection in human embryonic kidney HEK-293T cells, BAG3 was collected and purified by chromatographic techniques such as IMAC and SEC, respectively. Subsequently, through Surface Plasmon Resonance (SPR) all the compounds were evaluated for their binding ability to BAG3, highlighting the compound **FB49** as the one having the greatest affinity for the protein ($K_d = 45 \pm 6$ μM) also against the reference compound **28**. Further analysis carried out by Saturation Transfer Difference (STD) Nuclear Magnetic Resonance (NMR) spectroscopy further confirmed the highest affinity of **FB49** for the protein. *In vitro* biological investigation showed that compound **FB49** is endowed with an antiproliferative activity in the micromolar range in three human tumoral cell lines and more importantly is devoid of toxicity in human peripheral mononuclear cell deriving from healthy donors. Moreover, **FB49** was able to block cell cycle in G1 phase and to induce apoptosis as well as autophagy in medulloblastoma HD-MB03 treated cells. In addition, **FB49** demonstrated a synergistic effect when combined with a chemotherapy cocktail of Vincristine, Etoposide, Cisplatin, Cyclophosphamide (VECC). In conclusion we have demonstrated that **FB49** is a new derivative able to bind human BAG3 with high affinity and could be used as BAG3 modulator in cancers correlated with overexpression of this protein.

1. Introduction

The Bcl-2-associated athanogene 3 (BAG3) is a 75 kDa protein member of the BAG family of co-chaperone proteins, which is predominantly localized in the cytoplasm and ubiquitously expressed in all tissues. The expression of this protein is regulated by several endogenous physiological factors such as the heat shock transcription factor 1 (HSF1) upon stress, which could be mediated by cell treatments [1]. BAG3 is ubiquitously expressed in almost all normal tissues, but most prominently in heart and skeletal muscles, while its deregulation has

been reported in many cancers, where it is involved in altered protein homeostasis, cell proliferation and migration, adaptation to stress stimuli, and finally autophagy and resistance to apoptosis. Indeed, the main important role of BAG proteins is to maintain cellular protein homeostasis by i) monitoring the proper folding of nascent proteins, ii) shuttling proteins, or iii) targeting unfolded proteins to degradation by the ubiquitin proteasome system, especially in highly proliferating cells such as neoplastic cells [2]. The co-chaperon activity is allowed by the presence of the common shared domain, namely BAG, through which BAG family members can interact with the ATPase domain of the heat shock protein 70 (Hsp70). Furthermore, the presence of additional protein domains, makes BAG3 a multifaceted protein involved in a multitude of major cell oncogenic pathways such as migration and invasion (epithelial-to-mesenchymal transition), aberrant angiogenesis, cytoskeleton re-organization, apoptosis and selective macroautophagy [3]. Considering the autophagic contribute to drug resistance in different malignancies, the deregulation of BAG3 in cancers correlates with this phenomenon, influencing the invasiveness and the most aggressive behavior [1]. Thereby, upregulation of BAG3 leads to inhibition of tumor cell apoptosis, while the downregulation of BAG3 may be an effective strategy to overcome tumor growth and resistance to treatments. The oncogenic role of BAG3 has been described in both solid cancers - such as melanoma [4], glioblastoma [5], prostate carcinoma [6], colorectal cancer [7] and leukemia [8]. So far, the main strategy adopted to inhibit BAG3 has been the disruption of BAG3-HSP70 interaction with benzothiazole-rhodacyanines allosteric inhibitors such as MKT-077 [9], YM-08 [10], and JG-98 [11] (Fig. 1), but their effective use in therapy is hampered by significant liabilities (e.g., poor solubility, renal toxicity). The lack of the full-length crystallized structure of BAG3 undoubtedly impairs progress on the development of future BAG3 inhibitors. Recently, the 2,4-thiazolidinedione derivative **28** (Fig. 1) has been reported as BAG3 modulator identified through a structure-based virtual screening [12].

In the present work, an extensive structure-activity relationship (SAR) exploration was performed by introducing and/or replacing new chemical groups in compound **28** to improve its binding affinity for BAG3 and antiproliferative activity against different cancer cell lines (Fig. 2).

1.1. Design strategy of new BAG3 modulators based on compound 28

The design of new molecules started from the 3-position of the 2,4-thiazolidinedione core. Substituents of varying steric bulk were introduced to explore the space surrounding the ester moiety and at the α-position to its carbonyl function. The ester function was also replaced with amides and other functional groups such as lactones and ethers.
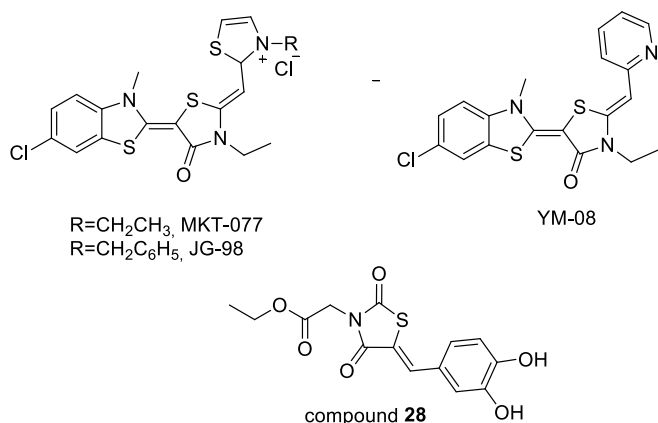

Fig. 1. Chemical structures of BAG3 modulators MKT-077, JG-98, YM-08 and compound **28**.
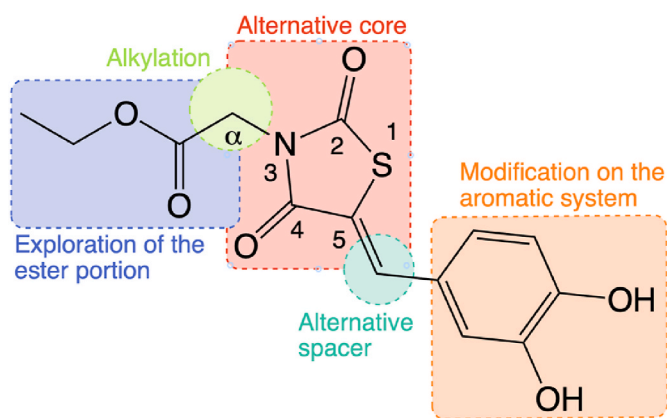

Fig. 2. SAR exploration on compound **28**.

Subsequently, the SAR exploration was focused onto replacement of the catechol ring in order to understand if the two hydroxy groups are necessary to retain the binding affinity to BAG3 (as hydrogen bond donors), or if they can be substituted with other groups. Then, the reduction and the methylation of the double bond at the 5 position of the 2,4-thiazolidinedione was considered to verify if these modifications are tolerated while removing a possible metabolic hot spot. Finally, some explorative core replacements were considered to access a new series of BAG3 modulators, allowing the discovery of a new proprietary class of inhibitors.

1.1.1. SAR exploration on position 3 of the 2,4-thiazolidinedione

The SAR exploration was initially focused on the Left-Hand-Side (LHS) of the reference molecule **28**, corresponding to the 3-position of the 2,4-thiazolidinedione core. Substituents of varying steric bulk were introduced to explore the space surrounding the ester moiety and at the α-position to its carbonyl function (Fig. 3).

The replacement of the ethyl ester with a bulky and flexible substituent like a benzyl ester for derivative **FB19**, can furnish useful information about the extent of hydrophobic interactions needed to increase the binding surface within the protein. On conversely, the introduction of an acidic functionality, like the carboxylic acid in the compound **28**, could reveal if a positive ionic interaction or hydrogen bonding could take place with the surrounding amino acid side chains. The ether analogue **FB23** was design to verify if the carbonyl group of the ester is essential for binding to the protein, in particular to evaluate whether the loss of planarity, due to the removal of the carbonyl function, the increased flexibility, and the removal of a putative hydrogen bond acceptor (HBA) could be tolerated. The five-member lactone ring of compound **FB31** was designed as a cyclized version of the ethyl ester of compound **28**, to restrict the flexible ethyl group in a rigid conformation and to study the space around the carbonyl.

As replacing a labile ester linkage with an amide group is known to impart an improved stability to the molecule, secondary and tertiary amides with dimethylamine, morpholine and methylamine to furnish compounds **FB21**, **FB22** and **FB37**, respectively, were designed to prevent future problems due to this metabolic hot spot. For the morpholino derivative **FB22**, we have also evaluated the replacement of catechol moiety with *N*-phenylmethanesulfonamide and 3′,5′-dicloro-4′-hydroxyphenyl groups in compounds **FB53** and **FB54**, respectively.

As part of the LHS exploration, also the introduction of alkyl groups in the α-position of the carbonyl moiety was considered to obtain information about the space available in this region and if positive hydrophobic interactions can occur with the protein surface. Starting with small substituents, such as methyl and ethyl groups, then expanding to larger substituents, such as the bulkier cyclopropyl and phenyl groups, four analogues were designed corresponding to derivatives **FB20**, **FB28**, **FB24** and **FB25**, respectively.
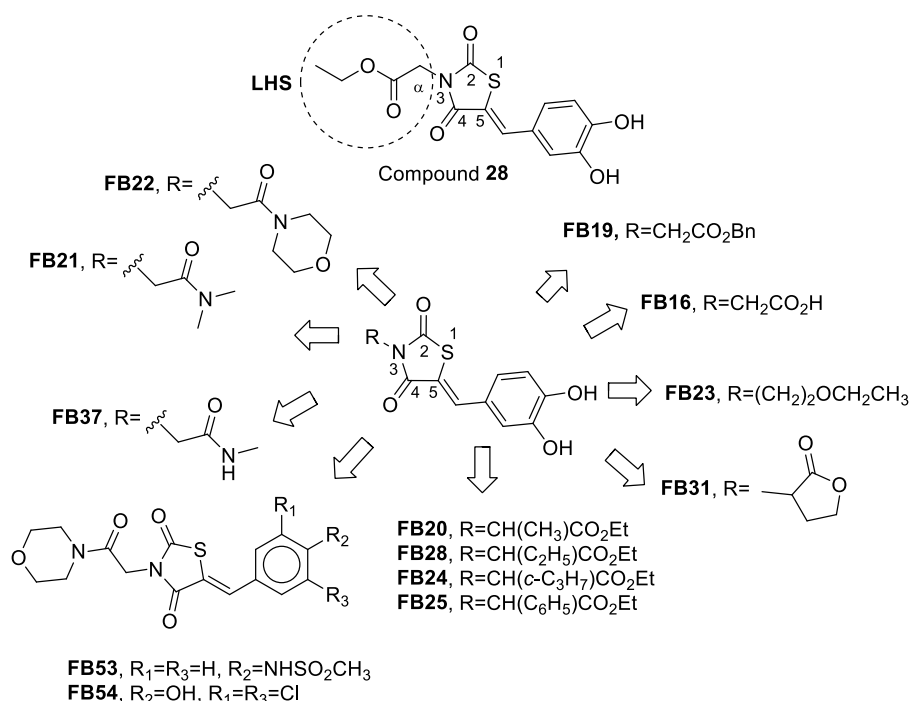
Fig. 3. Designed derivatives for the SAR exploration on the LHS of the thiazolidinedione series.

Further amide analogues were designed maintaining the methyl group in the α-position of the carbonyl group (see compounds **FB32-33** and **FB35-36**, Fig. 4). The first amide, **FB32** was designed to verify if the morpholine and the α methyl group could have a synergistic effect on the binding affinity. The piperidine derivative **FB33** was exploited to verify if the oxygen of **FB32** can effectively make a positive interaction with the protein. Some variations on the morpholine ring were also considered, like the spiro derivatives **FB35** and **FB36**. Finally, the catechol ring attachment point of compound **FB32** was switched, affording the 2,3-dihydroxyphenyl derivative **FB49,** or replaced by a 4′-phenylmorpholine or 4′-phenylpyrrolidine to furnish compounds **FB48** and **FB50**, respectively.

1.1.2. SAR exploration on position 5 of the 2,4-thiazolidinedione

The SAR exploration on the right-hand-side (RHS) of the 2,4-thiazolidinedione series (Fig. 5), was initially focused on the replacement of the catechol ring with more suitable moieties to avoid formation of semiquinone radicals and ortho-benzoquinones as possible side reactions. In the first set of derivatives described, the left portion of

compound **28** was fixed, so the SAR changes only concern the catechol ring (Fig. 5). To verify if the two-hydroxy groups were both essential to retain the BAG3 binding affinity, the two phenolic derivatives, **FB10** and **FB14**, were designed. In either compound, an acidic phenolic hydroxyl group is still present and can act as HBD/HBA and can possibly be involved in ionic interactions with the protein. The 3-fluorophenol derivative **FB8** was designed to evaluate the effect of an electron withdrawing substituent (fluorine) instead of an electron releasing group (hydroxyl). The *meta*-fluorine can also act as HBA and mask the *para*-–hydroxyl with an intramolecular hydrogen bond. The effect of an electron withdrawing group (EWG), such as a fluorine or chlorine, was also examined in the *para*-fluorine derivative **FB7** and in the 3,4-dichloro derivative **FB18**. The di-methoxy derivative **FB9** and its cyclized version **FB13** were designed to further evaluate if the two-hydroxy groups present in the catechol ring are involved in some specific HBD interactions with the protein. Both the compounds possess two HBA groups, such as the ortho-methoxy pyridine derivative **FB11**.

As reported in Fig. 6, a new set of analogues were designed with a SAR exploration on the LHS fixing as the racemic ethyl propanoate at the
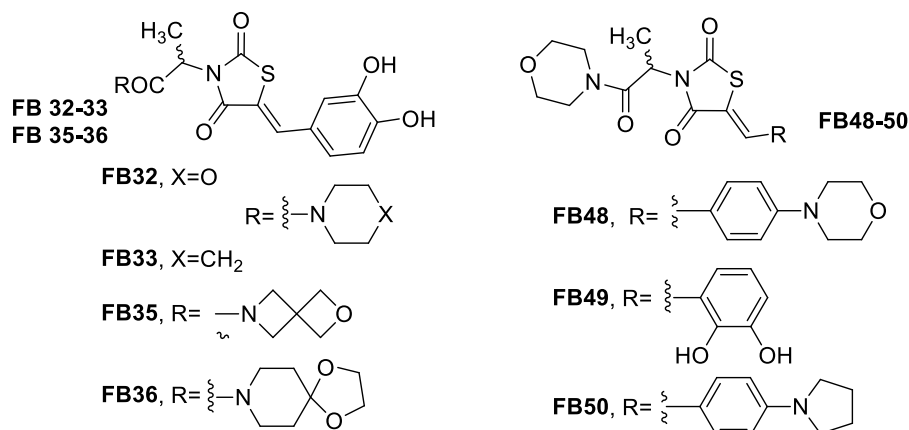

Fig. 4. Structure of compounds **FB32-33**, **FB35-36** and **FB48-50**.
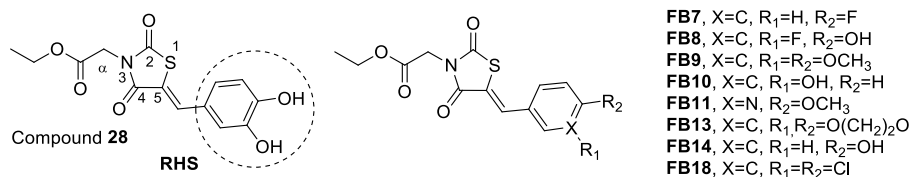
FB7, X=C, R$_1$=H, R$_2$=F
FB8, X=C, R$_1$=F, R$_2$=OH
FB9, X=C, R$_1$=R$_2$=OCH$_3$
FB10, X=C, R$_1$=OH, R$_2$=H
FB11, X=N, R$_2$=OCH$_3$
FB13, X=C, R$_1$,R$_2$=O(CH$_2$)$_2$O
FB14, X=C, R$_1$=H, R$_2$=OH
FB18, X=C, R$_1$=R$_2$=Cl

Fig. 5. The RHS of the thiazolidinedione series with ethyl acetate moiety at the N-3 position of 2,4-thiazolidinedione core.

FB41, R=3'-Cl, 4'-OH-C$_6$H$_3$
FB46, R=3'-OH, 4'-F-C$_6$H$_3$
FB47, R=3',5'-(OH)$_2$, 4'-F-C$_6$H$_2$
FB43, R=3'-OH, 4'-Cl-C$_6$H$_3$
FB45, R=3',5'-Cl$_2$, 4'-OH-C$_6$H$_2$
FB44, R=4'-NHSO$_2$CH$_3$-C$_6$H$_4$

R= **FB38**

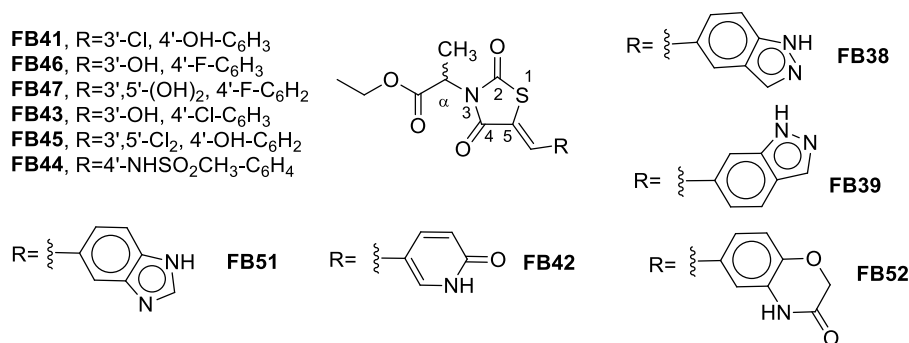R= **FB39**

R= **FB51**

R= **FB42**

R= **FB52**

Fig. 6. The RHS of the thiazolidinedione series with racemic ethyl propanoate at the N-3 position of 2,4-thiazolidinedione core.

N-3 position of 2,4-thiazolidinedione.

Further derivatives which bear EWGs, such as fluorine and chlorine, on both *meta-* and *para*-positions where designed. In compound **FB46** the fluorine and the hydroxy group were inverted from those of compound **FB8**, to verify if this reversed pattern of HBD/HBA is well tolerated. As the fluorine is a small substituent, whose dimension is comparable to a hydrogen atom, further analogues with larger groups, such as chlorine, were considered. In compound **FB41** the *meta*-hydroxy group of the catechol is replaced with a chlorine, while in compound **FB43** the *para*-hydroxy moiety has been replaced with a chlorine. In the 3′5′-difluoro and 3′,5′-dichloro phenol

derivatives, **FB47** and **FB45**, respectively, a second EWG near the *para*-hydroxy group was introduced to increase the acidity of the latter.

Other mild acidic groups and HBD/HBA moieties were introduced to replace the catechol, such as the methylsulphonamide **FB44** and the hydroxy pyridine **FB42**. Compound **FB52** is a derivative of **FB13** where a HBA was replaced with a HBD by substitution with an amide group. The benzimidazole **FB51** and the two indazole derivatives **FB38** and **FB39** are some examples of catechol bioisosteres replacement.

1.1.3. SAR exploration on the linker between the 5-position of the 2,4-thiazolidinedione ring and catechol moiety

To complete the SAR exploration, the double bond of compound **28** was reduced by hydrogenation, affording compound **FB15** (Fig. 7).

The transformation from a sp^2 carbon to a sp^3 leads to an increase in

the degrees of freedom of the system, which switches from a rigid double bond in the *Z* configuration to a rotatable single bond. Another modification investigated is the introduction of a methyl group on the double bond to give compound **FB17**.

1.1.4. Thiazolidinedione "core" replacement and exploratory derivatives

As part of the SAR exploration, the 2,4-thiazolidinedione core was replaced with alternative heterocycles, such as hydantoins, thiazole and quinolone cores with the aim of obtaining a new series of compounds. The hydantoin core presents a nitrogen in place of the sulphur atom of the thiazolidinedione core. Two derivatives were designed, the first one with the free NH (**FB29**), and the second one its *N*-methylated analogue **FB30** obtained as a 1:2 mixture of *Z/E* geometric isomers.

The thiazole derivative **FB40** (Fig. 8) was designed as an aromatic replacement of the 2,4-thiazolidinedione core of compound **28**. The double bond in position 5 was replaced by the oxygen of a phenoxy group and the catechol ring was replaced with a *para*-hydroxyphenyl group to reduce the electronic density of the aromatic ring. As shown in the models reported in Supplementary Fig. S1, the calculated minimum energy conformations for thiazole derivative **FB40** showed a good overlapping with compound **28**.
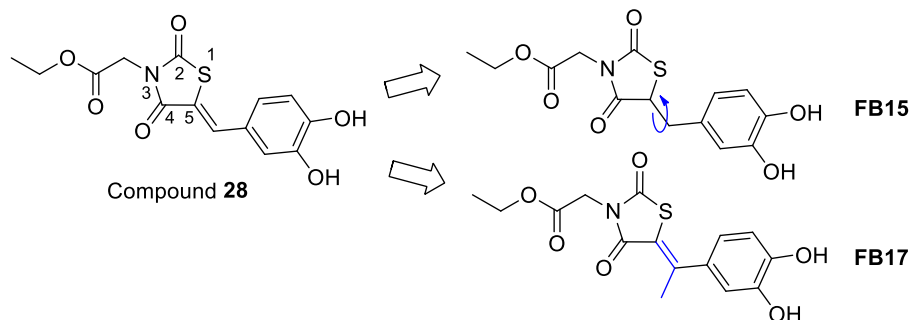

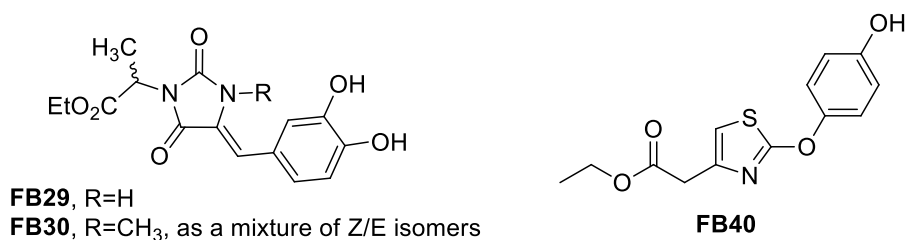**Fig. 7.** Structure of synthesized compounds **FB15** and **FB17**.

Fig. 8. Structures of hydantoin (**FB29** and **FB30**), and thiazole (**FB40**) derivatives.

2. Results and discussions

2.1. Chemistry

Compounds **FB7-11**, **FB13-14** and **FB18** were prepared by an efficient, previously described convergent approach reported in the Scheme 1, via a Knoevenagel condensation reaction of different aromatic aldehydes with ethyl 2-(2,4-dioxothiazolidin-3-yl)acetate **1** in the presence of a catalytic amount of piperidinium acetate in refluxing toluene as solvent for 18h. The common intermediate **1** was prepared by a SN$_2$ reaction of thiazolidine-2,4-dione with ethyl bromoacetate in the presence of K$_2$CO$_3$ and CH$_3$CN. Following the same synthetic approach, compound **FB17** was synthesized by a Knoevenagel condensation between the commercially available 1-(3,4-dihydroxyphenyl) ethanone with *N*-substituted-2,4-thiazolidinedione **1** in refluxing toluene for 48h. *N*-substituted-2,4-thiazolidinedione derivatives **2-4** with different alkyl chains were synthesized in good yields by the *N*-3 alkylation of

thiazolidine-2,4-dione with the appropriate alkyl bromide [2-bromoacetic acid (phenylmethyl) ester, 1-bromo-2-ethoxyethane and 3-bromo-2-oxolanone, respectively)] using K$_2$CO$_3$ as base in CH$_3$CN. The subsequent Knoevenagel condensation with 3,4-dihydroxybenzaldehyde afforded the corresponding final compounds **FB19**, **FB23** and **FB31**. Compounds **FB15**, characterized by the presence of a more flexible methyl linker at the 5-position of 2,4-thiazolidinedione scaffold, was prepared starting from compound **28**, by catalytic hydrogenation of the conjugated double bond over 10% palladium on charcoal (Pd/C). The hydrolysis of the ester group of compound **28** with a mixture of 37% HCl in water and acetic acid furnished the desired 2,4-thiazolidinedione *N*-acetic acid derivative **FB16**.

The preparation of *N*-acetamido-(Z)-5-arylidene-2,4-thiazolidinedione derivatives **FB21-22** and **FB53-54** is outlined in the Scheme 2. The *N*-substituted 2,4-thiazolidinediones **5** and **6** were synthesized in good yields by coupling the 2,4-thiazolidinedione with the required 2-chloro-1-(morpholin-4-yl)ethan-1-one or 2-chloro-N,N-dimethylacetamide,
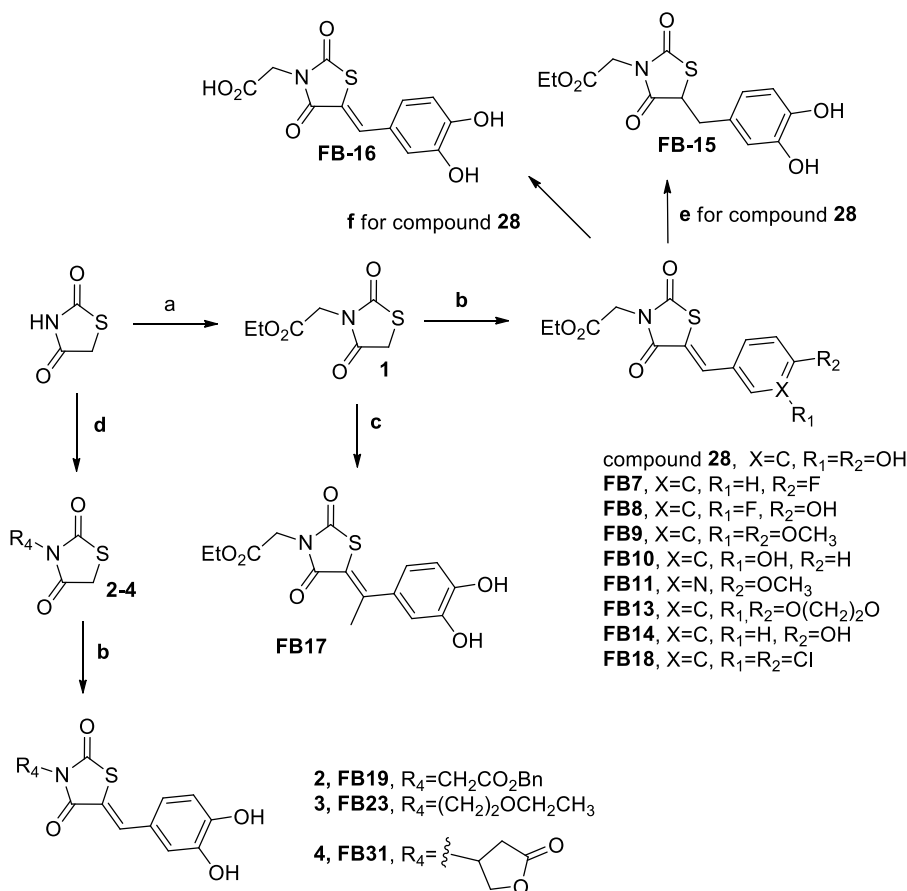
Scheme 1. Reagents: **a**: BrCH$_2$CO$_2$Et, K$_2$CO$_3$, CH$_3$CN, rt, 18h; **b**: appropriate aromatic aldehyde, pyridine acetate (cat.), toluene, rx, 18h; **c**: 1-(3,4-dihydroxyphenyl) ethanone, pyridine acetate (cat.), toluene, rx, 72 h; **d**: appropriate bromoalkyl derivative, K$_2$CO$_3$, CH$_3$CN, rt, 18h; **e**: Pd/C 10% wet, H$_2$, EtOH, rt, 18 h; **f**: 37% HCl in water-CH$_3$COOH, 120 °C, 2h.
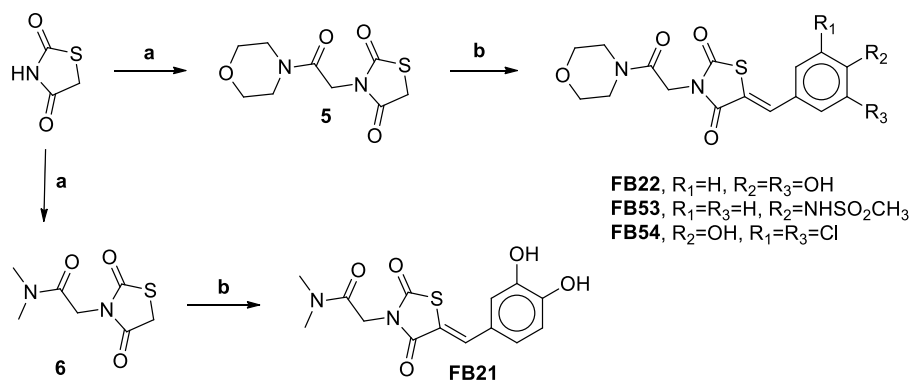
Scheme 2. Reagents: **a**: 2-chloro-1-(morpholin-4-yl)ethan-1-one or 2-chloro-N,N-dimethylacetamide, K$_2$CO$_3$, CH$_3$CN/DMF, 75 °C, 2h; **b**: appropriate aromatic aldehyde, pyridine acetate (cat.), toluene, rx, 18h.

respectively, in a mixture of CH$_3$CN/DMF at 75 °C for 2 h in the presence of K$_2$CO$_3$ as base. The subsequent Knoevenagel condensation with different aromatic aldehydes furnished the (*Z*)-5-arylidene-2,4-thiazolidinediones **FB21-22** and **FB53-54.**

Compounds **FB20**, **FB24-25** and **FB28** characterized by a common 3′,4′-dihydroxybenzylidene moiety and different substituents in the α-position to the carbonyl of the acetate moiety at the 5- and 3-positions, respectively of the thiazolidinedione ring, were prepared following the procedure reported in the Scheme 3. The *N*-substituted 2,4-thiazolidinedione derivatives **7-10** were synthesized by the *N*-alkylation of 2,4-thiazolidinedione with the appropriate ethyl α-substituted bromoacetate using NaH as base in DMF. The subsequent Knoevenagel condensation with 3,4-dihydroxy benzaldehyde furnished in good yields the final compounds **FB20**, **FB24-25** and **FB28**.

Derivatives **FB38-39**, **FB41-47** and **FB51-52** characterized by a common ethyl 2-(2,4-dioxothiazolidin-3-yl)propanoate system and different arylidene at its 5-position were synthesized according to a short synthetic pathway reported in Scheme 4, by the Knoevenagel condensation of previously synthesized compound **7** (see Scheme 3) with suitable aromatic aldehydes.

Compounds **FB32-33** and **FB35-37** were synthesized as shown in Scheme 5. After protection of the phenolic groups of the catechol moiety of compound **FB20** to yield the bis-*tert*-butyldimethylsilyl (TBDMS) analogue **11**, the acid hydrolysis of ethyl ester was accomplished by the concomitant removal of both TBDMS-protecting groups, to afford compound **12**. Final derivatives **FB32-33** and **FB35-37** were obtained by an amide coupling of different amines with the derivative **12**, using O-(7-azabenzotriazol-1-yl)-N,N,N′,N′tetramethyluronium hexafluorophosphate (HATU) as coupling agent and triethylamine (TEA) as base in anhydrous DMF at room temperature. All the final amides were obtained as racemic mixtures due to the presence of a chiral center.

The preparation of compounds **FB48-50** involved a straightforward reaction sequence in three steps (Scheme 6). Staring from the previously

reported compound **7** (see Scheme 4), it was hydrolysed under acid catalysed conditions to furnish the corresponding carboxylic derivative **13** and then transformed in the morpholino amide **14** by using morpholine as amine and HATU and TEA as coupling reagents. Finally, this latter compound was employed as key intermediate for the preparation of final compounds **FB48-50** under Knoevenagel condensation with the appropriate benzaldehydes.

For the preparation of hydantoin derivatives **FB29** and **FB30**, the following synthetic Scheme 7 was employed. The first step is a S$_N$2 reaction on the hydantoin core with ethyl 2-bromopropanoate in the presence of potassium carbonate. The reaction was selective for the succinimide-like nitrogen affording the common intermediate **15** which was then condensed with the 3,4-dihydroxybenzaldehyde in the Knoevenagel conditions, to give **FB29**. Hydantoin was also methylated, in the presence of potassium carbonate and iodomethane, affording intermediate **16**, which was then condensed with 3,4-dihydroxybenzaldehyde, affording compound **FB30** as a 1:2 mixture of Z/E geometric isomers.

Compound **FB40** was synthesized in two steps starting from commercially available ethyl 2-aminothiazole-4-acetate (Scheme 8). The first step is the Sandmeyer bromination of the aminothiazole **17**, affording intermediate **18**, which then reacts with 1,4-dihydroxybenzene in a nucleophilic aromatic substitution (SNAr) reaction affording the desired compound **FB40**.

2.2. Assessment of BAG3 binding capacity of designed compounds

2.2.1. BAG3 protein expression and purification

To assess the affinity of putative BAG3 inhibitors, human BAG3 sequence was efficiently cloned into pcDNA3.1-C-His vector, and then transiently transfected into human embryonic kidney HEK-293T cells to obtain the overexpression of C *terminus* His-tagged BAG3 protein (BAG3-His). BAG3-His protein was then collected by cell lysis and the soluble fraction was subjected first to Immobilized Metal Affinity

7, **FB20**, R= (R,S)-CH$_3$
8, **FB28**, R= (R,S)-C$_2$H$_5$
9, **FB24**, R= (R,S)-C$_3$H$_5$
10, **FB25**, R= (R,S)-C$_6$H$_5$
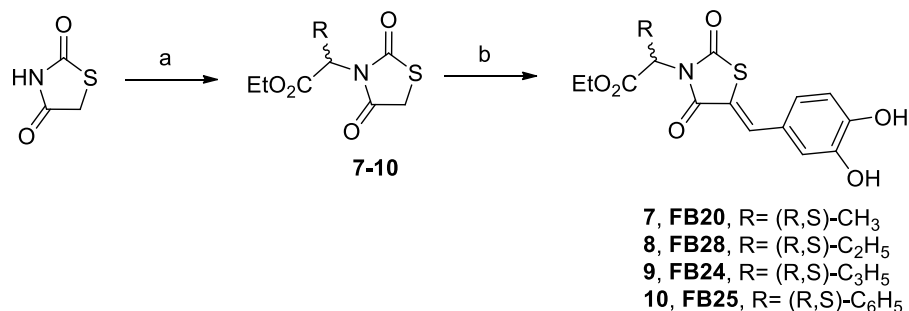
Scheme 3. Reagents: **a**: 2-bromopropanoic acid ethyl ester, ethyl 2-bromobutanoate, 2-bromo-2-(cyclopropyl) acetate, 2-bromo-2-phenylacetic acid ethyl ester (for the preparation of compounds **7-10**, respectively), NaH, DMF, rt, 18 h; **b**: 3,4-dihydroxybenzaldehyde, pyridine acetate (cat.), toluene, rx, 18h.
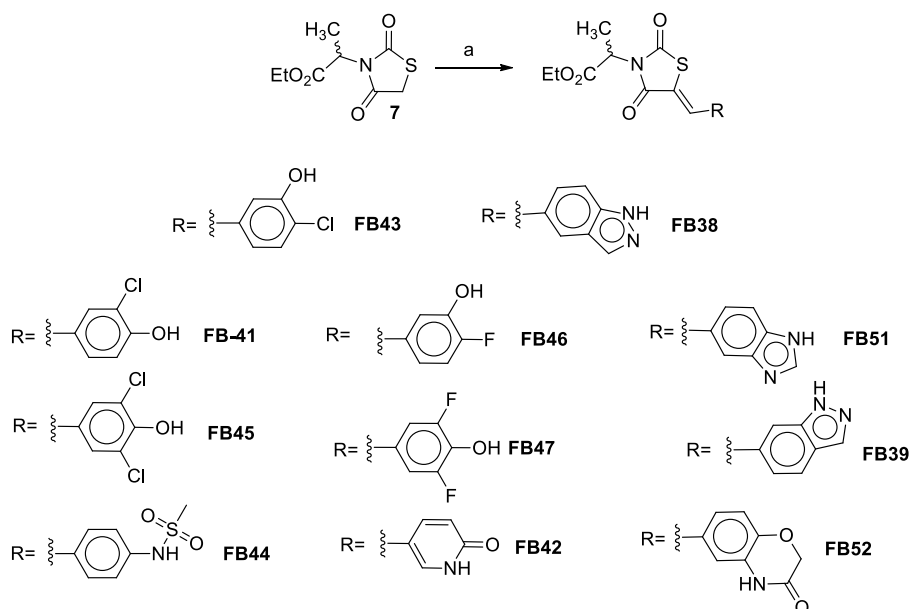
Scheme 4. Reagents: **a**: appropriate aromatic aldehyde, pyridine acetate (cat.), toluene, rx, 18h.
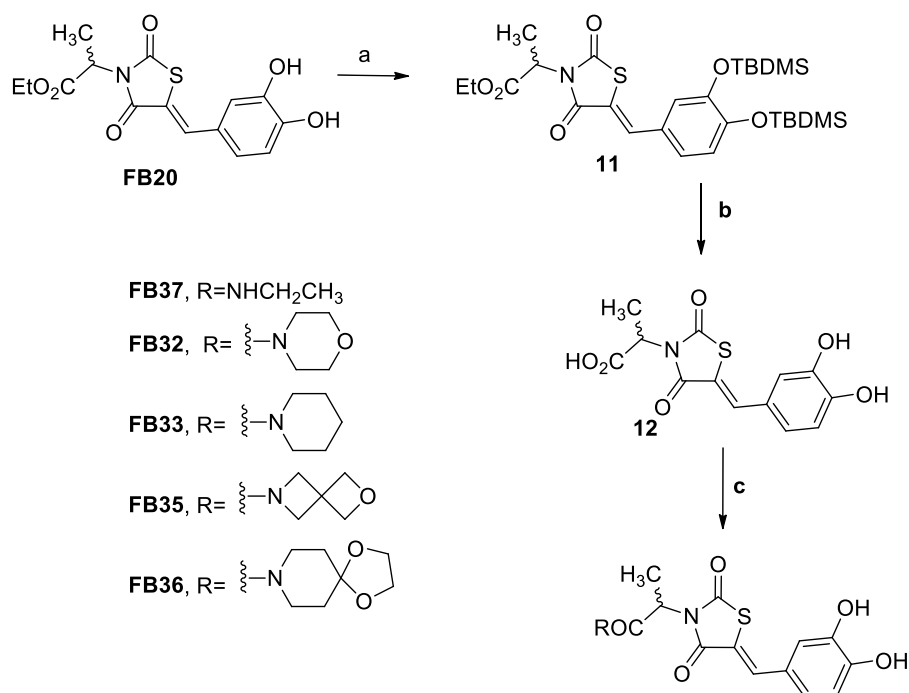
Scheme 5. Reagents: **a**: TBDMSCl, DMAP (cat.), DMF, rt, 18h; **b**: 37% HCl in water-CH$_3$COOH, 100 °C, 2h; **c**: DIPEA, HATU, appropriate amine, DMF, rt, 4h.

Chromatography (IMAC) and then to Size Esclusion Chromatography (SEC) to ensure high final purity (see Material & Methods for detailed experimental procedures). By Tandem Mass Spectrometry (MS-MS), 71 BAG3 unique peptides were identified, with 97.7% of sequence coverage.

2.2.2. Assessment of BAG3 binding capacity by Surface Plasmon Resonance (SPR)

In order to shortlist the synthetized compounds, putative BAG3 inhibitors were preliminarily screened for their BAG3-binding capacity by Surface Plasmon Resonance (SPR) technique at a single concentration (50 μM) (Fig. 9). As expected, very small chemical compounds give rise

to very low SPR signals (few Resonance Units, RU), however it was possible to discriminate between positive and negative BAG3 binders. The BAG3 binding capacity of compound **28** was tested as reference (Supplementary Fig. S2A). Of note, the injection of compound **28** causes a relevant increase of RU on both BAG3-immobilized and control-surface sensorchips. Similar results were obtained for all the other compounds tested (data not shown). However, the high aspecific SPR signal did not hamper the determination of a specific binding when the sensorgram is blank-subtracted.

As shown in Fig. 9, out of the 44 small molecules tested (excluding compound **28**), 26 compounds resulted completely unable to bind BAG3, while other 10 (**FB31, FB36, FB38, FB39, FB40, FB43, F48,**
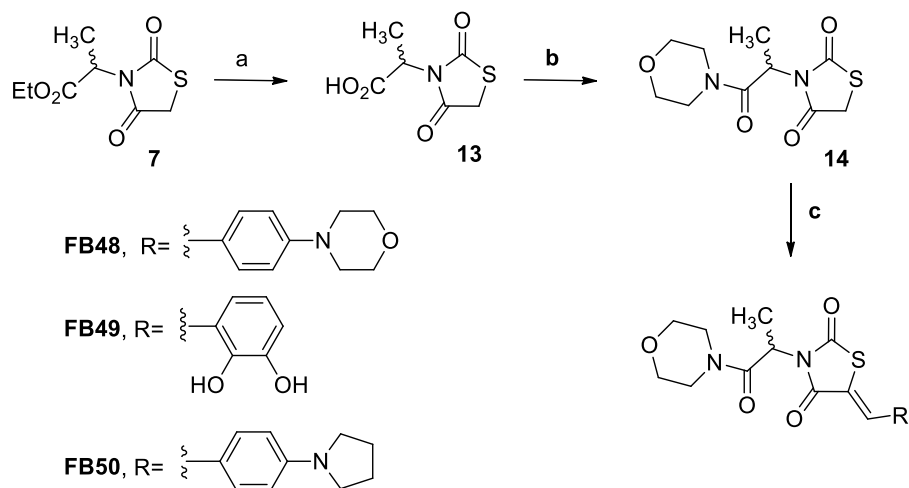
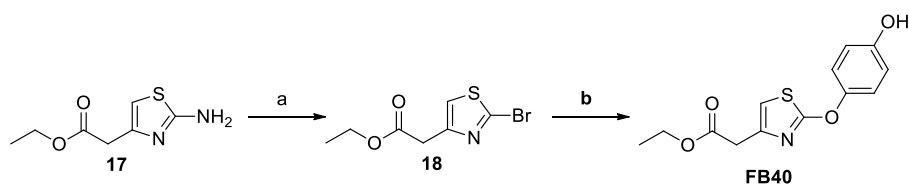**Scheme 6.** Reagents: **a**: 37% HCl in water-CH$_3$COOH, 120 °C, 1h; **b**: DIPEA, HATU, morpholine, DMF, rt, 4h; **c**: appropriate aromatic aldehyde, pyridine acetate (cat.), toluene, rx, 18h.
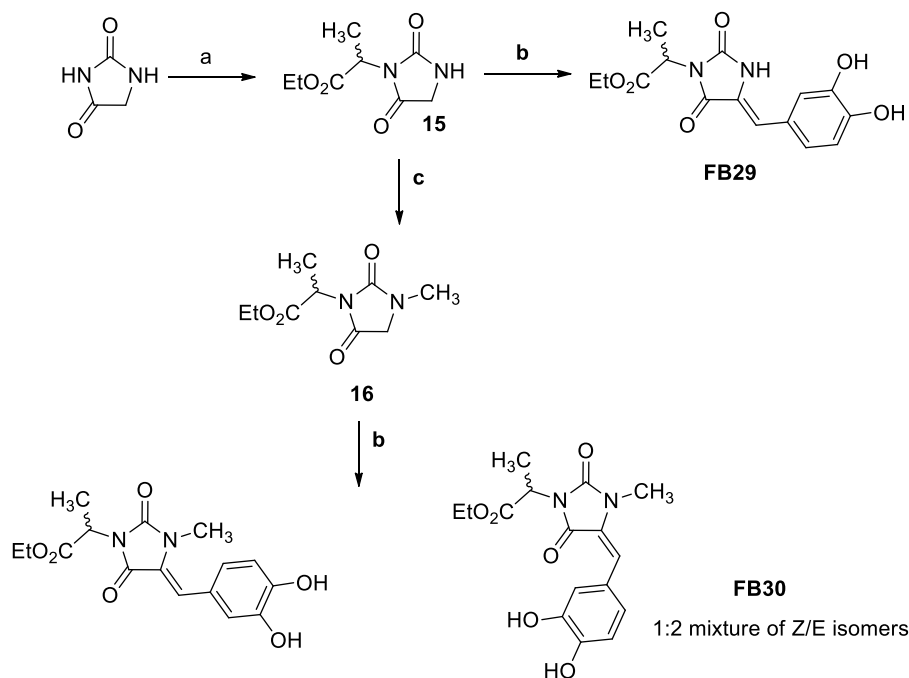
Scheme 7. Reagents: **a**: BrCH(CH$_3$)CO$_2$Et, K$_2$CO$_3$,THF, 85 °C, 18h; **b**: 3,4-dihydroxybenzaldehyde, pyridine acetate (cat.), toluene, rx, 18h; **c**: CH$_3$I, K$_2$CO$_3$, DMF, 25 °C, 18 h.

Scheme 8. Reagents: **a**: *t*-butyl nitrite, copper (II) bromide, MeCN, 25 °C, 18 h; **b**: 1,4-dihydroxybenzene, K$_2$CO$_3$, DMF, 140 °C, 18 h.

FB45, FB48 and FB50) showed a very limited binding capacity (<5.0 RU) and were no further considered. Conversely, **FB20, FB22, FB24, FB25, FB28, FB33, FB49, FB51**, as well as reference compound **28**, showed high binding capacity (>5.0 RU) (Fig. 9), and were then subjected to further dose-dependent binding analysis to calculate the affinity of their interaction with BAG3.

A dose-dependent interaction with surface-immobilized BAG3 was observed for all tested compounds, but signal saturation was observed only for **FB49**. An explicative blank-subtracted sensorgram derived from a single cycle analysis of derivative **FB49** injected at increasing
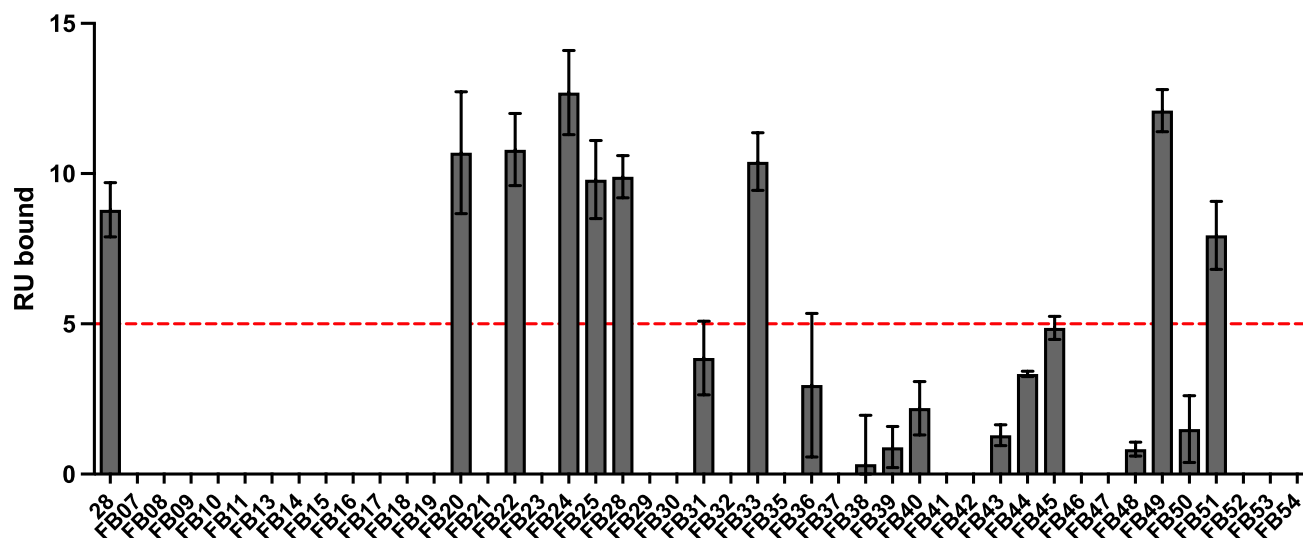
Fig. 9. Assessment of the BAG3-binding capacity of the synthetized compounds. The indicated compounds were injected onto the BAG3-containing biosensor at a single dose (50 μM) and the amount of bound RU was measured at equilibrium. The data reported represent the mean values ± Standard Error Mean (SEM) of 3–10 repeated analyses for each compound. The red dashed line indicates the cut-off under which the compounds were not taken in further consideration.

concentrations on the BAG3-containing biosensor with the related steady state analysis are shown in Supplementary Figs. S1B–C. All the other compounds bind BAG3 in a dose-dependent but not saturable manner (data not shown). Compared to the reference compound **28**, the introduction of a substituent in the α-position of the ester group (**FB20**, **FB24**, **FB33** and **FB49**) is well tolerated (Table 1). Instead, compound **FB25,** which presents a bulky phenyl group in that position, showed a detrimental effect on the binding affinity for BAG3. The replacement of the catechol ring with its benzoimidazole bioisoster **FB51** and its 2,3-dihydroxybenzyl isomer **FB49** is well tolerated. Moreover, the replacement of the ester group with the amides **FB22**, **FB33** and **FB49** had a positive impact on the binding affinity (Table 1). Finally, in agreement with its capacity to reach a saturation binding, derivative **FB49** displayed the highest BAG3 binding affinity, being endowed with a K_d equal to 45 ± 6 μM, that is statistically lower than those of all the other compounds tested (Table 1). Collectively, the SPR data demonstrated that the best compounds reported in this study bind to BAG3 to a similar extent (**FB20**, **FB24**, **FB25**, **FB51**), or even stronger (**FB22**, **FB33** and **FB49**) than the previously reported compound **28**.

Worth of note is the significant discrepancy present between the Kd value measured for parental compound **28** in our experimental conditions (233 ± 58 μM) and that previously reported in the nanomolar range [12]. This could be likely due to different post-translational

modifications (i.e. glycosylation) of the different BAG3 protein preparations used in the different works. Indeed, here we have used a glycosylated BAG3 protein produced in mammalian cells instead of the non-glycosylated BAG3 protein from *E. coli* used previously [12]. Relevant to this point, it has been reported that the glycan shield can greatly impact the accessibility of the underlying protein surface [13], weakening or even hampering the binding of specific antibodies [14] and drugs [15].

*2.2.3. Biophysical investigation of FB49 binding to BAG3*

To better characterize the binding between BAG3 and the lead compound **FB49**, WaterLOGSY and Saturation Transferred Difference (STD) NMR experiments were carried out both in the presence and in the absence of BAG3. Compound **28** was also tested for comparison. In the waterLOGSY experiments, the signals of **FB49** and compound **28** in the presence of the protein assume the same negative sign as BAG3, indicating that the ligand acquired the protein magnetization as intermolecular Nuclear Overhauser Effect (NOE) due to the binding of the ligands to BAG3 (Supplementary Fig. S3). To understand which part of the molecule is more involved in the binding the epitope mapping was obtained by the STD experiments. First, these experiments inevitably proved that **FB49** binds to BAG3 (Fig. 10A). In fact, as shown in Fig. 10A, in the STD spectra in the presence of BAG3, the signals of the ligand appear indicating that in the on-resonance experiments, the molecules acquired the saturated protein magnetization via intermolecular spin-diffusion because of the formation of the protein-ligand complex. It should be noticed that the methyl groups of **FB49** at 1.5 and 1.2 ppm also appear in the STD spectra in the absence of the protein because it is partially saturated by the pulse train at 0.4 ppm since it resonates near this frequency (Fig. 10A). However, the intensity of their signals in the STD spectra in the presence of BAG3 is higher, indicating that the observed STD effect is also due to the protein magnetization transfer in the bound state between BAG3 and the ligand The analysis of STD NMR spectra allowed us to determine a complete ligands-binding epitope. Notably, the most substantiable STD effects (STD factor (%) in the range of 87–100%) are observed for the protons of the catechol moiety of **FB49** (Fig. 10B): the magnetization transfer from the protein to this portion is more efficient, proving the proximity of the catechol moiety to BAG3 upon binding. In contrast, lower STD effects (STD factor (%) in the range of 22–65%) can be noticed for the protons of the LHS, evincing that this

Table 1
K_d values of the binding to immobilized-BAG3 of the selected compounds.

Compound	K_d (μM) mean ± SEM	Number of measurements	Student T-test (**FB49** *vs* other compounds)
28	233 ± 58	(6)	p = 0.0075
FB20	286 ± 86	(4)	p = 0.078
FB22	152 ± 25	(13)	p = 0.007
FB24	204 ± 32	(8)	p = 0.003
FB25	366 ± 93	(5)	p = 0.0037
FB28	n.d	(3)	n.d
FB33	150 ± 39	(3)	p = 0.008
FB49	45 ± 6	(6)	–
FB51	198 ± 82	(3)	p = 0.03

The data are presented as mean Kd value ± Standard Error Mean (SEM), n.d, not determined. In the right column, the results of Student T-test are reported that demonstrate that the Kd value for **FB49** is statistically lower than those of all the other compounds.
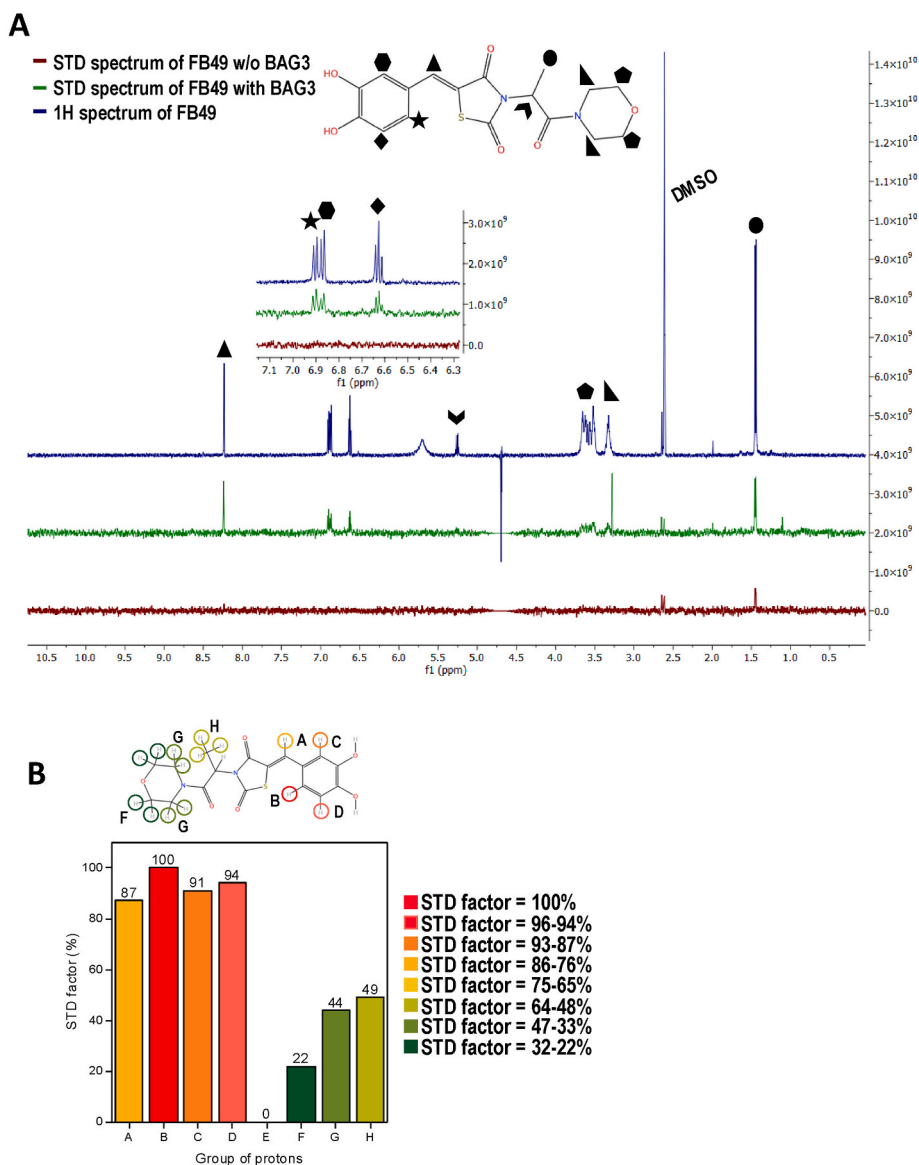
Fig. 10. Comparison between the ¹H spectrum and Saturation Transferred Difference (STD) spectra obtained by nuclear magnetic resonance (NMR) spectroscopy of lead compound **FB49** in the presence (5 μM) (1:25 protein:ligand molar ratio) and in the absence of BAG3 protein (**A**) and its proposed binding epitope mapping (**B**). The strongest STD signal in the spectrum was set to the value of 100% and used as reference to calculate relative STD effects accordingly.

portion of the molecule is less in contact with the protein surface or more solvent exposed (Fig. 10B). A slightly different binding epitope was determined for compound **28** (Supplementary Fig. S4B): high STD factors (STD factor in the range of 68–96%) are experienced by the catechol moiety as well as by the methyl group (STD factor = 100%) of the RHS. This experimental evidence support that the chemical modifications introduced in the RHS of compound **28** (resulting in the generation of **FB49** play a pivotal role in enhancing the binding affinity leading to a 5-fold increase in the binding affinity (**FB49**: Kd = 45 μM; compound **28**: Kd = 233 μM).

2.3. In vitro antiproliferative activity of BAG3 inhibitors

To assess the cytotoxicity of putative BAG3 inhibitors, cell viability resazurin assay was performed in three different tumoral cell lines (Table 2). All compounds presented GI$_{50}$ in the micromolar range, in accordance to previously reported BAG3 inhibitors [12,16]. The GI$_{50}$ values of the lead BAG3 inhibitor identified by SPR and NMR analysis **FB49** were 11.2 ± 0.03 μM in HD-MB03 medulloblastoma cells, 6.7 ±

0.15 μM in RS4; 11 leukemia cells, and 28.0 ± 0.52 in A549 lung carcinoma cells, while the GI$_{50}$ values of the reference compound **28** were 14.82 ± 0.03 μM, 6.39 ± 0.72 μM, and 42.49 ± 1.29 μM, respectively. Accordingly, all positive BAG3 binders **FB20, FB22, FB24, FB25, FB28,** and **FB33** displayed a similar cytotoxic profile on the three tested cell lines, except for compound **FB51** that presented poor cytotoxic properties compared to other BAG3-binders. Oppositely, non-binder compounds, such as **FB13,** were not cytotoxic in all tested cancer cell lines (GI$_{50}$ > 100 μM), thus strengthening the specificity of selected BAG3 inhibitors.

Notably, all BAG3-binders showed a comparable and higher cytotoxicity on the RS4; 11 leukemia cells with GI$_{50}$ < 10 μM (except **FB22**). Indeed, several studies have reported that leukemia cells are highly BAG3-dependent and thus more sensitive to BAG3 inhibitors [17,18]. A549 lung carcinoma cells, on the contrary, were generally more resistant to BAG3 inhibitors, possibly suggesting that pharmacological BAG3 inhibition may not be effective *per se* for this pathology.

Finally, to exclude a cytotoxic potential of the identified lead compound, **FB49** was evaluated *in vitro* against peripheral blood

Table 2
In vitro inhibitory effects of synthetized compounds.

Compound	GI$_{50}$ (μM)		
	HD-MB03	RS4;11	A549
28	14.8 ± 0.03	6.4 ± 0.72	42.5 ± 1.29
FB07	34.7 ± 0.26	>100	>100
FB08	58.3 ± 0.13	>100	>100
FB09	45.0 ± 0.07	>100	>100
FB10	40.7 ± 0.16	55.00 ± 2.1	>100
FB11	41.1 ± 1.10	>100	>100
FB13	>100	>100	>100
FB14	29.5 ± 0.33	>100	>100
FB15	49.00 ± 0.20	27.6 ± 0.82	>100
FB16	>100	>100	>100
FB17	6.4 ± 0.38	7.25 ± 0.01	44.2 ± 0.92
FB18	>100	>100	>100
FB19	n.d.	n.d.	n.d.
FB20	25.3 ± 0.04	5.1 ± 0.39	32.5 ± 1.57
FB21	36.39 ± 0.12	25.63 ± 2.22	48.3 ± 0.90
FB22	33.1 ± 1.13	24.8 ± 0.67	49.4 ± 3.23
FB23	17.8 ± 0.11	6.1 ± 0.02	34.3 ± 2.62
FB24	15.48 ± 0.09	6.83 ± 0.09	28.1 ± 0.34
FB25	17.6 ± 0.12	9.53 ± 0.01	33.3 ± 0.74
FB28	11.7 ± 0.62	5.13 ± 0.55	29.31 ± 0.23
FB29	16.9 ± 0.02	11.9 ± 0.35	54.1 ± 3.65
FB30	53.3 ± 1.73	17.8 ± 0.77	52.6 ± 3.65
FB31	20.7 ± 0.74	18.1 ± 0.62	50.2 ± 1.42
FB32	48.73 ± 1.62	14.09 ± 0.12	47.93 ± 0.33
FB33	13.9 ± 0.25	8.6 ± 0.09	29.4 ± 0.68
FB35	>100	>100	>100
FB36	31.4 ± 0.46	13.4 ± 0.55	44.1 ± 3.04
FB37	53.1 ± 1.29	24.8 ± 0.20	70.9 ± 1.66
FB38	28.3 ± 0.37	50.5 ± 1.99	68.0 ± 2.83
FB39	26.3 ± 1.23	17.8 ± 0.02	57.5 ± 1.67
FB40	>100	>100	>100
FB41	265 ± 0.72	38.1 ± 0.81	49.4 ± 0.99
FB42	>100	>100	>100
FB43	5.26 ± 0.21	60.56 ± 0.54	>100
FB44	17.63 ± 0.22	50.27 ± 0.78	>100
FB45	45.6 ± 1.42	47.24 ± 0.34	72.5 ± 1.15
FB46	>100	>100	>100
FB47	>100	>100	>100
FB48	>100	>100	>100
FB49	11.2 ± 0.03	6.7 ± 0.15	28.0 ± 0.52
FB50	7.4 ± 1.36	5.2 ± 0.88	69.0 ± 1.23
FB51	42.5 ± 1.65	>100	>100
FB52	40.7 ± 0.68	28.1 ± 0.59	>100
FB53	47.4 ± 1.88	12.4 ± 0.66	47.7 ± 2.23
FB54	>100	>100	>100

GI$_{50}$ = compound concentration (μM) required to inhibit cell proliferation by 50%, in comparison with cells treated with the maximum amount of DMSO (0.25%) and considered as 100% viability. Data are expressed as the mean ± SEM from the dose-response curves of at least three independent experiments. n. d. = not determined.

mononuclear cells (PBMC) collected from healthy donors. **FB49** showed GI$_{50}$ > 100 μM) both in quiescent and hytohaemagglutinin-activated (PHA) lymphocytes (Table 3). These results indicated that this

Table 3
Effects of compound **FB49** in non-tumoral cells.

Compound	GI$_{50}$ (μM)	
	PBMC$_{resting}^{a}$	PBMC$_{PHA}^{b}$
28	>100	>100
FB49	>100	>100

GI$_{50}$ = compound concentration (μM) required to inhibit cell proliferation by 50%, in comparison with cells treated with the maximum amount of DMSO (0.25%) and considered as 100% viability. [a] PBMC not stimulated with PHA. [b] PBMC stimulated with PHA. Data are expressed as the mean ± Standard Error Mean (SEM) from the dose-response curves of at least three independent experiments. PBMC: Peripheral Blood Mononuclear Cells; PHA: Phytohaemagglutinin.

compound has very low toxicity in normal cells in comparison to tumor cells, suggesting potential for an optimal therapeutic index.

2.4. BAG3 as therapeutic target in medulloblastoma (MB) cells

Besides its well described role in leukemia disease, high BAG3 expression has been associated with poor prognosis also in medulloblastoma [19], a pediatric brain tumor with extremely poor response to conventional chemotherapeutics and tendency to relapse [20]. As a matter of fact, the cytotoxic activity of BAG3-binders observed in HD-MB03 medulloblastoma cells, reinforces the idea that BAG3 may be an interesting molecular target also in this tumor. In order to verify the contribution of BAG3 to drug response in medulloblastoma cells, BAG3 was efficiently silenced in HD-MB03 through specific small interfering RNA (siRNA) (Fig. 11A). While BAG3 depletion did not affect HD-MB03 cell viability *per se* (data not shown), BAG3 silencing slightly sensitized HD-MB03 cells exposed to a cocktail of the four most common chemotherapeutics used to treat medulloblastoma (Vincristine, Etoposide, Cisplatin and Cyclophosphamide, hereafter namely VECC) (Fig. 11B). Similarly, the efficacy of **FB49**, the most relevant BAG3 binder identified by SPR, was evaluated in combination with VECC chemotherapy on HD-MB03 cells. As shown in Fig. 11C–D, the pharmacological inhibition of BAG3 improved HD-MB03 cell response to chemotherapy, as confirmed by the positive Highest Single Agent (HSA) synergistic score (Fig. 11D, dark pink area) [21].

2.5. FB49 caused G1 cell cycle arrest and apoptosis

To discriminate if the observed reduction of cell viability was due to cell cycle arrest and/or cell death, both cell processes were further investigated. Indeed, treatment with **FB49** caused a cell cycle arrest in G1 phase at the expenses of S phase, which became evident only at 72h of cell treatment with sublethal dose of BAG3 inhibitors (10 μM) (Fig. 12A), as previously reported for different BAG3 inhibitor in MCF7 breast cancer cells [11].

On the other hand, to evaluate the mode of cell death induced by **FB49**, the annexin-V/Propidium Iodide (AV/PI) assay was performed. HD-MB03 cells were treated with 20 μM **FB49** for 48h and 72h. As shown in Fig. 12B, **FB49** induced a time-dependent accumulation of apoptotic cells (AV+PI- CTR vs. 48h p = 0.0042, and AV+PI + CTR vs. 72h and p < 0.0001).

2.6. FB49 induced cell autophagy

Since BAG3 have been described as multifunctional hub molecule regulating the crosstalk between apoptosis and autophagy signaling [22], the autophagic flux was evaluated after treatment with **FB49** in HD-MB03 cells, by visualizing the co-localization of fluorescently labeled LC3 and lysosomal marker. **FB49** induced a significant increase in LC3 signal (green fluorescence) in correspondence to acidic vesicles (red fluorescence), thus indicating a strong induction of autophagy, which can be counteracted by chloroquine (CQ) autophagy inhibitor (Fig. 13A–B). Intriguingly, by blocking autophagy with CQ, the percentage of apoptotic cells significantly increase (Fig. 13C), hence hastening the apoptotic effect of **FB49**. The autophagic effect can be also observed from brightfield images through the formation of autophagic vacuoles in HD-MB03 brightfield images upon **FB49** treatment, while CQ prevented vacuoles formation at the expense of cell shrinkage and membrane blebbing, indicative of apoptosis (Fig. 13D).

Collectively this data suggested that **FB49**-mediated BAG3 inhibition may have a dual role also in medulloblastoma cells, by first triggering autophagy and then unleashing cell apoptosis at later time points.

3. Conclusions

By means of different medicinal chemistry strategies, a set of
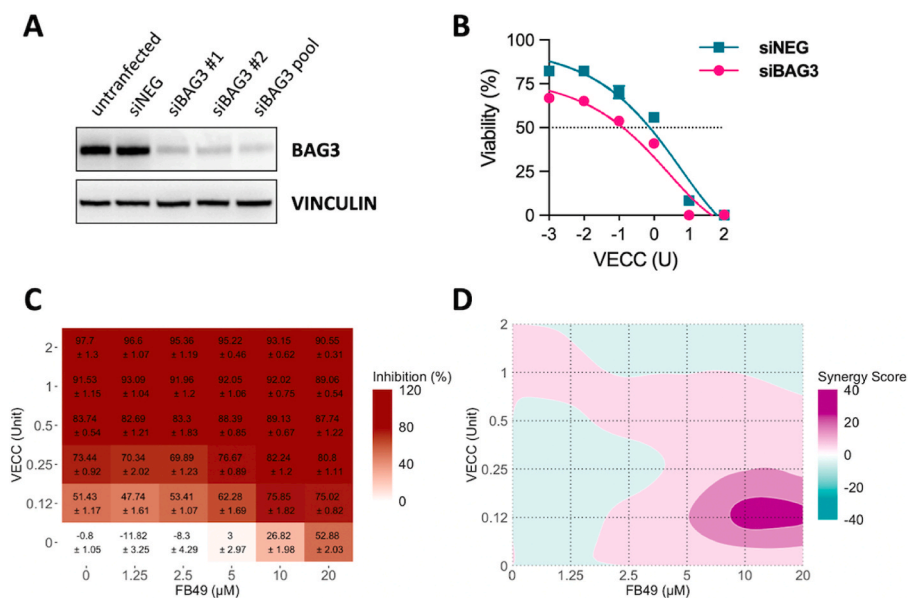
Fig. 11. Targeting BAG3 lead to Medulloblastoma sensitization to chemotherapy

A) Western Blot analysis demonstrating the efficient silencing of BAG3 in HD-MB03 medulloblastoma cells with two different siRNAs. **B)** Dose-response curves for HD-MB03 cells treated with decreasing concentration of VECC chemotherapy cocktail (Vincristine, Etoposide, Cisplatin, and Cyclophosphamide). For detailed VECC description see Material and Method. **C)** Cell viability inhibition matrix calculated for **FB49** lead compound in combination with VECC and (**D**) relative HSA synergy matrix. Interaction has been considered synergistic when HSA$\geq$20, antagonistic when HSA $\leq$ -20, and non-interactive for 10>HSA > -10.
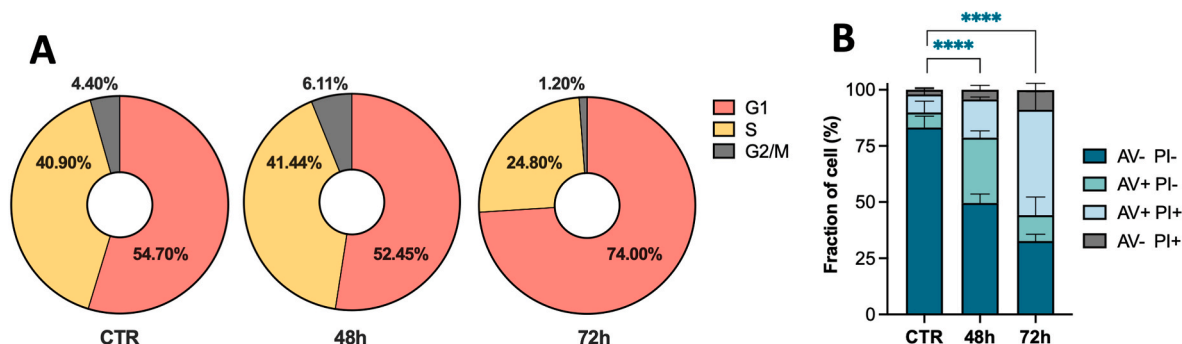
Fig. 12. FB49 induces G1 cell cycle arrest and apoptosis in Medulloblastoma cells

A) Cytofluorimetric analysis of cell cycle upon **FB49** treatment. HD-MB03 cells were treated with sub-lethal dose (10 μM) of **FB49** for 48 h and 72 h respectively. Data represent the mean fraction of cells (%) of three independent experiments. 2-way ANOVA statistical analysis with Tukey correction for multiple comparison was applied. Only significant comparison between treatment and CTR are shown. **B)** Cytofluorimetric analysis of cell death by Annexin V (AV) and Propidium Iodide (PI) staining. HD-MB03 cells were treated with 20 μM **FB49** for 24h and 48h. Histograms represent the mean $\pm$ Standard Error Mean (SEM) of three independent experiments. 2-way ANOVA statistical analysis with Tukey correction for multiple comparison was applied. Only significant comparison between live cell (AV- PI-) are shown. *p < 0.05; **p < 0.01; ***p < 0.001.

putative BAG3 inhibitors was designed. Through SAR evaluation, which encompassed *in vitro* cytotoxicity and SPR analysis, we identified a new highly selective BAG3 inhibitor, namely **FB49**. The interaction of the lead compound **FB49** with the full-length BAG3, for the first time produced in HEK-293T mammalian host system, was also confirmed by NMR analysis. Notably, the substitution of the ethyl ester group with a morpholine amide demonstrated a favorable effect on the binding affinity. This finding highlights the potential of this structural modification in enhancing compound efficacy in targeting BAG3. From the point of view of biological activity, the results obtained demonstrate a good correlation between the ability to bind to BAG3 and the antiproliferative activity. Furthermore, the further biological evaluation of **FB49** pointed out the relevance of the pharmacological inhibition of BAG3 in medulloblastoma, thus strengthening BAG3 as an attractive candidate for drug development. Indeed, BAG3 inhibition mediated by **FB49** induced cell cycle arrest, apoptosis as well as autophagy in HD-MB03 cells.

Intriguingly, the inhibition of BAG3-mediated autophagy significantly increased the cytotoxic effect of **FB49**, hence revealing new therapeutic opportunities to further boost the observed synergistic effect with conventional chemotherapy.

4. Experimental procedures

4.1. Chemistry

4.1.1. Materials and methods

All the reagents and solvents were obtained from commercial sources and used as supplied.

[1]H nuclear magnetic resonance (NMR) spectroscopy was carried out using one of the following instruments: a Bruker Avance 400 or a Bruker Avance III 400. ^{13}C NMR spectra were recorded on a Varian 400 Mercury Plus or a Bruker Avance III 400 spectrometer. Chemical shifts (δ) are
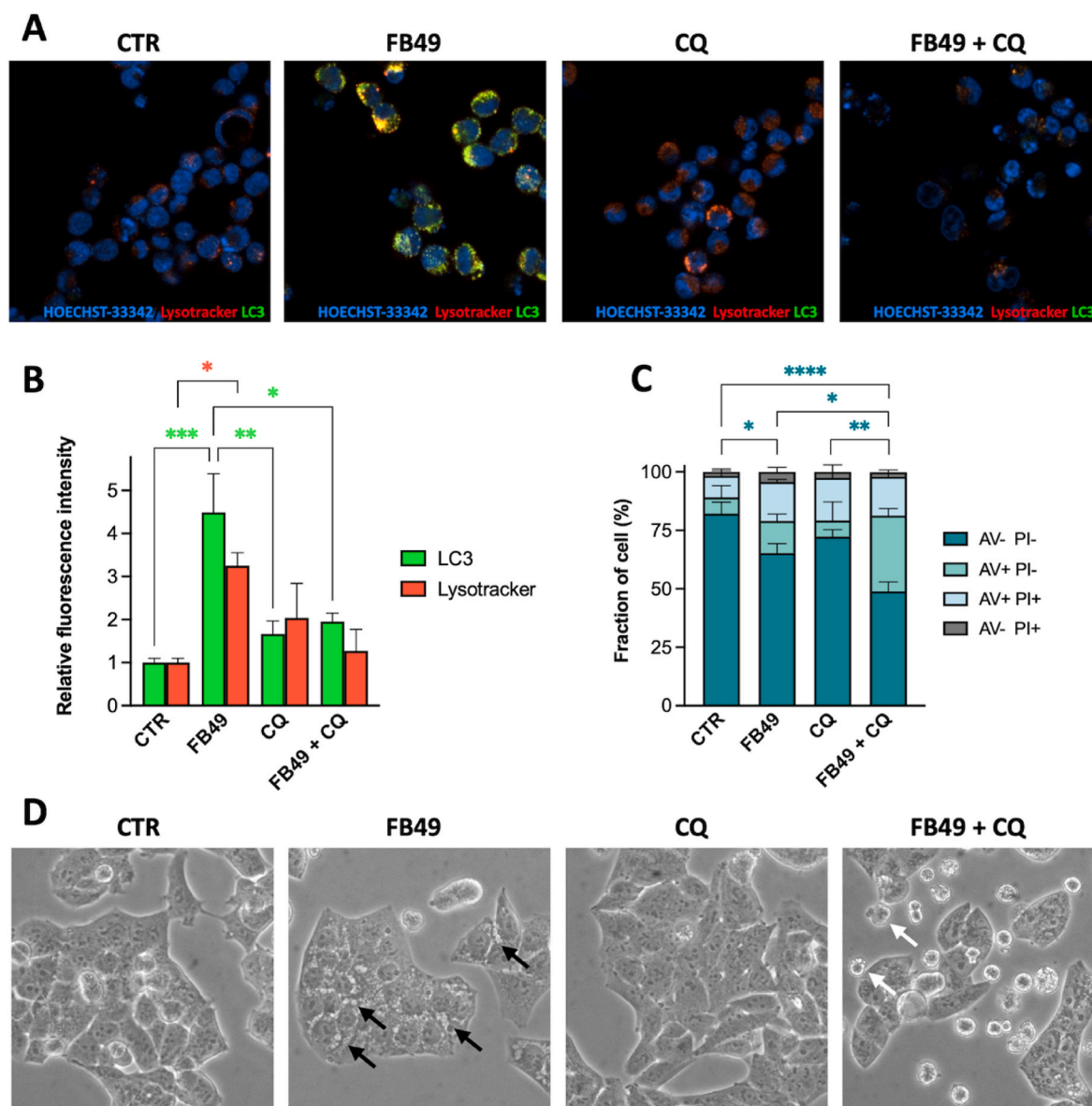
Fig. 13. FB49 triggers autophagy in Medulloblastoma cells
A) Representative immunofluorescence images of LC3 (in green) and Lysotraker (in red) staining to evaluate the autophagic flux upon **FB49** treatment. HD-MB03 cells were treated with 20 μM of BAG3 inhibitor with or without 10 μM of Chloroquine (CQ) autophagy inhibitor for 24 h. The co-localization of green and red fluorescence in **FB49** single treatment indicated the induction of autophagy, which can be reverted by CQ treatment. **B**) Quantification of the total fluorescence intensity per field of green (LC3) and red (Lysotracker) fluorescence. Both green and red fluorescence of DMSO-treated control cells (CTR) were arbitrary set to 1 and used as reference to calculate relative fluorescence intensity accordingly. Histograms represent the mean ± Standard Deviation (SD) of three independent experiments and 2-way ANOVA statistical analysis with Tukey correction for multiple comparison was applied. **C**) Cytofluorimetric analysis of cell death by Annexin V (AV) and Propidium Iodide (PI) staining. Histograms represent the mean ± Standard Error Mean (SEM) of three independent experiments. 2-way ANOVA statistical analysis with Tukey correction for multiple comparison was applied. Only significant comparison between live cell (AV- PI-) are shown **D**) Representative brightfield images of HD-MB03 cells showing the presence of autophagic vacuoles (black arrows) upon **FB49** treatment, while the co-treatment with CQ dramatically reduced vacuoles formation and triggered cell apoptosis. White arrows indicate membrane blebbing in apoptotic cells. *p < 0.05; **p < 0.01; ***p < 0.001; ****p < 0.0001.

given in in parts per million (ppm) downfield relative to the residual solvent peak and the spectra were acquired in the stated solvent at around room temperature (unless otherwise stated). In all cases, NMR data were consistent with the proposed structures. Characteristic chemical shifts (δ) are given in ppm using conventional abbreviations for designation of major peaks: e.g., s, singlet; d, doublet; t, triplet; q, quartet; dd, doublet of doublets; dt, doublet of triplets; and br, broad.

When thin layer chromatography (TLC) has been used it refers to silica gel TLC using Merck precoated aluminum-backed silica gel 60 F_{254} plates with UV at 254 nm. TLC plates were stained using $KMnO_4$.

Column chromatography purifications were performed using an automatic flash chromatography (FC) system (Biotage SP1 or Isolera) over Biotage Sfär KP-Amino D 50 μm cartridges or Biotage Sfär Silica D 60 μm 100 Å cartridges. Reversed phase flash chromatography purifications were performed using Biotage Sfär C18 D 30 μm 100 Å cartridges. Chromatography purifications were also performed by preparative TLC plates on PLC silica gel 60 F_{254} 0.5 mm (20 × 20 cm) plates (Merck).

Liquid Chromatography-Mass Spectrometry (LC-MS): Total ion current (TIC) and diode-array detector (DAD) UV chromatographic traces together with MS and UV spectra associated with the peaks were taken on an UPLC/MS Acquity™ system equipped with a photodiode array

(PDA) detector and coupled to a Waters single quadrupole mass spectrometer operating in alternated positive and negative electrospray ionization mode.

Compound UPLC/MS retention times (Rt) were obtained using the following methods.

Method A: Acquity UPLC CSH C18 column (50 mm × 2.1 mm, 1.7 μm particle size) at 40 °C, a linear gradient from 3 to 100% B over 2 min [A = 0.1% v/v solution of HCOOH in water, B = 0.1% v/v solution of HCOOH in acetonitrile (MeCN)] and a flow rate of 0.9 mL/min.

Method B: Acquity UPLC Peptide BEH C18 column (50 mm × 2.1 mm, 1.7 μm particle size) at 40 °C, a linear gradient from 3 to 60% B over 4 min [A = 0.05% v/v solution of TFA in water, B = 0.05% v/v solution of TFA in MeCN] and a flow rate of 0.7 mL/min. LC-MS was used for monitoring the reactions and for the characterization of intermediates and final compounds.

When high-performance liquid chromatography (HPLC) purification was performed, compounds were purified using a semipreparative MDAP Fractionlynx (Waters) equipped with a mass spectrometry detector (MS: ZQ2000). Method used: XSelect semipreparative column C-18 CSH (30 × 100 mm, 5 μm, from Waters), solvent A = 0.1% v/v solution of HCOOH in water, B = MeCN, gradient from 35.0% B1 to 55.0% B1 in 10min, flow rate of 40 mL/min. Detection: UV/Vis detection range 210 nm–350 nm, MS(ES+/ES-) Scan range 100–1000 AMU.

When stereochemistry is not stated, the compounds with a chiral center are racemic mixtures.

Preparation of ethyl 2-(2,4-dioxo-1,3-thiazolidin-3-yl)acetate (1). To a stirring suspension of thiazolidine-2,4-dione (2 g, 17.08 mmol) and K_2CO_3 anhyd. (4.73 g, 34.22 mmol) in dry MeCN (300 mL), ethyl 2-bromoacetate (1.89 mL, 17.08 mmol) was added dropwise at room temperature under nitrogen atmosphere. After 18 h, the reaction was concentrated *in vacuo* and the residue partitioned between EtOAc and water. The aqueous phase was extracted with EtOAc (3 x), then the organic phases were collected, dried over Na_2SO_4, filtered and concentrated under *vacuum*. The residue was purified by flash chromatography (cartridge: Biotage sfär Silica D 25 g; gradient conditions: EtOAc in cyclohexane (CHX), from 0% to 40%, 8 CV) to afford the title compound **1** (2.82 g, 13.88 mmol, 81% yield) as a colourless oil. ^{1}H NMR (400 MHz, CDCl₃) δ 4.37 (s, 2H), 4.25 (q, J = 7.1 Hz, 2H), 4.06 (s, 2H), 1.31 (t, J = 7.1 Hz, 3H). $C_7H_9NO_4S$; UPLC-MS acidic (method A) r.t. 0.64 min, MS (ESI) *m/z* = 204.0 [M+H] [+].

Preparation of benzyl 2-(2,4-dioxothiazolidin-3-yl)acetate (2). To a stirring suspension of thiazolidine-2,4-dione (0.5 g, 4.3 mmol) and K_2CO_3 anhyd. (1.19 g, 8.6 mmol) in dry MeCN (75 mL), benzyl 2-bromoacetate (0.68 mL, 4.3 mmol) was added dropwise at room temperature under nitrogen atmosphere. After 18 h, the reaction was concentrated *in vacuo* and the residue partitioned between EtOAc and water. The aqueous phase was extracted with EtOAc (3 x), then the organic phases were collected, dried over Na_2SO_4, filtered and concentrated under *vacuum*. The residue was purified by flash chromatography (cartridge: Biotage sfär Silica D 25 g; gradient conditions: EtOAc in CHX, from 0% to 40%, 8 CV) to afford the title compound **2** (0.84 g, 3.18 mmol, 74% yield) as a colourless oil. ^{1}H NMR (400 MHz, CDCl₃) δ 7.36–7.48 (m, 5H), 5.32 (s, 2H), 4.84 (s, 2H), 4.34 (s, 2H). $C_{12}H_{11}NO_4S$; UPLC-MS acidic (method A) r.t. 0.78 min, MS (ESI) *m/z* = 266.3 [M+H] [+].

Preparation of 3-(2-ethoxyethyl)-1,3-thiazolidine-2,4-dione (3). To a stirring suspension of thiazolidine-2,4-dione (100 mg, 0.85 mmol) and K_2CO_3 anhyd. (236 mg, 1.71 mmol) in a mixture of dry MeCN (1 mL) and DMF (1 mL), 1-bromo-2-ethoxyethane (0.1 mL, 0.85 mmol) was added at room temperature. Then, the reaction was heated to 75 °C and left stirring for 2 h. The reaction was concentrated under reduced pressure and the residue was partitioned between EtOAc and water. The aqueous phase was extracted with EtOAc (2x) and the organic layers were collected, dried over Na_2SO_4, filtered and concentrated under *vacuum*. The residue was subjected to direct phase flash chromatography (cartridge: Biotage sfär Silica D 10 g; gradient conditions: EtOAc in CHX,

from 0% to 100%, 8 CV) to afford compound **3** (102 mg, 0.54 mmol, 63% yield) as an amorphous white solid. ^{1}H NMR (400 MHz, DMSO-d_6) δ 4.21 (s, 2H), 3.65 (t, J = 5.9 Hz, 2H), 3.48 (t, J = 5.8 Hz, 2H), 3.41 (q, J = 7.0 Hz, 2H), 1.05 (t, J = 7.0 Hz, 3H). $C_7H_{11}NO_3S$; UPLC-MS acidic (method A) r.t. 0.60 min, MS (ESI) *m/z* = 190.0 [M+H] [+].

Preparation of 3-(2-oxooxolan-3-yl)-1,3-thiazolidine-2,4-dione (4). To a stirring suspension of thiazolidine-2,4-dione (40 mg, 0.34 mmol) and K_2CO_3 anhyd. (142 mg, 1 mmol) in dry DMF (2.5 mL), 3-bromo-2-oxolanone (113 mg, 0.68 mmol) was added at room temperature. Then, the reaction was heated to 50 °C and left stirring for 18 h. The reaction mixture was left reach room temperature and then partitioned between EtOAc and water. The aqueous phase was extracted with EtOAc (2 x), the organic phases were collected, dried over Na_2SO_4, filtered and concentrated under *vacuum*. The residue was subjected to direct phase flash chromatography (cartridge: Biotage sfär Silica D 10 g; gradient conditions: EtOAc in CHX, from 0% to 100%, 12 CV) to afford compound **4** (19 mg, 0.094 mmol, 28% yield) as a colourless oil. ^{1}H NMR (400 MHz, DMSO-d_6) δ 5.08-5.01 (m, 1H), 4.61 (td, J = 9.2, 2.4 Hz, 1H), 4.46-4.30 (m, 1H), 4.03 (s, 2H), 2.71-2.62 (m, 1H), 2.58-2.48 (m, 1H). $C_7H_7NO_4S$; UPLCMS acidic (method A) r.t. 0.42 min, MS (ESI) *m/z* = 201.9 [M+H] [+].

Preparation of 3-[2-(morpholin-4-yl)-2-oxoethyl]-1,3-thiazolidine-2,4-dione (5). To a stirring suspension of thiazolidine-2,4-dione (1 g, 8.54 mmol) and K_2CO_3 anhyd. (2.36 g, 17.1 mmol) in dry MeCN (51 mL), 2-chloro-1-(morpholin-4-yl)ethan-1-one (1.4 g, 8.54 mmol) was added at room temperature. The reaction mixture was heated to 80 °C and stirred for 18 h. Solvents were removed under reduced pressure, then water was added, and the resulting mixture was extracted with DCM (3x). The combined organic layers were dried over Na_2SO_4, filtered and concentrated *in vacuo* to afford compound **5** (1.87 g, 7.66 mmol, 90% yield) as a colourless oil. ^{1}H NMR (400 MHz, DMSO-d_6) δ 4.42 (s, 2H), 4.31 (s, 2H), 3.61 (t, J = 4.7 Hz, 2H), 3.56 (t, J = 4.9 Hz, 2H), 3.51 (t, J = 4.8 Hz, 2H), 3.41 (t, J = 4.9 Hz, 2H). $C_9H_{12}N_2O_4S$; UPLCMS acidic (method A) r.t. 0.42 min, MS (ESI) *m/z* = No ionization.

Preparation of 2-(2,4-dioxo-1,3-thiazolidin-3-yl)-N,N-dimethylacetamide (6). To a stirring suspension of thiazolidine-2,4-dione (100 mg, 0.85 mmol) and K_2CO_3 anhyd. (236 mg, 1.71 mmol) in a mixture of dry MeCN (4 mL) and dry DMF (1 mL), 2-chloro-*N,N*-dimethylacetamide (0.09 mL, 0.85 mmol) was added at room temperature. The reaction mixture was heated to 75 °C and left stirring for 2 h. Then, the reaction was concentrated *in vacuo*, the residue was taken up in EtOAc and washed with water. The aqueous phase was extracted with EtOAc (2 x) and then the organic phases were collected, dried over Na_2SO_4, filtered and concentrated under *vacuum*. The residue was subjected to direct phase flash chromatography (cartridge: Biotage sfär Silica D 10 g; gradient conditions: EtOAc in CHX, from 0% to 100%, 8 CV) to afford compound **6** (135 mg, 0.67 mmol, 78% yield) as a white solid, mp: 110–111 °C. ^{1}H NMR (400 MHz, DMSO-d_6) δ 4.38 (s, 2H), 4.30 (s, 2H), 3.02 (s, 3H), 2.82 (s, 3H).

$C_7H_{10}N_2O_3S$; UPLC-MS acidic (method A) r.t. 0.40 min, MS (ESI) *m/z* = 203.0 [M+H] [+].

Synthesis of (+/−)-ethyl 2-(2,4-dioxo-1,3-thiazolidin-3-yl)propanoate (7). To a solution of thiazolidine-2,4-dione (200 mg, 1.71 mmol) in dry DMF (1 mL), sodium hydride (as a 60% dispersion in mineral oil; 75 mg, 1.88 mmol) was added under N_2 atmosphere at 0 °C, and the resulting reaction mixture was left stirring for 10 min. Then the reaction was left reach room temperature and 2-bromopropanoic acid ethyl ester (0.21 mL, 1.88 mmol) was added dropwise. After stirring overnight, the reaction mixture was diluted with water and extracted with EtOAc (2 x). The combined organic phases were collected, dried over Na_2SO_4, filtered and concentrated under reduced pressure. The residue was subjected to direct phase flash chromatography (cartridge: Biotage sfär Silica D 25 g; gradient conditions: EtOAc in CHX, from 0% to 40%, 8 CV) to afford compound **7** (300 mg, 1.38 mmol, 81% yield) as a colourless oil. ^{1}H NMR (400 MHz, DMSO-d_6) δ 4.91 (q, J = 7.1 Hz, 1H), 4.38-4.21 (m, 2H), 4.17-4.04 (m, 2H), 1.41 (d, J = 7.1 Hz, 3H), 1.15 (t, J = 7.1 Hz, 3H).

$C_8H_{11}NO_4S$; UPLC-MS acidic (method A) r.t. 0.75 min, MS (ESI) m/z = 218.0 [M+H] +.

Synthesis of (+/−)-Ethyl 2-(2,4-dioxo-1,3-thiazolidin-3-yl)butanoate (8). A solution of thiazolidine-2,4-dione (100 mg, 0.85 mmol) in dry DMF (2 mL) was cooled to 0 °C with an ice-bath, then sodium hydride (as a 60% dispersion in mineral oil; 27 mg, 1.11 mmol) was added and the mixture was left stirring for 15 min. Then the reaction was left reach room temperature and ethyl 2-bromobutanoate (0.13 mL, 0.85 mmol) was added. After stirring overnight, the reaction mixture was diluted with water and then extracted with EtOAc (2 x). The combined organic phases were collected, dried over Na_2SO_4, filtered and concentrated under reduced pressure. The residue was subjected to direct phase flash chromatography (cartridge: Biotage sfär Silica D 10 g; gradient conditions: EtOAc in CHX, from 0% to 100%, 8 CV) to afford compound **8** (100 mg, 0.43 mmol, 51% yield) as an amorphous white solid. ^{1}H NMR (400 MHz, DMSO-d_6) δ 4.73 (dd, J = 10.3, 5.0 Hz, 1H), 4.37 (d, J = 4.1 Hz, 2H), 4.18-4.03 (m, 2H), 2.11-1.98 (m, 1H), 1.97-1.83 (m, 1H), 1.15 (t, J = 7.1 Hz, 3H), 0.81 (t, J = 7.5 Hz, 3H). $C_9H_{13}NO_4S$; UPLC-MS acidic (method A) r.t. 0.87 min, MS (ESI) m/z = 232.1 [M+H] +.

Synthesis of (+/−)-ethyl 2-cyclopropyl-2-(2,4-dioxo-1,3-thiazolidin-3-yl)acetate (9). To a solution of thiazolidine-2,4-dione (50 mg, 0.43 mmol) in dry DMF (1 mL), sodium hydride (as a 60% dispersion in mineral oil; 11 mg, 0.47 mmol) was added at 0 °C, and the reaction mixture was left stirring for 10 min. Then the reaction was left reach room temperature and ethyl 2-bromo-2-(cyclopropyl) acetate (0.07 mL, 0.47 mmol) was added. After stirring overnight, the reaction mixture was quenched with water and then partitioned between EtOAc and water. The aqueous phase was extracted with EtOAc (2 x) and then the organic phases were collected, dried over Na_2SO_4, filtered and concentrated under reduced pressure. The residue was subjected to direct phase flash chromatography (cartridge: Biotage sfär Silica D 25 g; gradient conditions: EtOAc in CHX, from 0% to 100%, 10 CV) to afford compound **9** (103 mg, 0.423 mmol, 99% yield) as a colourless oil. ^{1}H NMR (400 MHz, DMSO-d_6) δ 4.39 (d, J = 2.3 Hz, 2H), 4.15-4.10 (m, 2H), 1.58-1.47 (m, 1H), 1.24-1.12 (m, 4H), 0.76-0.67 (m, 1H), 0.63-0.56 (m, 1H), 0.42 (ddd, J = 8.1, 4.4, 2.2 Hz, 1H), 0.17-0.08 (m, 1H). $C_{10}H_{13}NO_4S$; UPLC-MS acidic (method A) r.t. 0.88 min, MS (ESI) m/z = 244.0 [M+H]+.

Synthesis of (+/−)-ethyl 2-(2,4-dioxo-1,3-thiazolidin-3-yl)-2-phenylacetate (10). To a stirring suspension of thiazolidine-2,4-dione (50 mg, 0.43 mmol) in dry DMF (1 mL), sodium hydride (as a 60% dispersion in mineral oil; 11 mg, 0.47 mmol) was added under N_2 atmosphere at 0 °C, and the resulting reaction mixture was left stirring for 10 min. Then the reaction was left reach room temperature and 2-bromo-2-phenylacetic acid ethyl ester (0.08 mL, 0.47 mmol) was added. After stirring overnight, the reaction mixture was diluted with water and then extracted with EtOAc (2x). The combined organic phases were collected, dried over Na_2SO_4, filtered and concentrated under reduced pressure. The residue was subjected to direct phase flash chromatography (cartridge: Biotage sfär Silica D 25 g, gradient conditions: EtOAc in CHX, from 0% to 100%, 10 CV) to afford compound **10** (66 mg, 0.24 mmol, 55% yield) as a colourless oil. ^{1}H NMR (400 MHz, DMSO-d_6) δ 7.47-7.26 (m, 5H), 6.05 (s, 1H), 4.49-4.33 (m, 2H), 4.22-4.11 (m, 2H), 1.17 (t, J = 7.1 Hz, 3H). $C_{13}H_{13}NO_4S$; UPLC-MS acidic (method A) r.t. 0.98 min, MS (ESI) m/z = 280.0 [M+H]

Synthesis of (+/−)-ethyl 2-[(5Z)-5-({3,4-bis[(tert-butyldimethylsilyl)oxy]phenyl}methylidene)-2,4-dioxo-1,3thiazolidin-3-yl]propanoate (11)

A stirring solution of compound **FB20** (634 mg, 1.9 mmol) and 4-dimethylaminopyridine (23 mg, 0.19 mmol) in dry DMF (3 mL) was placed under N_2 atmosphere. Then, TEA (0.65 mL, 4.7 mmol) and *tert*-butyldimethylsilyl chloride (708 mg, 4.7 mmol) were sequentially added and the resulting suspension was left stirring for 1 h at room temperature. The reaction was partitioned between EtOAc and NH_4Cl_{ss}, the organic phase was separated, washed with brine, dried over Na_2SO_4, filtered and concentrated under reduced pressure. The residue was purified by direct phase flash chromatography (cartridge: Biotage sfär

Silica D 25 g; gradient conditions: EtOAc in CHX, from 0% to 80%, 12 CV) to afford compound **11** (1.06 g, 1.87 mmol, 99.7% yield) as a colourless oil. ^{1}H NMR (400 MHz, CDCl$_3$) δ 7.79 (s, 1H), 7.02 (dq, J = 4.7, 2.4 Hz, 2H), 6.93-6.86 (m, 1H), 5.04 (q, J = 7.2 Hz, 1H), 4.30-4.15 (m, 2H), 1.65 (d, J = 7.2 Hz, 3H), 1.26 (t, J = 7.1 Hz, 3H), 1.00 (d, J = 5.0 Hz, 18H), 0.25 (d, J = 3.5 Hz, 12H). $C_{27}H_{43}NO_6Si_2S$; UPLCMS acidic (method A) r.t. 1.88 min, MS (ESI) m/z = No ionization.

Synthesis of (+/−)-2-[(5Z)-5-[(3,4-dihydroxyphenyl)methylene]-2,4-dioxo-thiazolidin-3-yl]propanoic acid (12). A mixture of compound **11** (910 mg, 1.61 mmol), glacial acetic acid (6 mL) and concentrated hydrogen chloride (3 mL, 36 mmol) was heated to 100 °C and left stirring for 2 h. The reaction was left reach room temperature, diluted with water and EtOAc. The organic phase was washed with NH_4Cl_{ss}, dried over Na_2SO_4, filtered, and concentrated under *vacuum*. The residue was purified by reversed phase flash chromatography (cartridge: Biotage sfär C18 D 12 g; gradient conditions: MeCN in water, in presence of 0.1% HCOOH, from 2% to 80%, 10 CV) to give the title compound **12** (393 mg, 1.27 mmol, 79% yield), as a yellow solid, mp: >300 °C. ^{1}H NMR (400 MHz, DMSO-d_6) δ 13.19 (s, 1H), 9.91 (s, 1H), 9.50 (s, 1H), 7.77 (s, 1H), 7.05-6.98 (m, 2H), 6.89 (d, J = 8.1 Hz, 1H), 4.97 (q, J = 7.1 Hz, 1H), 1.50 (d, J = 7.2 Hz, 3H). $C_{13}H_{11}NO_6S$; UPLC-MS acidic (method A) r.t. 0.78 min, MS (ESI) m/z = 310.0 [M+H] +.

Synthesis of (+/−)-2-(2,4-dioxothiazolidin-3-yl)propanoic acid (13). A mixture of compound **7** (500 mg, 2.3 mmol) in acetic acid (2 mL) and concentrated hydrochloric acid (1 mL, 12 mmol) was refluxed for 1 h. The reaction was concentrated *in vacuo* and the residue partitioned between water and EtOAc. The aqueous phase was extracted with EtOAc (3 x), the organic phases were collected, dried over Na_2SO_4, filtered and concentrated *in vacuo*. The residue was purified by reversed phase flash chromatography (cartridge: Biotage sfär C18 D 12 g; gradient conditions: MeCN in water, in presence of 0.1% HCOOH, from 2% to 50%, 10 CV) to afford compound **13** (606 mg, yield >95%) as a colourless oil. ^{1}H NMR (400 MHz, DMSO-d_6) δ 13.06 (s, 1H), 4.81 (q, J = 7.2 Hz, 1H), 4.38-4.19 (m, 2H), 1.42 (d, J = 7.2 Hz, 3H). $C_6H_7NO_4S$; UPLC-MS acidic (method A) r.t. 0.52 min, MS (ESI) m/z = 189.95 [M+H] +.

Synthesis of (+/−)-3-(1-methyl-2-morpholino-2-oxo-ethyl)thiazolidine-2,4-dione (14). To a solution of compound **13** (606 mg, 1.76 mmol) in dry DMF (3.5 mL), HATU (670 mg, 1.76 mmol) was added, and the resulting solution was left stirring for 10 min. Then DIPEA (0.46 mL, 2.64 mmol) and morpholine (0.15 mL, 1.76 mmol) were added and the resulting solution was left stirring at 25 °C for 4 h. The reaction mixture was diluted with $NaHCO_{3ss}$ and extracted with EtOAc (3 x). The organic phases were collected, dried over Na_2SO_4, filtered, and concentrated under reduced pressure. The residue was purified by direct phase flash chromatography (cartridge: Biotage sfär Silica D 10 g; gradient conditions: EtOAc in CHX, from 0% to 50%, 10 CV) to give compound **14** (391 mg, 1.51 mmol, 86% yield) as a white solid, mp: 176–178 °C. ^{1}H NMR (400 MHz, Chloroform-d) δ 5.04 (q, J = 7.2 Hz, 1H), 3.97 (d, J = 2.8 Hz, 2H), 3.79-3.23 (m, 8H), 1.63 (d, J = 7.2 Hz, 3H). $C_{10}H_{14}N_2O_4S$; UPLC-MS acidic (method A) r.t. 0.49–0.52 min, MS (ESI) m/z = 259.0 [M+H] +.

Synthesis of (+/−)-ethyl 2-(2,5-dioxoimidazolidin-1-yl)propanoate (15) To a stirring suspension of imidazolidine-2,4-dione (300 mg, 3 mmol) and potassium carbonate (456 mg, 3.3 mmol) in dry THF (9 mL), ethyl 2-bromopropanoate (0.37 mL, 3.3 mmol) was added at room temperature and the reaction was heated under reflux for 18 h. The mixture was allowed to reach room temperature and then partitioned between EtOAc and water. The organic phase was separated, dried over Na_2SO_4, filtered and concentrated under reduced pressure. The residue was subjected to direct phase flash chromatography (cartridge: Biotage sfär Silica D 10 g; gradient conditions: EtOAc in CHX, from 0% to 100%, 10 CV) to afford compound **15** (469 mg, 2.34 mmol, 78% yield) as a colourless oil. ^{1}H NMR (400 MHz, DMSO-d_6) δ 8.16 (s, 1H), 4.67 (q, J = 7.2 Hz, 1H), 4.10 (qd, J = 7.1, 2.1 Hz, 2H), 3.97 (d, J = 3.7 Hz, 2H), 1.42 (d, J = 7.2 Hz, 3H), 1.16 (t, J = 7.1 Hz, 3H). $C_8H_{12}N_2O_4$; UPLC-MS acidic (method A) r.t. 0.51 min, MS (ESI) m/z = 201.1 [M+H] +.

Preparation of (+/−)-ethyl 2-(3-methyl-2,5-dioxoimidazolidin-1-yl) propanoate (16). To a stirring solution of compound **15** (100 mg, 0.49 mmol) in dry DMF (2 mL), potassium carbonate (68 mg, 0.49 mmol) was added at room temperature. After 10 min, iodomethane (30 μL, 0.54 mmol) was added and reaction was left stirring at room temperature for 18 h. Then, the reaction was partitioned between EtOAc and water. The organic phase was separated, dried over Na_2SO_4, filtered and concentrated under reduced pressure. The residue was subjected to direct phase flash chromatography (cartridge: Biotage sfär Silica D 10 g; gradient conditions: EtOAc in CHX, from 0% to 80%, 10 CV) to afford compound **15** (97 mg, 0.45 mmol, 92% yield) as a yellow oil. ^{1}H NMR (400 MHz, DMSO-d_6) δ 4.68 (q, $J = 7.2$ Hz, 1H), 4.10 (q, $J = 7.0$ Hz, 2H), 4.03 (d, $J = 2.9$ Hz, 2H), 2.86 (s, 3H), 1.43 (d, $J = 7.2$ Hz, 3H), 1.16 (t, $J = 7.1$ Hz, 3H). $C_9H_{14}N_2O_4$; UPLC-MS acidic (method A) r.t. 0.57 min, MS (ESI) $m/z = 215.1$ [M+H]$^+$.

Preparation of ethyl 2-(2-bromothiazol-4-yl)acetate (18). To a solution of Copper (II) bromide (68 mg, 0.31 mmol) and 2-(2-amino-4-thiazolyl) acetic acid ethyl ester **17** (100 mg, 0.54 mmol) in MeCN (4 mL), *t*-butyl nitrite (50 μL, 0.4 mmol) was added and the reaction mixture was left stirring for 18 h at room temperature under N_2 atmosphere. The reaction mixture was diluted with DCM and washed with a 1 M solution of HCl. The phases were separated, the aqueous phase was re-extracted with DCM (2 x), and the combined organic layers were dried over Na_2SO_4, filtered and concentrated under reduced pressure. The residue was purified by direct phase flash chromatography (cartridge: Biotage sfär Silica D 10 g; gradient conditions: EtOAc in CHX, from 0% to 30%, 10 CV) to afford compound **18** (22 mg, 0.088 mmol, 16% yield) as a colourless oil. ^{1}H NMR (400 MHz, DMSO-d_6) δ 7.55 (d, $J = 0.8$ Hz, 1H), 4.10 (q, $J = 7.1$ Hz, 2H), 3.82 (d, $J = 0.9$ Hz, 2H), 1.19 (t, $J = 7.1$ Hz, 3H). $C_7H_8BrNO_2S$; UPLC-MS acidic (method A) r.t. 0.89 min, MS (ESI) $m/z =$ No ionization.

General procedure A for Knoevenagel condensation of N-substituted-2,4-thiazolidinedione with an aromatic aldehyde.

To a stirring solution of *N*-substituted-2,4-thiazolidinedione (1.0 eq.) and aromatic aldehyde (1.0 eq.) in dry toluene (0.34 M), piperidine (0.5 eq.) and acetic acid (0.5 eq.) were added at room temperature. The mixture was heated under reflux and left stirring overnight. After cooling to room temperature, the reaction mixture was diluted with EtOAc and washed with water. The organic phase was dried over Na_2SO_4, filtered and concentrated under *vacuum*. The purification was performed by flash chromatography using the gradient conditions reported below and the final products were characterized by ESI-MS and NMR spectra. The reaction was monitored by analytical LC-MS (A/a by UV and ESI-MS).

Synthesis of ethyl 2-[(5Z)-5-[(3,4-dihydroxyphenyl)methylidene]-2,4-dioxo-1,3-thiazolidin-3-yl]acetate (compound 28). Compound **28** was obtained from compound **1** (250 mg, 1.23 mmol) and 3,4-dihydroxybenzaldehyde (171.61 mg, 1.24 mmol), by following the general procedure A, as a yellow solid, mp: 163–164 °C (255 mg, 0.79 mmol, 64% overall isolated yield after purification by reversed phase flash chromatography); Cartridge: Biotage sfär C18 D 30 g, gradient conditions: MeCN in water, in presence of 0.1% HCOOH, from 2% to 100%, 10 CV. ^{1}H NMR (400 MHz, DMSO-d_6) δ 9.70 (s, 2H), 7.81 (s, 1H), 7.07-6.99 (m, 2H), 6.89 (d, $J = 8.0$ Hz, 1H), 4.47 (s, 2H), 4.17 (q, $J = 7.1$ Hz, 2H), 1.21 (t, $J = 7.1$ Hz, 3H). ^{13}C NMR (100 MHz, DMSO-d_6) δ 167.56, 167.23, 165.52, 149.79, 146.45, 135.40, 124.94, 124.40, 117.00, 116.79, 115.91, 62.04, 42.55, 14.41. $C_{14}H_{13}NO_6S$; UPLC-MS acidic (method A) r.t. 0.89 min, MS (ESI) $m/z = 324.1$ [M+H]$^+$.

Synthesis of ethyl 2-[(5Z)-5-[(4-fluorophenyl)methylidene]-2,4-dioxo-1,3-thiazolidin-3yl]acetate (FB7). Compound **FB7** was obtained from compound **1** (70 mg, 0.34 mmol) and 4-fluorobenzaldehyde (43 mg, 0.35 mmol), by following the general procedure A, as a yellow solid, mp: 127–128 °C (51.7 mg, 0.167 mmol, 49% overall isolated yield after purification by direct phase flash chromatography; Cartridge: Biotage sfär Silica D 10 g, gradient conditions: EtOAc in DCM, from 0% to 50%, 10 CV. ^{1}H NMR (400 MHz, DMSO-d_6) δ 8.03 (s, 1H), 7.80-7.68 (m, 2H),

7.47-7.35 (m, 2H), 4.50 (s, 2H), 4.18 (q, $J = 7.1$ Hz, 2H), 1.22 (t, $J = 7.1$ Hz, 3H). ^{13}C NMR (100 MHz, DMSO-d_6) δ 167.20, 165.33, 167.10 and 164.86 ($J_{1C-F} = 224$ Hz), 162.36, 133.52, 133.31 and 133.22 ($J_{3C-F} = 9$ Hz) (2C), 129.89, 120.67, 117.20 and 116.98 ($J_{2C-F} = 22$ Hz) (2C), 62.11, 42.71, 14.40. $C_{14}H_{12}FNO_4S$; UPLC-MS acidic (method A) r.t. 1.16 min, purity: >99%. MS (ESI) $m/z = 310.0$ [M+H]$^+$.

Synthesis of ethyl 2-[(5Z)-5-[(3-fluoro-4-hydroxyphenyl)methylidene]-2,4-dioxo-1,3-thiazolidin-3-yl]acetate (FB8). Compound **FB8** was obtained from compound **1** (70 mg, 0.34 mmol) and 3-fluoro-4-hydroxybenzaldehyde (49 mg, 0.35 mmol), by following the general procedure A, as a yellow solid, mp: 145–146 °C (60.8 mg, 0.338 mmol, 54% overall isolated yield after purification by direct phase flash chromatography); *First column purification:* cartridge: Biotage sfär Silica D 10g; gradient conditions: EtOAc in CHX, from 0% to 50%, 10 CV; *Second column purification:* cartridge: Biotage sfär Silica D 10 g; gradient conditions: MeOH in DCM, from 0% to 10%, 10 CV. ^{1}H NMR (400 MHz, DMSO-d_6) δ 10.90 (s, 1H), 7.91 (s, 1H), 7.51 (dd, $J = 12.4$, 2.2 Hz, 1H), 7.34 (dd, $J = 8.5$, 2.2 Hz, 1H), 7.12 (t, $J = 8.8$ Hz, 1H), 4.48 (s, 2H), 4.17 (q, $J = 7.1$ Hz, 2H), 1.21 (t, $J = 7.1$ Hz, 3H). ^{13}C NMR (100 MHz, DMSO-d_6) δ 167.26, 167.16, 165.40, 152.60, 150.18 and 148.63 ($J_{1C-F} = 240$ Hz), 148.52, 133.94, 127.89, 124.67 and 124.60 ($J_{3C-F} = 7$ Hz), 119.19 and 119.00 ($J_{2C-F} = 19$ Hz), 118.10, 62.10, 42.64, 14.40. $C_{14}H_{12}FNO_5S$; UPLC-MS acidic (method A) r.t. 1.04 min, purity: 95%. MS (ESI) $m/z = 326.1$ [M+H]$^+$.

Synthesis of ethyl 2-[(5Z)-5-[(3,4-dimethoxyphenyl)methylidene]-2,4-dioxo-1,3-thiazolidin-3-yl]acetate (FB9). Compound **FB9** was obtained from compound **1** (70 mg, 0.34 mmol) and 3,4-dimethoxybenzaldehyde (58 mg, 0.350 mmol), by following the general procedure A, as a yellow solid, mp: 116–117 °C (95 mg, 0.269 mmol, 78% overall isolated yield after purification by direct phase flash chromatography); Cartridge: Biotage sfär Silica D 10 g, gradient conditions: EtOAc in CHX, from 0% to 50%, 10 CV. ^{1}H NMR (400 MHz, DMSO-d_6) δ 7.96 (s, 1H), 7.32-7.22 (m, 2H), 7.21-7.11 (m, 1H), 4.48 (s, 2H), 4.17 (q, $J = 7.1$ Hz, 2H), 3.84 (s, 3H), 3.82 (s, 3H), 1.21 (t, $J = 7.1$ Hz, 3H). ^{13}C NMR (100 MHz, DMSO-d_6) δ 167.41, 167.19, 165.43, 151.72, 149.45, 134.94, 125.83, 124.55, 117.79, 114.01, 112.63, 62.08, 56.20, 56.04, 42.62, 14.41. $C_{16}H_{17}NO_6S$; UPLC-MS acidic (method A) r.t. 1.11 min, purity: 99%. MS (ESI) $m/z = 352.1$ [M+H]$^+$.

Synthesis of ethyl 2-[(5Z)-5-[(3-hydroxyphenyl)methylidene]-2,4-dioxo-1,3-thiazolidin-3yl]acetate (FB10). Compound **FB10** was obtained from compound **1** (70 mg, 0.34 mmol) and 3-hydroxybenzaldehyde (46 mg, 0.38 mmol), by following the general procedure A, as a pale-yellow solid, mp: 120–121 °C (64 mg, 0.208 mmol, 61% overall isolated yield after purification by reversed phase flash chromatography); Cartridge: Biotage sfär C18 D 12 g, gradient conditions: MeCN in water, in presence of 0.1% HCOOH, from 2% to 100%, 10 CV. ^{1}H NMR (400 MHz, DMSO-d_6) δ 9.91 (s, 1H), 7.91 (s, 1H), 7.35 (t, $J = 7.9$ Hz, 1H), 7.14-7.06 (m, 1H), 7.03 (t, $J = 2.1$ Hz, 1H), 6.92 (ddd, $J = 8.3$, 2.5, 0.9 Hz, 1H), 4.49 (s, 2H), 4.18 (q, $J = 7.1$ Hz, 2H), 1.22 (t, $J = 7.1$ Hz, 3H). ^{13}C NMR (100 MHz, DMSO-d_6) δ 167.35, 167.13, 165.37, 158.41, 134.80, 134.34, 130.97, 121.96, 120.71, 118.72, 116.58, 62.11, 42.66, 14.40. $C_{14}H_{13}NO_5S$; UPLC-MS acidic (method A) r.t. 1.01 min, purity: >99%. MS (ESI) $m/z = 308.1$ [M+H]$^+$.

Synthesis of ethyl 2-[(5Z)-5-[(6-methoxypyridin-3-yl)methylidene]-2,4-dioxo-1,3-thiazolidin-3-yl]acetate (FB11). Compound **FB11** was obtained from compound **1** (70 mg, 0.34 mmol) and 6-methoxy-3-pyridinecarboxaldehyde (52 mg, 0.38 mmol), by following the general procedure A, as a pale-yellow solid, mp: 110–111 °C (68 mg, 0.212 mmol, 61% overall isolated yield after purification by reversed phase flash chromatography; Cartridge: Biotage sfär C18 D 12 g, gradient conditions: MeCN in water, in presence of 0.1% HCOOH, from 2% to 100%, 10 CV. ^{1}H NMR (400 MHz, DMSO-d_6) δ 8.57 (d, $J = 2.6$ Hz, 1H), 8.01 (s, 1H), 7.95 (dd, $J = 8.8$, 2.6 Hz, 1H), 7.02 (d, $J = 8.7$ Hz, 1H), 4.49 (s, 2H), 4.18 (q, $J = 7.1$ Hz, 2H), 3.94 (s, 3H), 1.21 (t, $J = 7.1$ Hz, 3H). ^{13}C NMR (100 MHz, DMSO-d_6) δ 167.12, 167.04, 165.25, 164.95, 151.38, 139.60, 131.66, 123.14, 119.57, 112.00, 62.11, 54.31, 42.72, 14.40. $C_{14}H_{14}N_2O_5S$;

UPLC-MS acidic (method A) r.t. 1.10 min, purity: 99%. MS (ESI) m/z = 323.1 [M+H] $^+$.

Synthesis of ethyl 2-[(5Z)-5-[(2,3-dihydro-1,4-benzodioxin-6-yl)methylidene]-2,4-dioxo-1,3-thiazolidin-3-yl]acetate (FB13). Compound **FB13** was obtained from compound **1** (70 mg, 0.34 mmol) and 2,3-dihydro-1,4-benzodioxin-6-carboxaldehyde (62 mg, 0.38 mmol), by following the general procedure A, as a yellow solid, mp: 118–119 °C (85 mg, 0.242 mmol, 70% overall isolated yield after purification by reversed phase flash chromatography); Cartridge: Biotage sfär C18 D 12 g, gradient conditions: MeCN in water, in presence of 0.1% HCOOH, from 2% to 100%, 10 CV. ^{1}H NMR (400 MHz, DMSO-d_6) δ 7.90 (s, 1H), 7.20-7.14 (m, 2H), 7.04 (dd, J = 8.0, 0.7 Hz, 1H), 4.48 (s, 2H), 4.36-4.26 (m, 4H), 4.17 (q, J = 7.1 Hz, 2H), 1.21 (t, J = 7.1 Hz, 3H). ^{13}C NMR (100 MHz, DMSO-d_6) δ 167.29, 167.16, 165.41, 146.61, 144.24, 134.47, 126.46, 124.56, 119.58, 118.58, 118.33, 64.98, 64.43, 62.08, 42.63, 14.40. $C_{16}H_{15}NO_6S$; UPLC-MS acidic (method A) r.t. 1.15 min, purity: 99%. MS (ESI) m/z = 350.1 [M+H] +.

Synthesis of ethyl 2-[(5Z)-5-[(4-hydroxyphenyl)methylidene]-2,4-dioxo-1,3-thiazolidin-3yl]acetate (FB14). Compound **FB14** was obtained from compound **1** (70 mg, 0.34 mmol) and 4-hydroxybenzaldehyde (46 mg, 0.38 mmol), by following the general procedure A, as a yellow solid, mp: 159–160 °C (85.3 mg, 0.278 mmol, 81% overall isolated yield after purification by reversed phase flash chromatography); Cartridge: Biotage sfär C18 D 12 g, gradient conditions: MeCN in water, in presence of 0.1% HCOOH, from 2% to 100%, 10 CV. ^{1}H NMR (400 MHz, DMSO-d_6) δ 10.43 (s, 1H), 7.90 (s, 1H), 7.56-7.47 (m, 2H), 6.98-6.88 (m, 2H), 4.47 (s, 2H), 4.17 (q, J = 7.1 Hz, 2H), 1.21 (t, J = 7.1 Hz, 3H). ^{13}C NMR (100 MHz, DMSO-d_6) δ 167.49, 167.21, 165.55, 160.91, 135.02, 133.28 (2C), 124.08, 116.92 (2C), 116.25, 62.05, 42.58, 14.40. $C_{14}H_{13}NO_5S$; UPLC-MS acidic (method A) r.t. 0.99 min, purity: 97%. MS (ESI) m/z = 308.1 [M+H] $^+$.

Synthesis of ethyl 2-{5-[(3,4-dihydroxyphenyl)methyl]-2,4-dioxo-1,3-thiazolidin-3yl}acetate (FB15). Compound **FB12** (0.17 mL, 0.06 mmol) was dissolved in dry ethanol (10 mL). The mixture was degassed with N_2, then Pd/C 10% wet (20 mg, 0.02 mmol) was added followed by molecular hydrogen (0.12 mg, 0.06 mmol). The reaction was stirred at 6 atm of hydrogen for 18 h. Then the mixture was filtered over a pad of Celite (packed and washed with EtOH) and concentrated under *vacuum*. The residue was purified by direct phase flash chromatography (cartridge: Biotage sfär Silica D 10 g; gradient conditions: EtOAc in CHX, from 0% to 60%, 10 CV) to afford compound **FB15** (16.8 mg, 0.052 mmol, 83% yield), as a colourless oil. ^{1}H NMR (400 MHz, CDCl$_3$) δ 6.81 (d, J = 8.1 Hz, 1H), 6.76 (d, J = 2.1 Hz, 1H), 6.65 (dd, J = 8.1, 2.1 Hz, 1H), 5.50 (s, 2H), 4.49 (dd, J = 8.9, 4.3 Hz, 1H), 4.32 (s, 2H), 4.23 (q, J = 7.2 Hz, 2H), 3.41 (dd, J = 14.3, 4.3 Hz, 1H), 3.12 (dd, J = 14.3, 8.9 Hz, 1H), 1.30 (t, J = 7.2 Hz, 3H). ^{13}C NMR (100 MHz, DMSO-d_6) δ 173.76, 171.06, 167.05, 145.58, 144.91, 127.66, 120.25, 116.86, 116.02, 61.94, 51.97, 42.39, 37.50, 14.37. $C_{14}H_{15}NO_6S$; UPLC-MS acidic (method A) r. t. 0.80 min, purity: 93%. MS (ESI) m/z = 326.1 [M+H] $^+$.

Synthesis of 2-[(5Z)-5-[(3,4-dihydroxyphenyl)methylidene]-2,4-dioxo-1,3-thiazolidin-3yl]acetic acid (FB16). A mixture of compound **FB12** (2.39 g, 7.39 mmol), glacial acetic acid (18 mL) and concentrated hydrogen chloride (6.16 mL, 73.9 mmol) was stirred at 120 °C for 5 h. The reaction was left reach room temperature and precipitation of a yellow solid was observed. The solid was recovered by filtration and then washed with water to afford the title compound, **FB16** (2 g, 6.77 mmol, 92% yield) as a yellow solid, mp: 256–258 °C. ^{1}H NMR (400 MHz, DMSO-d_6) δ 13.39 (s, 1H), 9.92 (s, 1H), 9.50 (s, 1H), 7.80 (s, 1H), 7.06-7.00 (m, 2H), 6.89 (d, J = 8.1 Hz, 1H), 4.34 (s, 2H). ^{13}C NMR (100 MHz, DMSO-d_6) δ 168.51, 167.62, 165.67, 149.60, 146.41, 135.12, 124.84, 124.53, 117.02, 116.79, 116.24, 42.70. $C_{12}H_9NO_6S$; UPLC-MS acidic r.t. 0.70 min, purity: 99%. MS (ESI) m/z = 296.1 [M+H] $^+$.

Synthesis of 2-[(5Z)-5-[1-(3,4-dihydroxyphenyl)ethylidene]-2,4-dioxo-1,3-thiazolidin-3-yl]acetate (FB17). To a stirring suspension of **1** (140 mg, 0.68 mmol) and 1-(3,4-dihydroxyphenyl) ethanone (131 mg, 0.86 mmol) in dry toluene (10 mL), piperidine (84 μL, 0.86 mmol) and acetic

acid (40 μL, 0.86 mmol) were added and the reaction was heated under reflux for 2 days. The mixture was allowed to reach room temperature and then partitioned between EtOAc and water. The organic phase was washed with brine and then dried over Na$_2$SO$_4$, filtered, and concentrated under reduced pressure. The residue was subjected to direct phase flash chromatography (Cartridge: Biotage sfär Silica D 10 g; gradient conditions: EtOAc in CHX, from 0% to 50%, 10 CV) to afford compound **FB17** (106 mg, 0.32 mmol, 46% yield) as an amorphous yellow solid. ^{1}H NMR (400 MHz, DMSO-d_6) δ 9.62 (bs, 2H), 6.87 (d, J = 1.9 Hz, 1H), 6.84-6.77 (m, 2H), 4.41 (s, 2H), 4.17 (q, J = 7.1 Hz, 2H), 2.66 (s, 3H), 1.21 (t, J = 7.1 Hz, 3H). ^{13}C NMR (100 MHz, DMSO-d_6) δ 167.71, 167.38, 164.45, 153.01, 147.65, 145.94, 132.84, 119.21, 117.69, 116.21, 114.73, 61.98, 42.14, 22.38, 14.42. $C_{15}H_{15}NO_6S$; UPLC-MS acidic (method A) r.t. 0.92 min, purity: 94%. MS (ESI) m/z = 338.2 [M+H] $^+$.

Synthesis of ethyl 2-[(5Z)-5-[(3,4-dichlorophenyl)methylidene]-2,4-dioxo-1,3-thiazolidin3-yl]acetate (FB18). Compound **FB18** was obtained from compound **1** (50 mg, 0.25 mmol) and 3,4-dichlorobenzaldehyde (44 mg, 0.25 mmol), by following the general procedure A, as a yellow solid, mp: 156–158 °C (52 mg, 0.144 mmol, 59% overall isolated yield after purification by direct phase flash chromatography); Cartridge: Biotage sfär Silica D 25 g, gradient conditions: EtOAc in CHX, from 0% to 50%, 10 CV. ^{1}H NMR (400 MHz, DMSO-d_6) δ 8.01 (s, 1H), 7.97 (d, J = 2.1 Hz, 1H), 7.83 (d, J = 8.5 Hz, 1H), 7.61 (dd, J = 8.4, 2.1 Hz, 1H), 4.50 (s, 2H), 4.18 (q, J = 7.1 Hz, 2H), 1.22 (t, J = 7.1 Hz, 3H). ^{13}C NMR (100 MHz, DMSO-d_6) δ 167.04, 166.80, 165.10, 133.92, 133.72, 132.92, 132.59, 131.99 (2C), 129.53, 123.27, 62.14, 42.79, 14.40. $C_{14}H_{11}Cl_2NO_4S$; UPLC-MS acidic (method A) r.t. 1.36 min, purity: >99%. MS (ESI) m/z = 360.0 And 361.6 [M+H] $^+$.

Synthesis of benzyl 2-[(5Z)-5-[(3,4-dihydroxyphenyl)methylidene]-2,4-dioxo-1,3-thiazolidin-3-yl]acetate (FB19), Compound **FB19** was obtained from compound **2** (265 mg, 1 mmol) and 3,4-dihydroxybenzaldehyde (156 mg, 1 mmol) by following the general procedure A, as yellow solid (8.3 mg, 0.022 mmol, 17% yield) after direct phase flash chromatography (cartridge: Biotage sfär Silica D 10 g, gradient conditions: EtOAc in CHX, from 0% to 100%, 10 CV) to afford compound **1b** (208 mg, 0.54 mmol, 54% yield) as an amorphous yellow solid. ^{1}H NMR (400 MHz, DMSO-d_6) δ 7.81 (s, 1H), 7.44-7.29 (m, 5H), 7.07-6.99 (m, 2H), 6.88 (d, J = 8.0 Hz, 1H), 5.20 (s, 2H), 4.55 (s, 2H). ^{13}C NMR (100 MHz, DMSO-d_6) δ 167.58, 167.23, 165.54, 149.70, 146.43, 135.81, 135.46, 128.93 (2C), 128.74, 128.49 (2C), 124.94, 124.46, 117.05, 116.80, 115.95, 67.30, 42.57. $C_{19}H_{15}NO_6S$; UPLC-MS acidic (method A) r.t. 1.06 min, purity: 99%. MS (ESI) m/z = 386.1 [M+H] $^+$.

Preparation of (+/−)-ethyl 2-[(5Z)-5-[(3,4-dihydroxyphenyl)methylidene]-2,4-dioxo-1,3-thiazolidin-3yl]propanoate (FB20). Compound **FB20** was obtained from compound **7** (63 mg, 0.29 mmol) and 3,4-dihydroxybenzaldehyde (40 mg, 0.29 mmol), by following the general procedure A (conc. 0.18 M instead of 0.34 M), as a yellow solid, mp: 160–161 °C (77 mg, 0.23 mmol, 79% overall isolated yield after purification by reversed phase flash chromatography); Cartridge: Biotage sfär C18 D 28 g; gradient conditions: MeCN in water, in presence of 0.1% HCOOH, from 2% to 100%, 10 CV. ^{1}H NMR (400 MHz, DMSO-d_6) δ 7.79 (s, 1H), 7.10-6.97 (m, 2H), 6.88 (d, J = 7.9 Hz, 1H), 5.09 (q, J = 7.1 Hz, 1H), 4.13 (qq, J = 7.1, 3.7 Hz, 2H), 1.50 (d, J = 7.2 Hz, 3H), 1.15 (t, J = 7.1 Hz, 3H). ^{13}C NMR (100 MHz, DMSO-d_6) δ 169.05, 167.32, 165.36, 149.72, 146.44, 135.32, 124.90, 124.47, 117.01, 116.79, 115.85, 61.85, 50.52, 14.45, 14.39. $C_{15}H_{15}NO_6S$; UPLC-MS acidic (method A) r.t. 0.96 min, purity: 99%. MS (ESI) m/z = 338.2 [M+H] $^+$.

Synthesis of 2-[(5Z)-5-[(3,4-dihydroxyphenyl)methylidene]-2,4-dioxo-1,3-thiazolidin-3-yl]-N,N-dimethylacetamide (FB21). Compound **FB21** was obtained from compound **6** (50 mg, 0.25 mmol) and 3,4-dihydroxybenzaldehyde (34 mg, 0.25 mmol), by following the general procedure A, as a yellow solid, mp: 275–276 °C (58 mg, 0.18 mmol, 73% overall isolated yield after purification by trituration in MeOH, DCM, and water). ^{1}H NMR (400 MHz, DMSO-d_6) δ 7.76 (s, 1H), 7.08-6.97 (m, 2H), 6.88 (d, J = 8.1 Hz, 1H), 4.54 (s, 2H), 3.05 (s, 3H), 2.84 (s, 3H). ^{13}C NMR

(100 MHz, DMSO-d_6) δ 167.78, 165.94, 164.89, 149.61, 146.42, 134.70, 124.77, 124.53, 116.91, 116.77, 116.50, 43.05, 36.21, 35.66. $C_{14}H_{14}N_2O_5S$; UPLC-MS acidic (method A) r.t. 0.69 min, purity: >99%. MS (ESI) m/z = 323.0 [M+H]$^+$.

Synthesis of (5Z)-5-[(3,4-dihydroxyphenyl)methylidene]-3-[2-(morpholin-4-yl)-2-oxoethyl]-1,3-thiazolidine-2,4-dione (FB22). Compound **FB22** was obtained from compound **5** (62 mg, 0.25 mmol) and 3,4-dihydroxybenzaldehyde (35 mg, 0.25 mmol), by following the general procedure A, as a yellow solid, mp: >300 °C (66 mg, 0.18 mmol, 72% overall isolated yield after purification by trituration in MeOH, DCM, and water). ^{1}H NMR (400 MHz, DMSO-d_6) δ 7.76 (s, 1H), 7.09-6.96 (m, 2H), 6.88 (d, J = 8.1 Hz, 1H), 4.59 (s, 2H), 3.66-3.61 (m, 2H), 3.60-3.51 (m, 4H), 3.46-3.41 (m, 2H). ^{13}C NMR (100 MHz, DMSO-d_6) δ 167.77, 165.92, 163.96, 149.61, 146.43, 134.76, 124.79, 124.52, 116.93, 116.78, 116.46, 66.37 (2C), 44.99, 42.88, 42.39. $C_{16}H_{16}N_2O_6S$; UPLC-MS acidic (method A) r.t. 0.69 min, purity: >99%. MS (ESI) m/z = 365.1 [M+H]$^+$.

Synthesis of (5Z)-5-[(3,4-dihydroxyphenyl)methylidene]-3-(2-ethoxyethyl)-1,3-thiazolidine-2,4-dione (FB23). Compound **FB23** was obtained from compound **3** (100 mg, 0.48 mmol) and 3,4-dihydroxybenzaldehyde (66 mg, 0.48 mmol), by following the general procedure A, as a yellow solid, mp: 157–158 °C (67 mg, 0.215 mmol, 45% overall isolated yield after purification by direct phase flash chromatography and then by reversed phase flash chromatography); *First column purification*: cartridge: Biotage sfär Silica D 25 g; gradient conditions: EtOAc in CHX, from 0% to 100%, 10 CV; *Second column purification*: cartridge: Biotage sfär C18 D 12 g; gradient conditions: MeCN in water, in presence of 0.1% HCOOH, from 2% to 100%, 10 CV. ^{1}H NMR (400 MHz, DMSO-d_6) δ 9.82 (bs, 2H), 7.75 (s, 1H), 7.07-6.96 (m, 2H), 6.87 (d, J = 8.1 Hz, 1H), 3.80 (t, J = 5.8 Hz, 2H), 3.56 (t, J = 5.8 Hz, 2H), 3.43 (q, J = 7.0 Hz, 2H), 1.05 (t, J = 7.0 Hz, 3H). ^{13}C NMR (100 MHz, DMSO-d_6) δ 167.86, 166.20, 149.39, 146.37, 134.34, 124.66 (2C), 116.94, 116.75, 116.63, 66.04, 65.66, 41.29, 15.43. $C_{14}H_{15}NO_5S$; UPLC-MS acidic (method A) r.t. 0.88 min, purity: >99%. MS (ESI) m/z = 310.0 [M+H]$^+$.

Preparation of (+/−)-ethyl 2-cyclopropyl-2-[(5Z)-5-[(3,4-dihydroxyphenyl)methylidene]-2,4-dioxo-1,3-thiazolidin-3-yl]acetate (FB24). Compound **FB24** was obtained from compound **9** (62 mg, 0.25 mmol) and 3,4-dihydroxybenzaldehyde (35 mg, 0.25 mmol), by following the general procedure A, as an amorphous yellow solid (66 mg, 0.18 mmol, 72% overall isolated yield after purification by trituration in MeOH, DCM, and water). ^{1}H NMR (400 MHz, DMSO-d_6) δ 9.82 (bs, 1H), 7.76 (s, 1H), 7.09-6.96 (m, 2H), 6.88 (d, J = 8.1 Hz, 1H), 4.59 (s, 2H), 3.66-3.61 (m, 2H), 3.60-3.51 (m, 4H), 3.46-3.41 (m, 4H). ^{13}C NMR (100 MHz, DMSO-d_6) δ 168.09, 167.48, 165.54, 149.94, 146.46, 135.84, 125.04, 124.35, 117.03, 116.79, 115.40, 61.82, 61.09, 14.42, 11.36, 6.05, 2.87. $C_{17}H_{17}N_2O_6S$; UPLC-MS acidic (method A) r.t. 0.69 min, purity: >99%. MS (ESI) m/z = 365.1 [M+H]$^+$.

Synthesis of (+/−)-ethyl 2-[(5Z)-5-[(3,4-dihydroxyphenyl)methylidene]-2,4-dioxo-1,3-thiazolidin-3-yl]-2-phenylacetate (FB25). Compound **FB25** was obtained from compound **10** (63 mg, 0.2 mmol) and 3,4-dihydroxybenzaldehyde (28 mg, 0.2 mmol), by following the general procedure A (conc. 0.14 M instead of 0.34 M), as an amorphous yellow solid (49 mg, 0.12 mmol, 60% overall isolated yield after purification by direct phase flash chromatography and then by reversed phase flash chromatography); *First column purification*: cartridge: Biotage sfär Silica D 25 g; gradient conditions: EtOAc in CHX, from 0% to 100%, 10 CV; *Second column purification*: cartridge: Biotage sfär C18 D 12 g; gradient conditions: MeCN in water, in presence of 0.1% HCOOH, from 2% to 100%, 10 CV. ^{1}H NMR (400 MHz, DMSO-d_6) δ 9.75 (s, 2H), 7.84 (s, 1H), 7.48-7.42 (m, 2H), 7.41-7.33 (m, 3H), 7.07-7.00 (m, 2H), 6.93-6.85 (m, 1H), 6.25 (s, 1H), 4.20 (q, J = 7.1 Hz, 2H), 1.18 (t, J = 7.1 Hz, 3H). ^{13}C NMR (100 MHz, DMSO-d_6) δ 167.35, 167.21, 165.31, 150.13, 146.50, 136.21, 134.06, 129.64 (2C), 128.95, 128.73 (2C), 125.17, 124.25, 117.02, 116.80, 115.02, 62.23, 58.15, 14.39. $C_{20}H_{17}NO_6S$; UPLC-MS acidic (method A) r.t. 1.10 min, purity: >99%. MS (ESI) m/z = 400.1 [M+H]$^+$.

Preparation of (+/−)-ethyl 2-[(5Z)-5-[(3,4-dihydroxyphenyl)methylidene]-2,4-dioxo-1,3-thiazolidin-3yl]butanoate (FB28). Compound **FB28** was obtained from compound **8** (100 mg, 0.43 mmol) and 3,4-dihydroxybenzaldehyde (60 mg, 0.43 mmol), by following the general procedure A (conc. 0.22 M instead of 0.34 M), as an amorphous yellow solid (150 mg, 0.427 mmol, 99% overall isolated yield after purification by direct phase flash chromatography); Cartridge: Biotage sfär Silica D 25 g, gradient conditions: EtOAc in CHX, from 0% to 100%, 10 CV. ^{1}H NMR (400 MHz, CDCl$_3$) δ 7.79 (s, 1H), 7.05 (d, J = 2.1 Hz, 1H), 7.01 (dd, J = 8.3, 2.1 Hz, 1H), 6.95 (d, J = 8.3 Hz, 1H), 5.94 (s, 2H), 4.88 (dd, J = 10.5, 5.2 Hz, 1H), 4.24 (qq, J = 7.0, 3.6 Hz, 2H), 2.35-2.10 (m, 2H), 1.27 (t, J = 7.1 Hz, 3H), 0.94 (t, J = 7.5 Hz, 3H). ^{13}C NMR (100 MHz, DMSO-d_6) δ 168.50, 167.57, 165.68, 149.93, 146.48, 135.69, 125.01, 124.34, 117.01, 116.79, 115.31, 61.78, 56.47, 21.42, 14.39, 10.82. $C_{16}H_{17}NO_6S$; UPLC-MS acidic (method A) r.t. 1.04 min, purity: 99%. MS (ESI) m/z = 352.1 [M+H]$^+$.

Synthesis of (+/−)-ethyl 2-[(4Z)-4-[(3,4-dihydroxyphenyl)methylidene]-2,5-dioxoimidazolidin-1-yl]propanoate (FB29), To a stirring suspension of 3,4-dihydroxybenzaldehyde (41 mg, 0.3 mmol) and compound **15** (60 mg, 0.3 mmol) in dry toluene (2 mL), piperidine (16 μL, 0.15 mmol) and acetic acid (10 μL, 0.15 mmol) were added at room temperature and the reaction was then heated under reflux for 18 h. Then, the reaction mixture was concentrated *in vacuo* and the residue was partitioned between EtOAc and water. The organic phase was separated, dried over Na$_2$SO$_4$, filtered and concentrated under reduced pressure. The residue was subjected to direct phase flash chromatography (cartridge: Biotage sfär Silica D 25 g; gradient conditions: EtOAc in CHX, from 0% to 80%, 10 CV) to afford compound **14** (50 mg, 0.16 mmol, 52% yield) as a yellow solid, mp: 117–119 °C. ^{1}H NMR (400 MHz, DMSO-d_6) δ 7.04-6.98 (m, 2H), 6.80-6.73 (m, 1H), 6.41 (s, 1H), 4.81 (q, J = 7.2 Hz, 1H), 4.12 (qd, J = 7.1, 2.1 Hz, 2H), 1.50 (d, J = 7.2 Hz, 3H), 1.16 (t, J = 7.1 Hz, 3H). ^{13}C NMR (100 MHz, DMSO-d_6) δ 169.80, 163.85, 154.53, 147.40, 145.87, 124.37, 123.99, 122.27, 117.80, 116.29, 112.31, 61.67, 47.63, 15.03, 14.43. $C_{15}H_{16}N_2O_6$; UPLC-MS acidic (method A) r.t. 0.76 min, purity: 94%. MS (ESI) m/z = 321.2 [M+H]$^+$.

Synthesis of (+/−)-ethyl 2-[(4Z)-4-[(3,4-dihydroxyphenyl)methylene]-3-methyl-2,5-dioxoimidazolidin-1-yl]propanoate and ethyl 2-[(4E)-4-[(3,4-dihydroxyphenyl)methylene]-3methyl-2,5-dioxo-imidazolidin-1-yl]propanoate, obtained as a mixture of geometric isomers (FB30) To a stirring suspension of compound **16** (72 mg, 0.34 mmol) and 3,4-dihydroxybenzaldehyde (56 mg, 0.41 mmol) in dry toluene (2 mL), piperidine (20 μL, 0.17 mmol) and acetic acid (10 μL, 0.17 mmol) were added at room temperature and the reaction was heated for 18 h under reflux. After cooling to room temperature, the reaction mixture was partitioned between water and EtOAc (the black gummy solid residue was dissolved with 2 mL of DMSO and then added to the work up mixture). The organic phase was separated, dried over Na$_2$SO$_4$, filtered and concentrated under reduced pressure. The residue was purified by reversed phase flash chromatography (cartridge: Biotage sfär C18 D 12 g; gradient conditions: MeCN in water, in presence of 0.1% HCOOH, from 2% to 80%, 10 CV) and then by direct phase flash chromatography (Cartridge: Biotage sfär Silica D 10 g, gradient conditions: EtOAc in CHX, from 0% to 80%, 10 CV) to afford compound **30** (35 mg, 0.104 mmol, 31% yield) as an amorphous brown solid and a mixture 1:2 of Z/E regioisomers. By NOE correlation it was possible to assign the regiochemistry to the two isomers: the minor isomer has the Z configuration, while the major isomer has the E configuration.

Minor isomer: ^{1}H NMR (400 MHz, DMSO-d_6) δ 6.81 (d, J = 2.0 Hz, 1H), 6.78 (d, J = 8.1 Hz, 1H), 6.76-6.73 (m, 1H), 6.69 (s, 1H), 4.89 - 4.83 (m, 1H), 4.14 (q, J = 7.1 Hz, 2H), 2.98 (s, 3H), 1.51 (d, J = 7.2 Hz, 3H), 1.18 (t, J = 7.1 Hz, 3H). Major Isomer: ^{1}H NMR (400 MHz, DMSO-d_6) δ 7.71 (d, J = 2.1 Hz, 1H), 7.31 (dd, J = 8.5, 2.1 Hz, 1H), 6.74 (d, J = 8.3 Hz, 1H), 6.43 (s, 1H), 4.86 (q, J = 7.2 Hz, 1H), 4.13 (q, J = 7.1 Hz, 2H), 3.15 (s, 3H), 1.51 (d, J = 7.2 Hz, 3H), 1.16 (t, J = 7.1 Hz, 3H). Mixture of isomers: ^{13}C NMR (100 MHz, DMSO-d_6) δ 169.69, 169.62, 162.85,

160.90, 152.15, 147.53, 146.70, 145.31, 145.02, 127.63, 125.98, 124.55, 124.20, 123.30, 122.30, 119.83, 117.91, 117.36, 115.78, 115.51, 113.51, 61.67, 61.59, 48.14, 47.73, 30.85, 26.69, 14.93, 14.36. UPLC-MS acidic (method A) r.t. 0.81 and 0.83 min, MS (ESI) m/z = 335.2 [M+H] $^+$.

Synthesis of (5Z)-5-[(3,4-dihydroxyphenyl)methylidene]-3-(2-oxooxolan-3-yl)-1,3-thiazolidine-2,4-dione (FB31). Compound **FB31** was obtained from compound **4** (19 mg, 0.094 mmol) and 3,4-dihydroxybenzaldehyde (13 mg, 0.094 mmol), by following the general procedure A (conc. 0.035 M instead of 0.34 M), as a yellow solid, mp: 211–212 °C (14 mg, 0.044 mmol, 46% overall isolated yield after purification by direct phase flash chromatography); Cartridge: Biotage sfär Silica D 10 g, gradient conditions: EtOAc in CHX, from 0% to 100%, 10 CV. ^{1}H NMR (400 MHz, DMSO-d_6) δ 9.80 (bs, 2H), 7.80 (s, 1H), 7.07-6.98 (m, 2H), 6.90-6.86 (m, 1H), 5.40 (t, J = 10.0 Hz, 1H), 4.51 (td, J = 8.8, 2.6 Hz, 1H), 4.42-4.32 (m, 1H), 2.62-2.53 (m, 1H), 2.49-2.43 (m, 1H). ^{13}C NMR (100 MHz, DMSO-d_6) δ 172.86, 167.34, 165.21, 149.84, 146.45, 135.68, 125.00, 124.42, 117.02, 116.82, 115.57, 66.60, 50.57, 25.59. $C_{14}H_{11}NO_6S$; UPLC-MS acidic (method A) r.t. 0.76 min, purity: 97%. MS (ESI) m/z = 322.1 [M+H] $^+$.

Synthesis of (+/−)-(5Z)-5-[(3,4-dihydroxyphenyl)methylene]-3-(1-methyl-2-morpholino-2-oxoethyl)thiazolidine-2,4-dione (FB32). A stirring solution of compound **12** (30 mg, 0.1 mmol) in dry DMF (1 mL) was cooled to 0 °C, then DIPEA (20 μL, 0.1 mmol) was added followed by HATU (37 mg, 0.1 mmol). After 10 min, morpholine (10 μL, 0.1 mmol) was added and the resulting mixture was left stirring at room temperature for 4 h. The mixture was diluted with NH₄Cl$_{ss}$ and extracted with EtOAc. The organic phase was separated, dried over Na₂SO₄, filtered and concentrated under *vacuum*. The residue was purified by direct phase flash chromatography (cartridge: Biotage sfär Silica D 10 g; gradient conditions: EtOAc in CHX, from 0% to 80%, 10 CV). The product containing fractions were collected and solvents were removed under reduced pressure. The residue (13 mg) was triturated in Et₂O to remove traces of tetramethylurea. The organic solvents were removed by filtration and the solid product was dried under *vacuum* to afford compound **FB32** (11 mg, 0.03 mmol, 30% yield) as an amorphous yellow solid. 1H NMR (400 MHz, DMSO-d_6) δ 7.74 (s, 1H), 7.05-6.97 (m, 2H), 6.87 (d, J = 8.0 Hz, 1H), 5.22 (q, J = 7.1 Hz, 1H), 3.67-3.42 (m, 8H), 1.51 (d, J = 7.1 Hz, 3H). ^{13}C NMR (100 MHz, DMSO-d_6) δ 167.36, 166.92, 165.73, 149.68, 146.44, 134.93, 124.86, 124.52, 116.98, 116.78, 115.79, 66.48 (2C), 50.41 (2C), 42.42, 15.06. $C_{17}H_{18}N_2O_6S$; UPLC-MS acidic (method A) r.t. 0.74 min, purity: 95%. MS (ESI) m/z = 379.2 [M+H] $^+$.

Synthesis of (+/−)-(5Z)-5-[(3,4-dihydroxyphenyl)methylene]-3-[1-methyl-2-oxo-2-(1-piperidyl) ethyl]thiazolidine-2,4-dione (FB33). A stirring solution of compound **12** (30 mg, 0.1 mmol) in dry DMF (1 mL) was cooled to 0 °C, then DIPEA (40 μL, 0.2 mmol) was added followed by HATU (37 mg, 0.1 mmol). After 10 min, piperidine (10 μL, 0.1 mmol) was added and the resulting mixture was left stirring at room temperature for 4 h. The mixture was diluted with NH₄Cl$_{ss}$ and extracted with EtOAc. The organic phase was separated, dried over Na₂SO₄, filtered and the solvent was removed under *vacuum*. The residue was purified by direct phase flash chromatography (cartridge: Biotage sfär Silica D 10 g; gradient conditions: EtOAc in CHX, from 0% to 100%, 12 CV) to afford compound **FB33** (18.5 mg, 0.05 mmol, 51% yield) as an amorphous yellow solid. ^{1}H NMR (400 MHz, Methanol-d4) δ 7.78 (s, 1H), 7.03 (d, J = 2.2 Hz, 1H), 6.99 (dd, J = 8.3, 2.2 Hz, 1H), 6.88 (d, J = 8.2 Hz, 1H), 5.25 (q, J = 7.0 Hz, 1H), 3.88-3.65 (m, 1H), 3.42-3.33 (m, 2H), 3.30-3.21 (m, 1H), 1.74-1.57 (m, 4H), 1.56 (d, J = 7.0 Hz, 3H), 1.52-1.35 (m, 2H). ^{13}C NMR (100 MHz, DMSO-d_6) δ 167.30, 166.31, 165.72, 149.63, 146.44, 134.87, 124.84, 124.55, 116.99, 116.78, 115.84, 50.51, 46.28, 43.54, 26.17, 25.77, 24.37, 15.22. $C_{18}H_{20}N_2O_5S$; UPLC-MS acidic (method A) r.t. 0.88 min, purity: 93%. MS (ESI) m/z = 377.2 [M+H] $^+$.

Synthesis of (+/−)-(5Z)-5-[(3,4-dihydroxyphenyl)methylene]-3-[1-methyl-2-(2-oxa-6-azaspiro [3.3]heptan-6-yl)-2-oxo-ethyl]thiazolidine-2,4-dione (FB35). To a stirring solution of compound **12** (55 mg, 0.18

mmol) in dry DMF (2 mL), HATU (67 mg, 0.18 mmol) was added at room temperature. After 10 min, DIPEA (60 μL, 0.36 mmol) and 2-oxa-6-azaspiro[3.3]heptane (18 mg, 0.18 mmol) were added and the resulting mixture was left stirring for 4 h. The mixture was diluted with NH₄Cl$_{ss}$ and extracted with EtOAc. The organic phase was separated, dried over Na₂SO₄, filtered and the solvent was removed under *vacuum*. The residue was purified by direct phase flash chromatography (cartridge: Biotage sfär Silica D 10 g; gradient conditions: EtOAc in CHX, from 0% to 100%, 10 CV, and then MeOH in EtOAc from 0% to 25%, 6 CV) to afford 30 mg of the title product as a yellow solid which was further purified by reversed phase flash chromatography (cartridge: Biotage sfär C18 D 12 g; gradient conditions: MeCN in water, in presence of 0.1% HCOOH, from 2% to 60%, 10 CV) to give the title compound **FB35** (17 mg, 0.044 mmol, 25% yield) as an amorphous yellow solid. ^{1}H NMR (400 MHz, DMSO-d_6) δ 7.75 (s, 1H), 7.04-6.99 (m, 2H), 6.88 (d, J = 8.1 Hz, 1H), 4.96 (q, J = 7.1 Hz, 1H), 4.66-4.55 (m, 4H), 4.26 (d, J = 9.0 Hz, 1H), 4.12-4.03 (m, 2H), 4.00 (d, J = 10.3 Hz, 1H), 1.42 (d, J = 7.1 Hz, 3H). ^{13}C NMR (100 MHz, DMSO-d_6) δ 168.50, 167.08, 165.31, 149.62, 146.43, 135.06, 124.86, 124.58, 117.02, 116.78, 115.92, 80.20, 79.75, 60.25, 58.50, 49.69, 38.25, 14.21. $C_{18}H_{18}N_2O_6S$; UPLC-MS acidic (method A) r.t. 0.71 min, purity: 99%. MS (ESI) m/z = 391.2 [M+H] $^+$.

Synthesis of (+/−)-(5Z)-5-[(3,4-dihydroxyphenyl)methylene]-3-[2-(1,4-dioxa-8-azaspiro[4.5] decan-8-yl)-1-methyl-2-oxo-ethyl]thiazolidine-2,4-dione (FB36). To a stirring solution of compound **12** (55 mg, 0.18 mmol) in dry DMF (2 mL), HATU (67 mg, 0.18 mmol) was added at room temperature. After 10 min, DIPEA (60 μL, 0.36 mmol) and 1,4-dioxa-8-azaspiro[4.5]decane (25 mg, 0.18 mmol) were added and the resulting mixture was left stirring for 4 h. The mixture was diluted with NH₄Cl$_{ss}$ and extracted with EtOAc. The organic phase was separated, dried over Na₂SO₄, filtered and the solvent was removed under *vacuum*. The residue was purified by direct phase flash chromatography (cartridge: Biotage sfär Silica D 10 g; gradient conditions: EtOAc in CHX, from 0% to 100%, 10 CV) to afford 18 mg of the title product as a yellow solid, which was further purified by reversed phase flash chromatography (cartridge: Biotage sfär C18 D 12 g; gradient conditions: MeCN in water, in presence of 0.1% HCOOH, from 2% to 60%, 10 CV) to give the title compound **FB36** (13.3 mg, 0.031 mmol, 17% yield) as a yellow solid, mp: 233–234 °C. ^{1}H NMR (400 MHz, DMSO-d_6) δ 7.75 (s, 1H), 7.10-6.96 (m, 2H), 6.86 (d, J = 7.9 Hz, 1H), 5.23 (q, J = 7.0 Hz, 1H), 3.87 (s, 4H), 3.38-3.27 (m, 4H), 1.72-1.53 (m, 2H), 1.52-1.37 (m, 2H), 1.48 (d, J = 6.9 Hz, 3H). ^{13}C NMR (100 MHz, DMSO-d_6) δ 167.29, 166.59, 165.68, 149.72, 146.44, 135.01, 124.92, 124.49, 116.98, 116.79, 115.69, 106.56, 64.29 (2C), 50.44, 43.40 (2C), 35.96 (2C), 15.23. $C_{20}H_{22}N_2O_7S$; UPLC-MS acidic (method A) r.t. 0.83 min, purity: 96%. MS (ESI) m/z = 435.4 [M+H] $^+$.

Synthesis of (+/−)-2-[(5Z)-5-[(3,4-dihydroxyphenyl)methylene]-2,4-dioxo-thiazolidin-3-yl]-N-ethylpropanamide (FB37). A stirring solution of compound **12** (60 mg, 0.2 mmol) in dry DMF (1 mL) was cooled to 0 °C, then DIPEA (40 μL, 0.2 mmol) was added followed by HATU (74 mg, 0.2 mmol). After 10 min, ethylamine (0.18 mL, 0.36 mmol, 1.8 equiv.) was added and after 0.5 h, the reaction mixture was allowed to reach room temperature and left stirring for further 4 h. The mixture was diluted with NH₄Cl$_{ss}$ and extracted with EtOAc. The organic phase was separated, dried over Na₂SO₄, filtered and concentrated under *vacuum*, to furnish compound **FB37** as an amorphous yellow solid (30 mg, 0.09 mmol, 45% overall isolated yield after purification by reversed phase flash chromatography); Cartridge: Biotage sfär Silica D 12 g, gradient conditions: MeCN in water, in presence of 0.1% HCOOH, from 2% to 60%, 10 CV. ^{1}H NMR (400 MHz, Methanol-d_4) δ 7.76 (s, 1H), 7.04 (d, J = 2.2 Hz, 1H), 6.98 (dd, J = 8.3, 2.2 Hz, 1H), 6.88 (d, J = 8.2 Hz, 1H), 4.96 (q, J = 7.2 Hz, 1H), 3.23 (q, J = 7.2 Hz, 2H), 1.60 (d, J = 7.2 Hz, 3H), 1.11 (t, J = 7.2 Hz, 3H). ^{13}C NMR (100 MHz, DMSO-d_6) δ 167.61, 167.55, 165.85, 149.63, 146.45, 134.16 (2C), 124.66, 124.57, 116.77 (2C), 51.80, 34.35, 15.08, 14.66. $C_{15}H_{16}N_2O_5S$; UPLC-MS acidic (method A) r.t. 0.75 min, purity: 98%. MS (ESI) m/z = 337.1 [M+H] +.

*Synthesis of (+/−)-ethyl 2-[(5Z)-5-(1H-indazol-5-ylmethylene)-2,4-

dioxo-thiazolidin-3-yl] *propanoate (FB38)*. Compound **FB38** was obtained from compound **7** (100 mg, 0.46 mmol) and indazole-5-carboxaldehyde (67 mg, 0.46 mmol), by following the general procedure A (conc. 0.23 M instead of 0.34 M), as an amorphous pale-yellow solid (78 mg, 0.23 mmol, 49% overall isolated yield after purification by reversed phase flash chromatography); Cartridge: Biotage sfär C18 D 12 g, gradient conditions: MeCN in water, in presence of 0.1% HCOOH, from 2% to 100%, 10 CV. ^{1}H NMR (400 MHz, DMSO-d_6) δ 13.42 (s, 1H), 8.26 (d, $J = 1.0$ Hz, 1H), 8.16-8.14 (m, 1H), 8.12 (s, 1H), 7.74-7.68 (m, 1H), 7.62 (dd, $J = 8.8$, 1.7 Hz, 1H), 5.13 (q, $J = 7.1$ Hz, 1H), 4.14 (qq, $J = 7.1$, 3.7 Hz, 2H), 1.52 (d, $J = 7.1$ Hz, 3H), 1.17 (t, $J = 7.1$ Hz, 3H). ^{13}C NMR (100 MHz, DMSO-d_6) δ 169.02, 167.26, 165.33, 140.62, 135.73, 135.70, 128.07, 125.73, 125.24, 123.84, 118.06, 111.81, 61.89, 50.65, 14.39 (2C). $C_{16}H_{15}N_3O_4S$; UPLC-MS acidic (method A) r.t. 1.02 min, purity: >99%. MS (ESI) $m/z = 346.1$ [M+H]$^+$.

Synthesis of (+/−)-ethyl 2-[(5Z)-5-(1H-indazol-6-yl-methylene)-2,4-dioxo-thiazolidin-3-yl]propanoate (FB39). Compound **FB39** was obtained from compound **7** (100 mg, 0.46 mmol) and *1H*-indazole-6-carboxaldehyde (67 mg, 0.46 mmol), by following the general procedure A (conc. 0.23 M instead of 0.34 M), as a pale-yellow solid, mp: 160–161 °C (62 mg, 0.18 mmol, 39% overall isolated yield after purification by reversed phase flash chromatography; Cartridge: Biotage sfär C18 D 12 g, gradient conditions: MeCN in water, in presence of 0.1% HCOOH, from 2% to 100%, 10 CV. ^{1}H NMR (400 MHz, DMSO-d_6) δ 13.41 (s, 1H), 8.20-8.14 (m, 2H), 7.93 (d, $J = 8.4$ Hz, 1H), 7.89 (s, 1H), 7.37 (dd, $J = 8.5$, 1.5 Hz, 1H), 5.14 (q, $J = 7.1$ Hz, 1H), 4.15 (qd, $J = 7.1$, 2.9 Hz, 2H), 1.53 (d, $J = 7.1$ Hz, 3H), 1.17 (t, $J = 7.1$ Hz, 3H). ^{13}C NMR (100 MHz, DMSO-d_6) δ 168.96, 167.11, 165.20, 140.32, 135.49, 134.31, 130.90, 124.16, 122.15, 121.86, 120.64, 113.51, 61.92, 50.74, 14.40 (2C). $C_{16}H_{15}N_3O_4S$; UPLC-MS acidic (method A) r.t. 1.05 min, purity:>99%. MS (ESI) $m/z = 346.1$ [M+H]$^+$.

Preparation of ethyl 2-[2-(4-hydroxyphenoxy)thiazol-4-yl]acetate (FB40). A mixture of hydroquinone (10 mg, 0.09 mmol), compound **18** (22 mg, 0.09 mmol) and potassium carbonate (12 mg, 0.09 mmol) in dry DMF (2 mL) was heated to 140 °C and left stirring at that temperature for 18 h under nitrogen atmosphere. The reaction mixture was left reach room temperature and then diluted with NH_4Cl_{ss} and EtOAc. The organic phase was separated, dried over Na_2SO_4, filtered and concentrated under reduced pressure. The residue was purified by reversed phase flash chromatography (cartridge: Biotage sfär C18 D 12 g; gradient conditions: MeCN in water, in presence of 0.1% HCOOH, from 2% to 100%, 12 CV) to afford the title compound **FB40** (3 mg, 0.011 mmol, 12% yield), as a brown oil. ^{1}H NMR (400 MHz, Methanol-d_4) δ 7.14-7.08 (m, 2H), 6.87-6.81 (m, 2H), 6.80-6.74 (m, 1H), 4.17 (q, $J = 7.1$ Hz, 2H), 3.63 (d, $J = 0.9$ Hz, 2H), 1.26 (t, $J = 7.1$ Hz, 3H). ^{13}C NMR (100 MHz, Methanol-d_4) δ 170.44, 154.79, 153.65, 147.06, 124.39, 115.97, 113.61 (2C), 109.74 (2C), 59.83, 36.30, 13.04. $C_{13}H_{13}NO_4S$; UPLC-MS acidic (method A) r.t. 0.89 min, purity: 98%. MS (ESI) $m/z = 280.1$ [M+H]$^+$.

Synthesis of (+/−)-ethyl 2-[(5Z)-5-[(3-chloro-4-hydroxy-phenyl)methylene]-2,4-dioxothiazolidin-3-yl]propanoate (FB41). Compound **FB41** was obtained from compound **7** (100 mg, 0.46 mmol) and 3-chloro-4-hydroxybenzaldehyde (72 mg, 0.46 mmol), by following the general procedure A (conc. 0.46 M instead of 0.34 M), as a pale-yellow solid, mp: 138–139 °C (130 mg, 0.37 mmol, 80% overall isolated yield after purification by reversed phase flash chromatography); Cartridge: Biotage sfär C18 D 12 g, gradient conditions: MeCN in water, in presence of 0.1% HCOOH, from 2% to 100%, 10 CV. ^{1}H NMR (400 MHz, DMSO-d_6) δ 11.21 (s, 1H), 7.88 (s, 1H), 7.70 (d, $J = 2.3$ Hz, 1H), 7.45 (dd, $J = 8.7$, 2.3 Hz, 1H), 7.11 (d, $J = 8.6$ Hz, 1H), 5.10 (q, $J = 7.1$ Hz, 1H), 4.13 (qq, $J = 7.2$, 3.7 Hz, 2H), 1.50 (d, $J = 7.2$ Hz, 3H), 1.16 (t, $J = 7.1$ Hz, 3H). ^{13}C NMR (100 MHz, DMSO-d_6) δ 168.98, 166.97, 165.21, 156.26, 133.58, 133.35, 130.51, 125.31, 121.21, 117.99, 117.86, 61.88, 50.65, 14.40 (2C). $C_{15}H_{14}ClNO_5S$; UPLC-MS acidic (method A) r.t. 1.13 min, purity: >99%. MS (ESI) $m/z = 356.0$ and 358.0 [M+H]$^+$.

Synthesis of (+/-) ethyl 2-[(5Z)-5-[(6-hydroxypyridin-3-yl)

methylidene]-2,4-dioxo-1,3-thiazolidin-3-yl]propanoate (FB42). Compound **FB42** was obtained from compound **7** (100 mg, 0.46 mmol) and 6-hydroxynicotinaldehyde (57 mg, 0.46 mmol), by following the general procedure A (conc. 0.46 M instead of 0.34 M), as a white solid, mp: 249–250 °C (89 mg, 0.28 mmol, 60% overall isolated yield after purification by filtration and trituration). *Purification steps*: After cooling the reaction mixture to toom temperature, the precipitate was recovered by filtration. The filtrate was discarded, while the solid on the filter was washed with water, triturated in DCM and MeOH and dried under *vacuum* to afford the title product. ^{1}H NMR (400 MHz, DMSO-d_6) δ 12.27 (s, 1H), 8.06 (d, $J = 2.8$ Hz, 1H), 7.83 (s, 1H), 7.64 (dd, $J = 9.7$, 2.8 Hz, 1H), 6.49 (d, $J = 9.7$ Hz, 1H), 5.09 (q, $J = 7.1$ Hz, 1H), 4.13 (qq, $J = 7.1$, 3.7 Hz, 2H), 1.49 (d, $J = 7.1$ Hz, 3H), 1.15 (t, $J = 7.1$ Hz, 3H). ^{13}C NMR (100 MHz, DMSO-d_6) δ 168.99, 166.74, 165.18, 161.71, 143.64, 138.83, 131.88, 121.21, 115.23, 112.31, 61.85, 50.62, 14.42 (2C). $C_{14}H_{14}N_2O_5S$; UPLC-MS acidic (method A) r.t. 0.80 min, purity: >99%. MS (ESI) $m/z = 323.1$ [M+H]$^+$

Synthesis of (+/-) ethyl 2-[(5Z)-5-[(4-chloro-3-hydroxyphenyl)methylidene]-2,4-dioxo-1,3thiazolidin-3-yl]propanoate (FB43). Compound **FB43** was obtained from compound **7** (100 mg, 0.46 mmol) and 4-chloro-3-hydroxy-benzaldehyde (72 mg, 0.46 mmol), by following the general procedure A (conc. 0.46 M instead of 0.34 M), as a white solid, mp: 159–160 °C (24 mg, 0.07 mmol, 15% overall isolated yield after purification by reversed phase flash chromatography and then by direct phase flash chromatography); *First column purification:* cartridge: Biotage sfär C18 D 12 g; gradient conditions: MeCN in water, in presence of 0.1% HCOOH, from 2% to 60%, 10 CV; *Second column purification:* cartridge: Biotage sfär Silica D 10 g; gradient conditions: EtOAc in CHX, from 0% to 80%, 12 CV. ^{1}H NMR (400 MHz, DMSO-d_6) δ 10.79 (s, 1H), 7.87 (s, 1H), 7.50 (d, $J = 8.2$ Hz, 1H), 7.21 (d, $J = 2.2$ Hz, 1H), 7.10 (dd, $J = 8.4$, 2.1 Hz, 1H), 5.12 (q, $J = 7.1$ Hz, 1H), 4.14 (qd, $J = 7.1$, 3.1 Hz, 2H), 1.51 (d, $J = 7.2$ Hz, 3H), 1.16 (t, $J = 7.1$ Hz, 3H). ^{13}C NMR (100 MHz, DMSO-d_6) δ 168.92, 166.94, 165.13, 154.18, 133.62, 133.04, 131.26, 123.16, 123.01, 121.21, 117.22, 61.92, 50.75, 14.39, 14.36. $C_{15}H_{14}ClNO_5S$; UPLC-MS acidic (method A) r.t. 1.16 min, purity: >99%. MS (ESI) $m/z = 356.1$ and 358.1 [M+H]$^+$.

Synthesis of (+/-) ethyl 2-[(5Z)-5-[[4-(methanesulfonamido)phenyl]methylene]-2,4-dioxothiazolidin-3-yl]propanoate (FB44). Compound **FB44** was obtained from compound **7** (100 mg, 0.46 mmol) and *N*-(4-formylphenyl)methanesulfonamide (130 mg, 0.65 mmol), by following the general procedure A (conc. 0.23 M instead of 0.34 M), as an amorphous yellow solid (46 mg, 0.116 mmol, 25% overall isolated yield after purification by reversed phase flash chromatography). Cartridge: Biotage sfär C18 D 12 g, gradient conditions: MeCN in water, in presence of 0.1% HCOOH, from 2% to 60%, 10 CV. ^{1}H NMR (400 MHz, DMSO-d_6) δ 10.33 (s, 1H), 7.91 (s, 1H), 7.70-7.56 (m, 2H), 7.39-7.26 (m, 2H), 5.11 (q, $J = 7.1$ Hz, 1H), 4.14 (qt, $J = 7.1$, 3.6 Hz, 2H), 3.09 (s, 3H), 1.51 (d, $J = 7.2$ Hz, 3H), 1.16 (t, $J = 7.1$ Hz, 3H). ^{13}C NMR (100 MHz, DMSO-d_6) δ 168.98, 167.15, 165.28, 141.77, 134.08, 132.39 (2C), 127.62, 119.10 (2C), 118.64, 61.88, 50.66, 40.61, 14.39 (2C). $C_{16}H_{18}N_2O_6S_2$; UPLC-MS acidic (method A) r.t. 1.03 min, purity: 95%. MS (ESI) $m/z = 399.1$ [M+H]$^+$.

Synthesis of (+/-) ethyl 2-[(5Z)-5-[(3,5-dichloro-4-hydroxy-phenyl)methylene]-2,4-dioxothiazolidin-3-yl]propanoate (FB45). Compound **FB45** was obtained from compound **7** (100 mg, 0.46 mmol) and 3,5-dichloro-4-hydroxy-benzaldehyde (88 mg, 0.46 mmol), by following the general procedure A (conc. 0.4 M instead of 0.34 M), as a pale orange solid, mp: 166–167 °C (94 mg, 0.24 mmol, 52% overall isolated yield after purification by reversed phase flash chromatography). *Purification steps*: After cooling the reaction mixture to toom temperature, the precipitate was recovered by filtration. The filtrate was discarded, while the solid on the filter was washed with water, followed by DCM and MeOH. The residue was further purified by reversed phase flash chromatography (cartridge: Biotage sfär C18 D 12 g; gradient conditions: MeCN in water, in presence of 0.1% HCOOH, from 2% to 100%, 10 CV) affording the title compound **FB45**. ^{1}H NMR (400 MHz, DMSO-d_6) δ 11.18 (s, 1H),

7.88 (s, 1H), 7.64 (s, 2H), 5.11 (q, J = 7.1 Hz, 1H), 4.13 (qt, J = 7.1, 3.6 Hz, 2H), 1.51 (d, J = 7.1 Hz, 3H), 1.16 (t, J = 7.1 Hz, 3H). ^{13}C NMR (100 MHz, DMSO-d_6) δ 168.91, 166.60, 165.01, 151.93, 132.18, 130.80 (2C), 125.96, 123.36 (2C), 120.01, 61.91, 50.77, 14.38 (2C). $C_{15}H_{13}Cl_2NO_5S$; UPLC-MS acidic (method A) r.t. 1.29 min, purity: 99%. MS (ESI) m/z = 389.9 and 391.9 [M+H] $^+$.

Synthesis of (+/−)-ethyl 2-[(5Z)-5-[(4-fluoro-3-hydroxy-phenyl)methylene]-2,4-dioxothiazolidin-3-yl]propanoate (FB46). Compound **FB46** was obtained from compound **7** (100 mg, 0.46 mmol) and 4-fluoro-3-hydroxy-benzaldehyde (65 mg, 0.46 mmol), by following the general procedure A (conc. 0.46 M instead of 0.34 M), as a pale-yellow solid, mp: 135–136 °C (122 mg, 0.36 mmol, 78% overall isolated yield after purification by direct phase flash chromatography); Cartridge: Biotage sfär Silica D 10 g, gradient conditions: EtOAc in CHX, from 0% to 40%, 10 CV. ^{1}H NMR (400 MHz, DMSO-d_6) δ 10.49 (s, 1H), 7.88 (s, 1H), 7.32 (dd, J = 11.1, 8.4 Hz, 1H), 7.23 (dd, J = 8.4, 2.3 Hz, 1H), 7.12 (ddd, J = 8.6, 4.3, 2.4 Hz, 1H), 5.11 (q, J = 7.1 Hz, 1H), 4.13 (qq, J = 6.9, 3.7 Hz, 2H), 1.51 (d, J = 7.2 Hz, 3H), 1.16 (t, J = 7.1 Hz, 3H). ^{13}C NMR (100 MHz, DMSO-d_6) δ 168.94, 167.04, 165.17, 151.63 and 154.10 ($^1J_{CF}$ = 247 Hz), 146.26 and 146.14 ($^3J_{CF}$ = 12.0 Hz), 133.89, 130.07, 123.17, 120.19, 119.02, 117.78 and 117.59 ($^2J_{CF}$ = 19.0 Hz), 61.91, 50.71, 14.38 (2C). $C_{15}H_{14}FNO_5S$; UPLC-MS acidic (method A) r.t. 1.10 min, purity: >99%. MS (ESI) m/z = 340.1 [M+H] $^+$.

Synthesis of (+/−) ethyl 2-[(5Z)-5-[(3,5-difluoro-4-hydroxy-phenyl)methylene]-2,4-dioxothiazolidin-3-yl]propanoate (FB47). Compound **FB47** was obtained from compound **7** (70 mg, 0.32 mmol) and 3,5-difluoro-4hydroxy-benzaldehyde (51 mg, 0.32 mmol), by following the general procedure A, as a pale-yellow solid, mp: 137–138 °C (75 mg, 0.21 mmol, 65% overall isolated yield after purification by reversed phase column chromatography). Cartridge: Biotage sfär C18 D 12 g, gradient conditions: MeCN in water, in presence of 0.1% HCOOH, from 2% to 100%, 10 CV. ^{1}H NMR (400 MHz, DMSO-d_6) δ 11.28 (s, 1H), 7.89 (s, 1H), 7.44-7.29 (m, 2H), 5.12 (q, J = 7.1 Hz, 1H), 4.14 (qq, J = 7.1, 3.7 Hz, 2H), 1.51 (d, J = 7.1 Hz, 3H), 1.16 (t, J = 7.1 Hz, 3H). ^{13}C NMR (100 MHz, DMSO-d_6) δ 168.92, 166.75, 165.08, 151.38 and 153.80 ($^1J_{CF}$ = 242 Hz). 151.45 and 153.87 ($^1J_{CF}$ = 242 Hz), 137.22, 132.80, 123.40, 119.90, 114.43 and 114.58 ($^2J_{CF}$ = 15.0 Hz), 114.35 and 114.51 ($^2J_{CF}$ = 17.0 Hz), 61.91, 50.74, 14.38 (2C). $C_{15}H_{13}F_2NO_5S$; UPLC-MS acidic r.t. 1.16 min, purity: >99%. MS (ESI) m/z = 358.0 [M+H] $^+$.

Preparation of (+/−)-(Z)-3-(1-morpholino-1-oxopropan-2-yl)-5-(4-morpholinobenzylidene)thiazolidine-2,4-dione (FB48). Compound **FB48** was obtained from compound **13** (60 mg, 0.23 mmol) and 4-(4-morpholinyl)benzaldehyde (44 mg, 0.23 mmol), by following the general procedure A, as a pale yellow solid, mp: 206–207 °C (53 mg, 0.124 mmol, 53% yield), purified by reversed phase FC on a C18 column (using as eluent a gradient of MeCN in water, in presence of 0.1% formic acid, from 2% to 100%, 10 CV). ^{1}H NMR (400 MHz, DMSO-d_6) δ 7.82 (s, 1H), 7.50 (d, J = 9.0 Hz, 2H), 7.14-7.04 (m, 2H), 5.22 (q, J = 7.0 Hz, 1H), 3.78-3.67 (m, 4H), 3.66-3.43 (m, 5H), 3.42 -3.31 (m, 3H), 3.32-3.26 (m, 4H), 1.51 (d, J = 7.1 Hz, 3H). ^{13}C NMR (100 MHz, DMSO-d_6) δ: 167.26, 166.93, 165.72, 152.71, 134.56, 132.70 (2C), 122.67, 114.79, 114.63 (2C), 66.26 (2C), 50.39, 47.15 (2C), 45.96 (2C), 42.87 (2C), 15.09. $C_{21}H_{25}N_3O_5S$; UPLC-MS acidic (method A) r.t 0.95 min, purity: >99%. MS (ESI) m/z = 432.1 [M+H]$^+$.

Preparation of (+/−)-(5Z)-5-[(2,3-dihydroxyphenyl)methylene]-3-(1-methyl-2-morpholino-2-oxo-ethyl) thiazolidine-2,4-dione (FB49). Compound **FB49** was obtained from compound **13** (40 mg, 0.16 mmol) and 2,3-dihydroxybenzaldehyde (22 mg, 0.16 mmol), by following the general procedure A (conc. 0.16 M instead of 0.34 M), as an amorphous brown solid (13 mg, 0.034 mmol, 22% overall isolated yield after purification by reversed phase flash chromatography). Cartridge: Biotage sfär C18 D 12 g, gradient conditions: MeCN in water, in presence of 0.1% HCOOH, from 2% to 80%, 10 CV. ^{1}H NMR (400 MHz, DMSO-d_6) δ 9.61 (s, 1H), 8.16 (s, 1H), 6.91 (dd, J = 7.6, 1.7 Hz, 1H), 6.84 (dd, J = 8.0, 1.7 Hz, 1H), 6.78 (t, J = 7.8 Hz, 1H), 5.24 (q, J = 7.1 Hz, 1H), 3.63-3.43 (m, 6H), 3.43-3.36 (m, 2H), 1.52 (d, J = 7.1 Hz, 3H). ^{13}C NMR (100 MHz,

DMSO-d_6) δ 167.53, 166.90, 165.83, 146.64, 146.33, 129.72, 120.88, 120.17, 119.13, 119.00, 118.26, 66.50 (2C), 50.51, 45.94, 42.87, 15.04. $C_{17}H_{18}N_2O_6S$; UPLC-MS acidic (method A) r.t. 0.80 min, purity: 98%. MS (ESI) m/z = 379.1 [M+H] $^+$.

Preparation of (+/−)-(Z)-3-(1-morpholino-1-oxopropan-2-yl)-5-(4-(pyrrolidin-1-yl)benzylidene)thiazolidine-2,4-dione (FB50). Compound **FB50** was obtained from compound **13** (60 mg, 0.23 mmol) and 4-(1-pyrrolidinyl)benzaldehyde (41 mg, 0.23 mmol), by following the general procedure A, as an orange solid, mp: 157–158 °C (49 mg, 0.118 mmol, 51% yield), purified by reversed phase FC on a C18 column (using as eluent a gradient of MeCN in water, in presence of 0.1% formic acid, from 2% to 100%, 10 CV). ^{1}H NMR (400 MHz, CDCl$_3$) δ 7.83 (s, 1H), 7.45-7.35 (m, 2H), 6.65-6.55 (m, 2H), 5.12 (q, J = 7.0 Hz, 1H), 3.82-3.48 (m, 6H), 3.42-3.35 (m, 4H), 3.35-3.16 (m, 2H), 2.14-2.01 (m, 4H), 1.61 (d, J = 7.0 Hz, 3H). ^{13}C NMR (100 MHz, DMSO-d_6) δ: 167.35, 166.97, 165.69, 149.65, 135.40, 133.18 (2C), 119.67, 112.71 (2C), 111.84, 66.51, 66.36, 50.17, 47.76 (2C), 45.92, 42.87, 25.37 (2C), 15.16. $C_{21}H_{25}N_3O_4S$; UPLC-MS acidic (method A) r.t 1.18 min, purity: 95%. MS (ESI) m/z = 416.1 [M+H]$^+$.

Synthesis of (+/−)-ethyl 2-[(5Z)-5-(1H-benzimidazol-5-ylmethylene)-2,4-dioxo-thiazolidin-3-yl] propanoate (FB51). Compound **FB51** was obtained from compound **7** (60 mg, 0.28 mmol) and 1H-benzimidazole-5-carbaldehyde (40 mg, 0.28 mmol), by following the general procedure A (conc. 0.14 M instead of 0.34 M), as a pale-yellow solid, mp: 148–149 °C (56 mg, 0.162 mmol, 59% overall isolated yield after purification by trituration in DCM). ^{1}H NMR (400 MHz, DMSO-d_6) δ 12.76 (s, 1H), 8.38 (s, 1H), 8.14 (s, 1H), 7.93 (d, J = 1.7 Hz, 1H), 7.75 (d, J = 8.4 Hz, 1H), 7.50 (dd, J = 8.5, 1.8 Hz, 1H), 5.13 (q, J = 7.1 Hz, 1H), 4.15 (qd, J = 7.1, 2.9 Hz, 2H), 1.52 (d, J = 7.1 Hz, 3H), 1.17 (t, J = 7.1 Hz, 3H). ^{13}C NMR (100 MHz, DMSO-d_6) δ 169.02, 167.26, 165.33, 145.18, 136.13 (2C), 130.82, 127.05, 124.91, 124.81, 120.77, 118.09, 61.89, 50.65, 14.43 (2C). $C_{16}H_{15}N_3O_4S$; UPLC-MS acidic (method A) r.t. 0.73 min, purity:>99%. MS (ESI) m/z = 346.1 [M+H] $^+$.

Synthesis of (+/−)-ethyl 2-[(5Z)-2,4-dioxo-5-[(3-oxo-4H-1,4-benzoxazin-6-yl)methylene] thiazolidin-3-yl]propanoate (FB52). Compound **FB52** was obtained from compound **7** (80 mg, 0.37 mmol) and 3-oxo-4H-1,4-benzoxazine-6-carbaldehyde (65 mg, 0.37 mmol), by following the general procedure A (conc. 0.18 M instead of 0.34 M), as a pale-yellow solid, mp: 189–190 °C (73 mg, 0.194 mmol, 53% overall isolated yield after purification direct phase flash chromatography). Cartridge: Biotage sfär Silica D 25 g, gradient conditions: EtOAc in CHX, from 0% to 50%, 10 CV. ^{1}H NMR (400 MHz, DMSO-d_6) δ 10.92 (s, 1H), 7.88 (s, 1H), 7.28 (dd, J = 8.5, 2.2 Hz, 1H), 7.17 (d, J = 2.2 Hz, 1H), 7.10 (d, J = 8.4 Hz, 1H), 5.11 (q, J = 7.1 Hz, 1H), 4.69 (s, 2H), 4.14 (qq, J = 6.9, 3.7 Hz, 2H), 1.51 (d, J = 7.2 Hz, 3H), 1.16 (t, J = 7.1 Hz, 3H). ^{13}C NMR (100 MHz, DMSO-d_6) δ 167.58, 165.82, 163.88, 141.46, 133.51, 132.31 (2C), 127.83, 119.32 (2C), 119.11, 66.37 (2C), 44.99 (2C), 43.00, 42.40. $C_{17}H_{16}N_2O_6S$; UPLC-MS acidic (method A) r.t. 1.03 min, purity: 99%. MS (ESI) m/z = 377.1 [M+H] $^+$.

Synthesis of N-[4-[(Z)-[3-(2-morpholino-2-oxo-ethyl)-2,4-dioxo-thiazolidin-5-ylidene] methyl]phenyl]methanesulfonamide (FB53). To a stirring solution of compound **5** (149 mg, 0.5 mmol) and N-(4-formylphenyl)methanesulfonamide (140 mg, 0.7 mmol) in ethanol (4 mL), piperidine (30 μL, 0.350 mmol) was added and the resulting mixture was heated under reflux for 3 h. After cooling the reaction mixture to room temperature, the yellow precipitate was recovered by filtration. The filtrate was discarded and the solid on the filter was washed with EtOH and then further purified by trituration in MeOH to afford compound **FB53** (14.5 mg, 0.034 mmol, 5% yield) as a pale-yellow solid, mp: >300 °C. ^{1}H NMR (400 MHz, DMSO-d_6) δ 10.30 (s, 1H), 7.89 (s, 1H), 7.66-7.59 (m, 2H), 7.37-7.27 (m, 2H), 4.61 (s, 2H), 3.64 (t, J = 4.7 Hz, 2H), 3.58 (t, J = 4.8 Hz, 2H), 3.58-3.51 (m, 2H), 3.44 (t, J = 4.7 Hz, 2H), 3.09 (s, 3H). ^{13}C NMR (100 MHz, DMSO-d_6) δ 167.58, 165.82, 163.88, 141.46, 133.51, 132.31 (2C), 127.83, 119.32, 119.11 (2C), 66.37 (2C), 44.99, 43.01, 42.40, 40.61. $C_{17}H_{19}N_3O_6S_2$; UPLC-MS acidic (method A) r.t. 0.77 min, purity: 99%. MS (ESI) m/z =

426.2 [M+H] $^+$.

Synthesis of (5Z)-5-[(3,5-dichloro-4-hydroxy-phenyl)methylene]-3-(2-morpholino-2-oxoethyl)thiazolidine-2,4-dione (FB54). To a stirring solution of compound **5** (70 mg, 0.23 mmol) and 3,5-dichloro-4-hydroxy-benzaldehyde (44 mg, 0.23 mmol) in ethanol (0.6 mL), piperidine (10 μL, 0.12 mmol) was added and the resulting mixture was heated under reflux for 3 h. After cooling the reaction mixture to room temperature, the yellow precipitate was recovered by filtration, the filtrate was discarded and then the solid on the filter was washed with EtOH. To remove the residual traces of piperazine present in the batch (detected by NMR), the solid was washed with NH_4Cl_{ss}, water and MeCN and then dried under *vacuum* at 50 °C for 5 h. To remove the residual traces of NH_4Cl (detected by NMR), the solid was taken up with water and sonicated for 20 min. Then the solid precipitate was recovered by filtration and dried under *vacuum* at 50 °C for 18 h to afford the title compound **6a** (46 mg, 0.11 mmol, 47% yield) as a pale yellow solid, mp: >300 °C. ^{1}H NMR (400 MHz, DMSO-d_6) δ 7.85 (s, 1H), 7.64 (s, 2H), 4.61 (s, 2H), 3.67-3.61 (m, 2H), 3.60-3.56 (m, 2H), 3.56-3.51 (m, 2H), 3.46-3.41 (m, 2H). ^{13}C NMR (100 MHz, DMSO-d_6) δ 167.02, 165.54, 163.79, 151.75, 131.66, 130.74 (2C), 126.13, 123.33 (2C), 120.64, 66.37 (2C), 44.99, 43.09, 42.41. $C_{16}H_{14}Cl_2N_2O_5S$; UPLC-MS acidic (method A) r.t. 0.99 min, purity: 99%. MS (ESI) $m/z = 417.1$ [M+H] $^+$.

4.2. Biological assays

4.2.1. Human BAG3 production

Human HEK-293T cell line was transient transfected through chemical method, based on plasmid DNA co-precipitation with calcium phosphate in 2X HBS solution (274 mM NaCl, 10 mM KCl, 1.4 mM Na2HPO4, 15 mM D-glucose, 42 mM HEPES; pH = 7.05–7.06), to introduce the pCDNA3.1 C-*ter* His-tagged BAG3 plasmid (namely BAG3-His, Genscript, Piscataway NJ). The day after the transfection, cell culture medium was removed and replaced with fresh complete DMEM, then 48 h following cells were harvested for protein collection.

4.2.2. C-terminus His-tagged BAG3 expression and purification

The cell lysate was loaded into a HisTrap™ column (Cytiva, Marlborough, MA, USA) previously equilibrated with 30 mM tris, pH = 8.3, and 20 mM imidazole, and the C-ter His-tagged BAG3 was then eluted using an imidazole linear gradient (from 20 to 500 mM). To ensure high final purity, the BAG3-His was further purified by Size Exclusion Chromatography (SEC) on a HiLoad™ 16/60 Superdex™ 75 prep grade column (Cytiva Marlborough, MA, USA), equilibrated with 50 mM sodium phosphate, pH 7.8, 150 mM NaCl, and 0.04% (w/v) NaN3.

4.2.3. Ligand binding analysis by nuclear magnetic resonance

All the NMR experiments were acquired at 298 K on a Bruker 600 MHz spectrometer equipped with an autosampler (69 samples). and a nitrogen-cooled cryoprobe and they were processed and analyzed by Topspin 4.3.1 (Bruker BioSpin GmbH. Rheinstetten. Germany).

Compounds were tested against BAG3-His performing Saturation Transferred Difference (STD) [23] and Water-Ligand Observed via Gradient SpectroscopY (WaterLOGSY) [24] experiments both in the absence and in the presence of the protein. A control experiment was carried out with **FB12** as lead compound. The NMR samples were prepared in 50 mM sodium phosphate, pH 7.8, 150 mM NaCl, and 0.04% (w/v) NaN3, and consisted of 125 μM compound in 1.3% deuterated-DMSO. 5% (v/v) deuterated water, and 5 μM BAG3-His. The WaterLOGSY experiments were acquired with 240 scans, a recovery delay of 4.5 s before each scan, and a mixing time of 1.5 s. They were performed with a 180° inversion pulse applied to the water signal at 4.7 ppm using a Gaussian-shaped selective pulse of 7.5 ms. STD experiments were acquired with 256 scans, and a recovery delay of 2 s before each scan. Selective saturation of the protein at 0.4 ppm was achieved by a 2.5 ms pulse train (60 Gaussian pulses of 50 ms separated by an inter-pulse delay of 1 ms) included in the relaxation delay, and a 25 ms

spin-lock was used to remove the broad residual protein signal. In both experiments, water suppression was achieved by the excitation sculpting pulse scheme [25]. For the STD experiments, the STD effect (STD_f) for the different groups of protons of the compounds was quantified according to the following equation:

$$STD_f = \frac{I_{(+p)} - I_{(-p)}}{I_0}$$

where $I_{(+p)}$. and $I_{(-p)}$ are the peak integral in the STD spectrum in the presence and in the absence of the protein respectively. while I_0 is the peak integral of the corresponding peak in the off-resonance spectrum in the presence of the protein. The strongest STD signal in the spectrum was set to the value of 100% and used as reference to calculate relative STD effects accordingly.

4.2.4. Surface Plasmon Resonance (SPR)

A BIAcore X100 instrument and research-grade CM4 carboxyl-methyl-dextran-coated sensorchips (Cytiva, Westborough, MA, USA) were used. Purified, His-tagged BAG3 protein was immobilized onto the CM4 sensorchip by the amine coupling procedure. Briefly, BAG3-His resuspended at 60 μg/mL in 10 mM acetate pH 2.8 was injected for 10 min at 10 μL/min onto one of the two flow cells of the sensorchip that has been previously activated with a mixture of 1-ethyl-3-(3-dimethyla-minopropyl) carbodiimide hydrochloride (0.2 M) and N-hydroxy-suc-cinimide (0.5 M). The surface was then deactivated with ethanolamine. The immobilization procedure led to the immobilization of 2.400 RU (equal to 19 femtomol/mm^2 of BAG3-His). The second flow cell was subjected to the activation and deactivation procedure in the absence of any protein and was used to evaluate aspecific binding and for blank subtraction. The BAG3 containing sensorchip was firstly used to screen the whole set of synthesized compounds for their BAG3-binding capacity: each compound was resuspended at 50 μM in PBS containing 5% DMSO and 0,05% surfactant P20 (binding buffer), injected onto the sensorchip for 90s at 30 μL/min (to allow their association to immobilized-BAG) and then washed with binding buffer until dissociation was observed. Then, the sensorchip was regenerated by a 15s wash at 30 μL/min of 10 mM Glycine pH 3 and re-equilibrated with binding buffer for subsequent analyses. The amount of compound that specifically bound to the immobilized BAG3 was measured as resonance unit (RU). As expected, the injection of compounds caused relevant increase of RU on both the BAG3-containing and the void flow cells, since the small molecules are resuspended in DMSO [26]. Nevertheless, the high aspecific signal does not hamper the determination of the specific compound-BAG3 interaction when the sensorgram is blank-subtracted. The analyses were repeated 3–10 times for each compound. Only those compounds that showed an average binding to BAG3 higher than 5.0 RU were then subjected to a complete dose-dependent assays aimed at evaluating the dissociation constant (Kd) value, that is inversely proportional to the affinity binding. The single cycle model was adopted that allows the performing of a series of injections without the harsh regeneration procedure, as to preserve the integrity and binding capacity of the immobilized BAG3 protein [27]. In detail, increasing concentrations of each selected compound were injected onto the BAG3-containing sensorchip at a flow rate of 30 μL/min and then washed as described above. The Kd value (that is inversely proportional to the binding affinity) was calculated by steady state analyses performed by fitting the proper form of Scatchard's equation for the plot of the bound RU at equilibrium *versus* the compound concentration in solution using the non-linear curve fitting software package X100 evaluation 2.0.1 embedded in the BIAcore X-100 instrument.

4.2.5. Cell cultures

RS4;11 B-lymphobastic leukemia cells and HD-MB03 medulloblastoma cell line were grown in RPMI-1640 medium, while A549 non-small lung adenocarcinoma cells were grown in the DMEM medium (all

purchased from Gibco, Milan, Italy). Both media were supplemented with 115 units/mL of penicillin G, 115 μg/mL of streptomycin, and 10% foetal bovine serum (FBS, all purchased from Invitrogen, Milan, Italy). Stock solutions (10 mM) of the different compounds were obtained by dissolving them in DMSO.

4.2.6. Compound screening and drug synergism

4.2.6.1. Cell seeding and drug screening.
Briefly, 2000 cells per well were seeded in 384-well plates in 27 μl of complete growth medium. After 24h, cells were treated with 3 μl of 10x BAG3 inhibitors. Each compound was tested in a 6-points 2-fold dose-response curve, and each dose was tested in duplicate within each plate, in two independent experiments. For drug synergism, cells were treated with 3 μl of 10x **FB49** as single agent or in combination with 3 μl of 10x VECC chemotherapy cocktail in a 6x6 matrix design. One Unit (1U) of VECC was determined as 2.5 nM Vincristine, 1 μM Etoposide, 1.8 μM Cisplatin, 6 μM Cyclophosphamide. Each drug was tested in a 6-points 2-fold dose-response curves, and each dose was tested in duplicate within each plate, in two independent experiments. A gas-permeable sealing membranes (Breathe-Easy, Merck, Readington Township, NJ) was used to avoid evaporation during treatment incubation. After 72 h of treatment, 3ul of resazurin (10x) was added to each well to reach a final concentration of 44 μM, incubated for 3 at 37 °C, and then the fluorescence signal was measured at 590 nm using a multi-well plate reader (Spark, Tecan, Männedorf, Switzerland). To ensure treatment reproducibility, all procedures, including cell seeding, drug dilutions, cell treatment and application of resazurin solution, were carried out through a 96-channel robotic liquid handler (Microlab STAR 96-CORE, Hamilton, Bonaduz, Switzerland).

4.2.6.2. Plate quality control.
The Z-prime (Z') quality control metrics was calculated for each plate to measure the separation between the positive control (POS, 1 μM Bortezomib) and negative control (NEG, 0.5% DMSO). For this screening, only plates with acceptable quality metrics (Z' > 0.5) were further analyzed.

4.2.6.3. Data analysis.
Raw data were normalized according to the following equation: cell viability (%) = (x−POS)/(NEG−POS)*100, where x is the relative fluorescence units (RFU) collected from each single well, NEG is the mean of intraplate negative controls, and POS is the mean of intraplate positive controls. Normalized data were then processed with R 3.6.3 and Rstudio Version March 1, 1056 using GRmetrics package to draw dose-response curves [28], and Synergy-Finder R package to finally compute the Highest Single Agent (HSA) synergy score for all technical replicates per dose per drug combination, according to the formula

$$y_{HSA} = \max(y1, y2)$$

where *y1* and *y2* are the monotherapy effect of combined drug 1 and drug 2 [21].

4.2.7. Antiproliferative assays in non-tumoral cells
To evaluate cytotoxicity on normal tissue, the lead compound and the reference compound were also tested in Peripheral Blood Mononuclear Cells (PBMC) collected from healthy donors as described previously [29].

4.2.8. Western Blot analysis
HD-MB03 cells were lysed on ice for 30 min using M-PER™ Mammalian Protein Extraction Reagent (Thermo Scientific, Waltham, MA, USA) added with Halt™ Protease and Phosphatase Inhibitor Cocktail 100X (Thermo Scientific, Waltham, MA, USA), then lysates were centrifuged at $15000 \times g$ at 4 °C for 10 min. The protein concentration was determined using the BCA Protein Assay (Pierce, Italy). Equal amounts of protein (10 μg) were resolved using sodium dodecyl sulfate-polyacrylamide gel electrophoresis (SDS-PAGE) (Criterion Precast, BioRad, Italy) and transferred to a PVDF Hybond-P membrane (GE Healthcare). Membranes were blocked with a bovine serum albumin solution (5% in Tween PBS 1X), the membranes being gently rotated overnight at 4 °C. Membranes were then incubated with primary antibodies against BAG3 (1:1000 LifeSpan Biosciences, Seattle, Washington USA) (for 2 h at room temperature. Membranes were next incubated with peroxidase labeled secondary antibodies for 60 min. All membranes were visualized using ECL Select (GE Healthcare), and images were acquired using the iBright FL1500 Imaging System (Thermo Fisher Scientific, Waltham, MA, USA). Anti-Vinculin (1:25000, Santa Cruz Biotechnology, Dallas, TX, USA) and Coomassie staining (Thermo Fisher Scientific, Waltham, MA, USA) were used as loading controls.

4.2.9. Cell cycle analysis
HD-MB03 cells were treated with the lead compound for 24 h, harvested, and then fixed with 70% (v/v) ice-cold ethanol. Cells were lysed with 0.1% (v/v) Triton X-100 containing 10 μg/ml RNase A and stained with 25 μg/ml of Propidium Iodide (PI). Samples were then analyzed by Cytomics FC500 instrument (Beckman Coulter, Brea, California, USA) and MultiCycle software (Phoenix Flow Systems, San Diego California, USA).

4.2.10. Annexin V-PI flow cytometric analysis
HD-MB03 cells were treated with the lead compound for the indicated time point, and then stained with both Propidium Iodide (PI) to stain DNA, and Annexin V-fluorescein isothiocyanate to stain membrane Phosphatidylserine (PS) exposed on the cell surface of apoptotic cells, according to manufacturer's instructions (Roche Diagnostics, Milan, Italy). The BD FACSCelesta™ Flow Cytometer (BD Bioscience USA) was used for the measurements.

4.2.11. Live cells imaging for autophagy evaluation
HD-MB03 cells were transfected with pmTorquoise2-LC3 (1 μg/μL) using TransIT-LT1 Transfection reagent according to manufacturer's instructions (Mirus, Madison, WI). After 24h, cells were treated with FB-49 (20 μM) alone and in combination with Chloroquine (100 μM), and 24h later cellular acidic compartments were stained incubating live cells with 50 nM LysoTracker Red DND-99 (Thermo Scientific, Waltham, MA, USA) and with 10 μM Hoechest-33342 (Thermo Scientific, Waltham, MA, USA) in Phosphate Buffered Saline (PBS, Biosera Cholet, France) for 30 min. After staining, cells were washed twice and then acquired with ZEISS LMS800 confocal microscope.

Declaration of competing interest

The authors declare that they have no known competing financial interests or personal relationships that could have appeared to influence the work reported in this paper.

Data availability

No data was used for the research described in the article.

Appendix A. Supplementary data

Supplementary data to this article can be found online at https://doi.org/10.1016/j.ejmech.2023.115824.

References

[1] E. Mariotto, G. Viola, C. Zanon, S. Aveic, A BAG's life: every connection matters in cancer, Pharmacol. Ther. 209 (2020), 107498.

[2] E. Sturner, C. Behl, The role of the multifunctional BAG3 protein in cellular protein quality control and in disease, Front. Mol. Neurosci. 10 (2017) 177.

[3] C. Behl, Breaking BAG: the Co-chaperone BAG3 in health and disease, Trends Pharmacol. Sci. 37 (2016) 672–688.

[4] L. Guerriero, G. Palmieri, M. De Marco, A. Cossu, P. Remondelli, M. Capunzo, M. C. Turco, A. Rosati, The anti-apoptotic BAG3 protein is involved in BRAF inhibitor resistance in melanoma cells, Oncotarget 8 (2017) 80393–80404.

[5] M. Festa, L. Del Valle, K. Khalili, R. Franco, G. Scognamiglio, V. Graziano, V. De Laurenzi, M.C. Turco, A. Rosati, BAG3 protein is overexpressed in human glioblastoma and is a potential target for therapy, Am. J. Pathol. 178 (2011) 2504–2512.

[6] S. Staibano, M. Mascolo, M. Di Benedetto, M.L. Vecchione, G. Ilardi, G. Di Lorenzo, R. Autorino, V. Salerno, A. Morena, A. Rocco, M.C. Turco, E. Morelli, BAG3 protein delocalisation in prostate carcinoma, Tumour Biol 31 (2010) 461–469.

[7] H. Shi, H. Xu, Z. Li, Y. Zhen, B. Wang, S. Huo, R. Xiao, Z. Xu, BAG3 regulates cell proliferation, migration, and invasion in human colorectal cancer, Tumour Biol 37 (2016) 5591–5597.

[8] H. Zhu, W. Wu, Y. Fu, W. Shen, K. Miao, M. Hong, W. Xu, K.H. Young, P. Liu, J. Li, Overexpressed BAG3 is a potential therapeutic target in chronic lymphocytic leukemia, Ann. Hematol. 93 (2014) 425–435.

[9] K. Koya, Y. Li, H. Wang, T. Ukai, N. Tatsuta, M. Kawakami, Shishido, L.B. Chen, MKT-077, a novel rhodacyanine dye in clinical trials, exhibits anticarcinoma activity in preclinical studies based on selective mitochondrial accumulation, Cancer Res. 56 (1996) 538–543.

[10] Y. Miyata, X. Li, H.F. Lee, U.K. Jinwal, S.R. Srinivasan, S.P. Seguin, Z.T. Young, J. L. Brodsky, C.A. Dickey, D. Sun, J.E. Gestwicki, Synthesis and initial evaluation of YM-08, a blood-brain barrier permeable derivative of the heat shock protein 70 (Hsp70) inhibitor MKT-077, which reduces tau levels, ACS Chem. Neurosci. 4 (2013) 930–939.

[11] X. Li, T. Colvin, J.N. Rauch, D. Acosta-Alvear, M. Kampmann, B. Dunyak, B. Hann, B.T. Aftab, M. Murnane, M. Cho, P. Walter, J.S. Weissman, M.Y. Sherman, J. E. Gestwicki, Validation of the Hsp70-Bag3 protein-protein interaction as a potential therapeutic target in cancer, Mol. Cancer Therapeut. 14 (2015) 642–648.

[12] S. Terracciano, G. Lauro, A. Russo, M.C. Vaccaro, A. Vassallo, M. De Marco, B. Ranieri, A. Rosati, M.C. Turco, R. Riccio, G. Bifulco, I. Bruno, Discovery and synthesis of the first selective BAG domain modulator of BAG3 as an attractive candidate for the development of a new class of chemotherapeutics, Chem. Commun. 54 (2018) 7613–7616.

[13] M. Yang, J. Huang, R. Simon, L.-X. Wang, A.D. MacKerell, Conformational heterogeneity of the HIV envelope glycan shield, Sci. Rep. 7 (2017) 4435.

[14] A.C. Walls, M.A. Tortorici, B. Frenz, J. Snijder, W. Li, F.A. Rey, F. DiMaio, B.-J. Bosch, D. Veesler, Glycan shield and epitope masking of a coronavirus spike protein observed by cryo-electron microscopy, Nat. Struct. Mol. Biol. 23 (2016) 899–905.

[15] G. Vergoten, C. Bailly, N-glycosylation of High Mobility Group Box 1 protein (HMGB1) modulates the interaction with glycyrrhizin: a molecular modeling study, Comput. Biol. Chem. 88 (2020), 107312.

[16] D. Ruggiero, S. Terracciano, G. Lauro, M. Pecoraro, S. Franceschelli, G. Bifulco, I. Bruno, Structural refinement of 2,4-thiazolidinedione derivatives as new anticancer agents able to modulate the BAG3 protein, Molecules 27 (2022).

[17] A. Rosati, A. Basile, A. Falco, M. d'Avenia, M. Festa, V. Graziano, V. De Laurenzi, C. Arra, M. Pascale, M.C. Turco, Role of BAG3 protein in leukemia cell survival and response to therapy, Biochim. Biophys. Acta Rev. Canc 1826 (2012) 365–369.

[18] M.F. Romano, M. Festa, G. Pagliuca, R. Lerose, R. Bisogni, F. Chiurazzi, G. Storti, S. Volpe, S. Venuta, M.C. Turco, A. Leone, BAG3 protein controls B-chronic lymphocytic leukaemia cell apoptosis, Cell Death Differ. 10 (2003) 383–385.

[19] D. Yang, J. Zhou, H. Wang, Y. Wang, G. Yang, Y. Zhang, High expression of BAG3 predicts a poor prognosis in human medulloblastoma, Tumor Biol. 37 (2016) 13215–13224.

[20] V. Kumar, V. Kumar, T. McGuire, D.W. Coulter, J.G. Sharp, R.I. Mahato, Challenges and recent advances in medulloblastoma therapy, Trends Pharmacol. Sci. 38 (2017) 1061–1084.

[21] M.C. Berenbaum, What is synergy? Pharmacol. Rev. 41 (1989) 93–141.

[22] D. Kögel, B. Linder, A. Brunschweiger, S. Chines, C. Behl, At the crossroads of apoptosis and autophagy: multiple roles of the Co-chaperone BAG3 in stress and therapy resistance of cancer, Cells 9 (2020) 574.

[23] M. Mayer, B. Meyer, Characterization of ligand binding by saturation transfer difference NMR spectroscopy, Angew Chem. Int. Ed. Engl. 38 (1999) 1784–1788.

[24] C. Dalvit, G. Fogliatto, A. Stewart, M. Veronesi, B. Stockman, WaterLOGSY as a method for primary NMR screening: practical aspects and range of applicability, J. Biomol. NMR 21 (2001) 349–359.

[25] T.L. Hwang, A.J. Shaka, Water suppression that works. Excitation sculpting using arbitrary wave-forms and pulsed-field gradients, J. Magn. Reson., Ser. A 112 (1995) 275–279.

[26] P. D'Ursi, M. Uggeri, C. Urbinati, E. Millo, G. Paiardi, L. Milanesi, R.C. Ford, J. Clews, X. Meng, P. Bergese, A. Ridolfi, N. Pedemonte, P. Fossa, A. Orro, M. Rusnati, Exploitation of a novel biosensor based on the full-length human F508del-CFTR with computational studies, biochemical and biological assays for the characterization of a new Lumacaftor/Tezacaftor analogue, Sensor. Actuator. B Chem. 301 (2019), 127131.

[27] H.H. Trutnau, New multi-step kinetics using common affinity biosensors saves time and sample at full access to kinetics and concentration, J. Biotechnol. 124 (2006) 191–195.

[28] M. Hafner, M. Niepel, M. Chung, P.K. Sorger, Growth rate inhibition metrics correct for confounders in measuring sensitivity to cancer drugs, Nat. Methods 13 (2016) 521–527.

[29] F.F. Castro-Navas, S. Schiaffino-Ortega, M.P. Carrasco-Jimenez, P. Rios-Marco, C. Marco, A. Espinosa, M.A. Gallo, E. Mariotto, G. Basso, G. Viola, A. Entrena-Guadix, L.C. Lopez-Cara, New more polar symmetrical bipyridinic compounds: new strategy for the inhibition of choline kinase alpha1, Future Med. Chem. 7 (2015) 417–436.